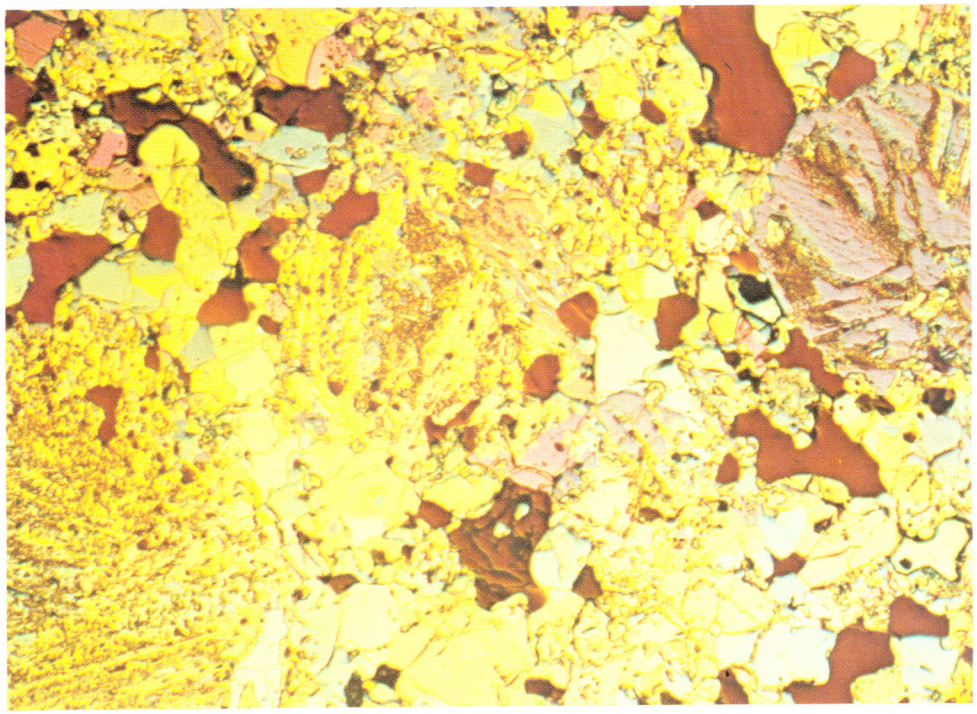

a.

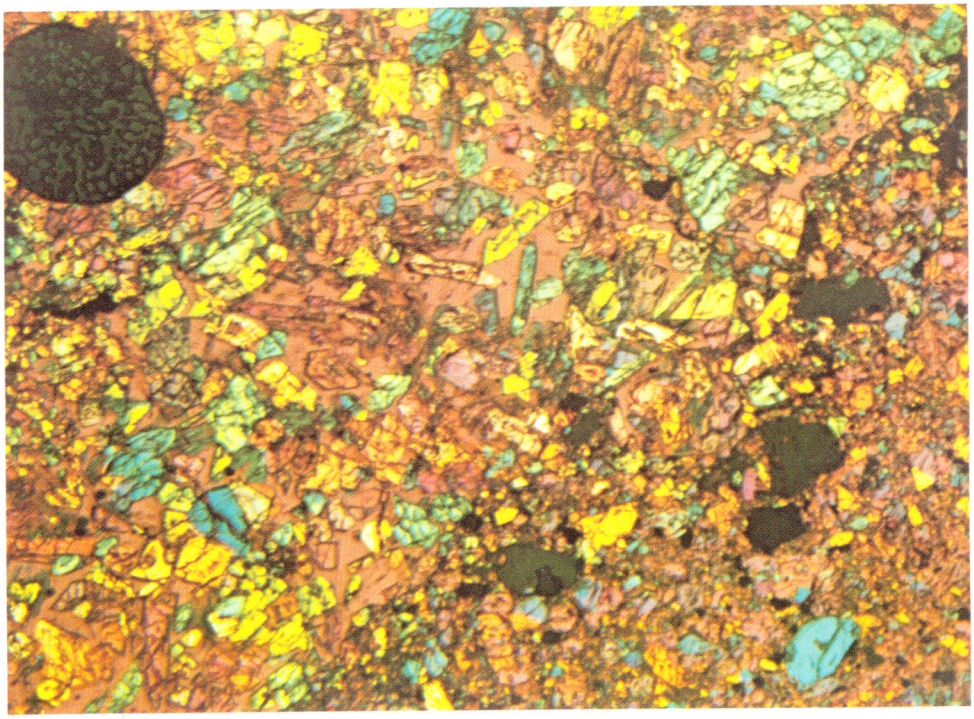

b.

a. Photomicrograph of thin (10μm) section of the Andura meteorite, an olivine bronzite-chondrite (H6). Note the strong contrast between the relatively coarse, equigranular, "metamorphic" texture of the matrix surrounding the chondrule, lower left, and the fine-grained, unrecrystallized texture of the chondrule itself and other parts of the matrix, a contrast that indicates a nonmetamorphic origin. Silicates, mostly olivine and pyroxene, show light pastel colors, metal (NiFe) brown, troilite (FeS) dark brown. This section also illustrates the extreme difficulties in performing a modal analysis optically. Length of section 2.3 mm. *b*. Photomicrograph of thin (10μm) section of the Pulsora olivine-bronzite chondrite (H3 to H7?). Upper left part consists of skeletal and zoned olivine (Fa_{13} to Fa_{16}) in silica-rich glass (H3). The normal matrix, lower right, containing numerous chondrules and fragments, is unsorted, mostly fine-grained and has the same (and constant) olivine-pyroxene composition as the chondrules. Some lithic fragments, also with constant olivine composition, show an "achondritic" (H7?) texture. Silicate minerals show varying pastel colors, the glass is pinkish, and the opaques (metal and troilite) are dark. Note the eutectic metal/troilite spherule, top left. This section clearly demonstrates that the Pulsora chondrite never suffered thermal metamorphism. Length of section 3.6 mm. (Fredriksson et al., "The Pulsora Anomaly.")

SMITHSONIAN CONTRIBUTIONS TO THE EARTH SCIENCES • NUMBER 14

Mineral Sciences Investigations 1972-1973

George S. Switzer
EDITOR

SMITHSONIAN INSTITUTION PRESS
City of Washington
1975

ABSTRACT

Switzer, George S., editor. Mineral Sciences Investigations, 1972–1973. *Smithsonian Contributions to the Earth Sciences,* number 14, 88 pages, 29 figures, and frontispiece, 1975.—Thirteen short contributions from the Smithsonian's Department of Mineral Sciences for 1972 and 1973 are gathered together in this volume. Scientific contributions include new data on some mercury minerals from Terlingua, Texas; a description of dashkesanite from St. Paul's Rocks; a note on high-alumina basalt from the Aleutian Trench; descriptions of samples from the Apollo 15 and 16 lunar missions; chondrule composition of the Allende meteorite; the Pulsora meteorite and metamorphic equilibration in chondrites; the possible survival of very large meteorites that encounter the earth's surface; data on eight observed-fall chondritic meteorites; chemical analyses of two microprobe standards; and a technological note on the preparation of multiple microprobe samples. A history of mineral sciences in the Smithsonian Institution and a list of meteorites in the Smithsonian collections complete the volume.

OFFICIAL PUBLICATION DATE is handstamped in a limited number of initial copies and is recorded in the Institution's annual report, *Smithsonian Year.* SI PRESS NUMBER 5138. SERIES COVER DESIGN: Aerial view of Ulawun Volcano, New Britain.

Library of Congress Cataloging in Publication Data
Switzer, George S., comp.
Mineral sciences investigations, 1972-1973.
(Smithsonian contributions to the earth sciences, no. 14)
Supt. of Docs. no.: SI 1.26: 14
"Thirteen short contributions from the Smithsonian's Department of Mineral Sciences."
1. Meteorites. 2. Mineralogy. 3. Lunar petrology. I. National Museum of Natural History. Dept. of Mineral Sciences. II. Title. III. Series: Smithsonian Institution. Smithsonian contributions to the earth sciences, no. 14.
QE1.S227 no. 14 [QE395] 550'.8s [549] 74-10590

For sale by the Superintendent of Documents, U.S. Government Printing Office
Washington, D.C. 20402 - Price $2.50 (paper cover)

Contents

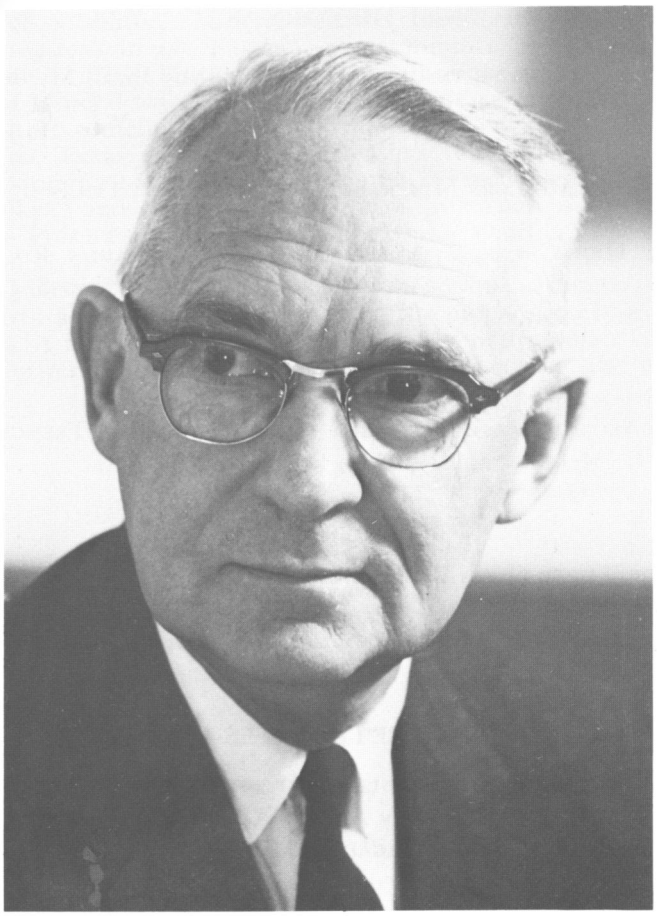

MINERAL SCIENCES INVESTIGATIONS
1972–1973

Dedicated to

EDWARD P. HENDERSON
Curator Emeritus, Department of Mineral Sciences
Smithsonian Institution

Mineral Sciences Investigations 1972-1973

Mineral Sciences in the Smithsonian Institution

Brian Mason

ABSTRACT

The Smithsonian Institution's interest in mineral sciences extends back to the founding of the Institution, whose founder, James Smithson, published a number of mineralogical papers. This account traces the development of the mineral sciences (including all of geology, except paleontology and stratigraphy) in the Smithsonian from its founding in 1846 to 1963.

Introduction

This history has been compiled to record the origin and development of mineral sciences as a part of the Smithsonian Institution. Mineral sciences are interpreted in a very broad sense as including all of geology, except paleontology and stratigraphy. This is essentially how the subject has evolved in the Institution, and the present Department of Mineral Sciences is responsible not only for mineralogy and petrology (both terrestrial and extraterrestrial—meteorites and lunar rocks), but also for most aspects of physical geology, including the exhibition hall "Our Restless Planet" and the answering of many queries from the public on general geology. The sources of this history include published information from annual reports and research papers, excerpts from manuscripts in the department's files (including a lengthy historical account written by Dr. G. P. Merrill near the end of his long curatorship), and verbal reminiscences by staff members and others. The account has been carried up to 1963, when the Department of Geology was divided into two departments, Paleobiology and Mineral Sciences. This seems to be a convenient point in time to stop, since subsequent developments are well known both from published reports and from the personal knowledge of the present staff.

Although the Department of Mineral Sciences was established as recently as 1963, the Smithsonian's interest in this field extends back to the establishment of the Institution—or even before, if we consider James Smithson's own contributions to mineralogy. He published a number of mineralogical papers, the most notable being one in the *Philosophical Transactions of the Royal Society* (1803), in which he showed that the material then known as calamine comprised two distinct minerals, zinc carbonate (now known as smithsonite) and zinc silicate (hemimorphite). Along with Smithson's monetary bequest, the Institution received his cabinet of minerals, described (Goode, 1897:305) as "a cabinet, which . . . proves to consist of a choice and beautiful collection of minerals, comprising probably eight or ten thousand specimens. The specimens, though generally small, are extremely perfect, and constitute a very complete geological and mineralogical series, embracing the finest varities of crystallization, rendered more valuable by

Brian Mason, Department of Mineral Sciences, National Museum of Natural History, Smithsonian Institution, Washington, D.C. 20560.

accompanying figures and descriptions by Mr. Smithson, and in his own writing. The cabinet also contains a valuable suite of meteoric stones, which appear to be suites of most of the important meteorites which have fallen in Europe during several centuries." This collection was unfortunately lost in the disastrous fire at the Institution in 1865.

The original charter of the Smithsonian Institution provided not only for a museum, but also for a chemical laboratory. The chemical laboratory was established by 1853, since in his report for 1854 the then Secretary, Joseph Henry (1854:18), recorded: "The laboratory of the Institution during the past year has been used by Professor J. Lawrence Smith in the examination of American minerals. . . . He also made a series of analyses of meteorites, among which were fourteen specimens belonging to the cabinet of James Smithson." This work was published as "Re-examination of American Minerals" (1853–1854) and "Memoir on Meteorites" (1855). Unfortunately, the specific meteorites from the Smithson collection are not identified and presumably were lost in the 1865 fire. J. Lawrence Smith moved to Louisville in the fall of 1854, after giving a series of lectures during the winter of 1853–1854 (for which he was paid $550, according to the financial records). Apparently, however, he worked in the Smithsonian chemical laboratory during several subsequent summers.

After the brilliant beginning provided by Smith, the mineral sciences languished for the next quarter century. Joseph Henry was unwilling to commit the Institution's limited income for the development of a museum. Indeed, he appears to have discouraged the accumulation of large collections. In 1861 Professor Thomas Egleston of the School of Mines at Columbia University, a prominent mineralogist, was employed in the Smithsonian laboratory examining and classifying the collections representing the acquisitions of the various land office surveys, exploring expeditions, and other sources (Henry, 1862:38). It is further recorded (Henry, 1873:51) that during the interval 1861–72 "a large number of specimens in mineralogy and geology were also packed up and transmitted to Professors Egleston and Newberry of the School of Mines of New York under the existing arrangements with those gentlemen to select and label a perfect single series for the U.S. National Museum and to exchange the duplicate specimens in its interest." This may not have been altogether in the interest of the Smithsonian Institution; Merrill comments:

> It is impossible, however, from the available records to state the full number in the collections at any one time, owing to the manner in which sets were made up to send out under the administration of Messrs. Egleston and Newberry. There is here shown a singular and inexplicable discrepancy between manifested intentions and actual accomplishment since under the administration of Egleston and Newberry these collections were largely, and in some cases almost completely dissipated or depleted.

In this connection the following excerpt (Merrill, c.1925) of a letter from W. P. Blake to G. P. Merrill dated 12 October 1899 is significant:

> I was also astonished in looking through the museum collection at Columbia College, New York to see the series of very remarkable concretions I collected on the Colorado desert in the cases. Wondering how they got there I inquired of Prof. Baird and he told me that an arrangement had been made with Newberry to look over the mass of material which had been accumulated with permission to him to take such duplicate material as he liked. [Merrill (c.1925) comments:] "Evidently Prof. N. made the most of his opportunity!"

In 1873 F. M. Endlich was appointed chemist and mineralogist in the Institution and served until 1879 when he resigned. During this period he was engaged during the summers as a geologist on the Hayden surveys in Colorado. Endlich reported in 1873 that the geological collections all told constituted 6300 specimens of which 3000 were minerals, representing 230 species; 2300 rocks and 500 ore specimens, with about 800 samples on hand awaiting classification. In his final report Endlich (1880: 333–335) listed 343 species and varieties of minerals in the collection.

The museum operations of the Smithsonian Institution were reorganized and greatly expanded in 1880, following the great accretion of collections from the Centennial Exhibition of 1876 and the provision of a large new building to house them (the present Arts and Industries Building). In a handwritten manuscript Merrill commented:

> It was a square squatty affair of red, blue and yellow brick, exteriorly an architectural horror, interiorly a barren waste. It presented but one redeeming feature—space; and as it was space that Baird was after I presume it may at first thought have been considered a success. One can here but be reminded of the reply made by a high official after being shown thru the then newly finished Pension Office building. "Well," it was asked, "have you any criticism?" "Yes," was the reply, "it is fireproof."

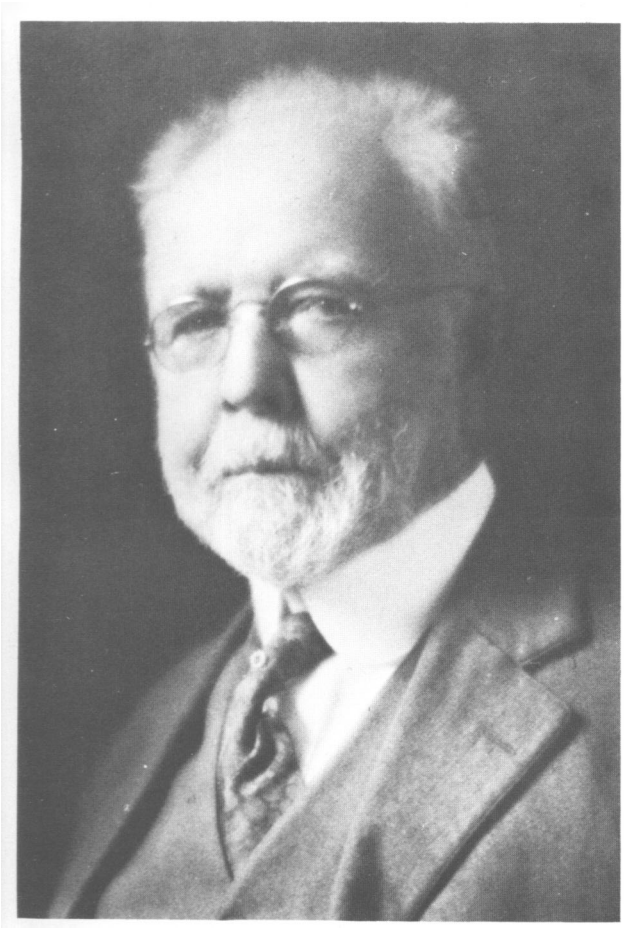

FIGURE 1.—George P. Merrill (1854–1929).

The expansion and reorganization of 1880 found expression in the creation of several departments and the appointment of salaried officials to take charge of the various collections. Dr. George W. Hawes was appointed curator of geology and mineralogy. In 1881 he was given three aids: F. P. Dewey for chemistry and metallurgy, G. P. Merrill for petrology (Figure 1), and W. S. Yeates for mineralogy. The organization thus formed was short-lived, being terminated by the death of Dr. Hawes on 22 June 1882. Upon the death of Dr. Hawes, Mr. Dewey was appointed an assistant curator and shortly afterwards full curator of a separate Department of Metallurgy and Economic Geology. In December 1883, Dr. F. W. Clarke of the U.S. Geological Survey was made honorary curator of the Department of Mineralogy, with Mr. Yeates as assistant. In the same year Dr. Merrill was made assistant acting curator in charge of the newly created Department of Lithology and Physical Geology. In 1889, after the resignation of Mr. Dewey to become assayer at the Bureau of the Mint, the two departments of Metallurgy and Economic Geology, and Lithology and Physical Geology were united under the title of Department of Geology, Systematic and Applied, and Dr. Merrill appointed curator. A complete reorganization in 1897 created a single Department of Geology, with three divisions: Physical and Chemical Geology, Mineralogy, and Stratigraphic Paleontology. Merrill was appointed head curator of the department, and was also curator of physical and chemical geology. Clarke remained as honorary curator of mineralogy, with Wirt Tassin assistant curator and Dr. L. T. Chamberlain as honorary custodian of gems and precious stones. The Department of Geology so constituted survived with minor modifications for over sixty years, until the creation of separate departments of Mineral Sciences and Paleobiology in

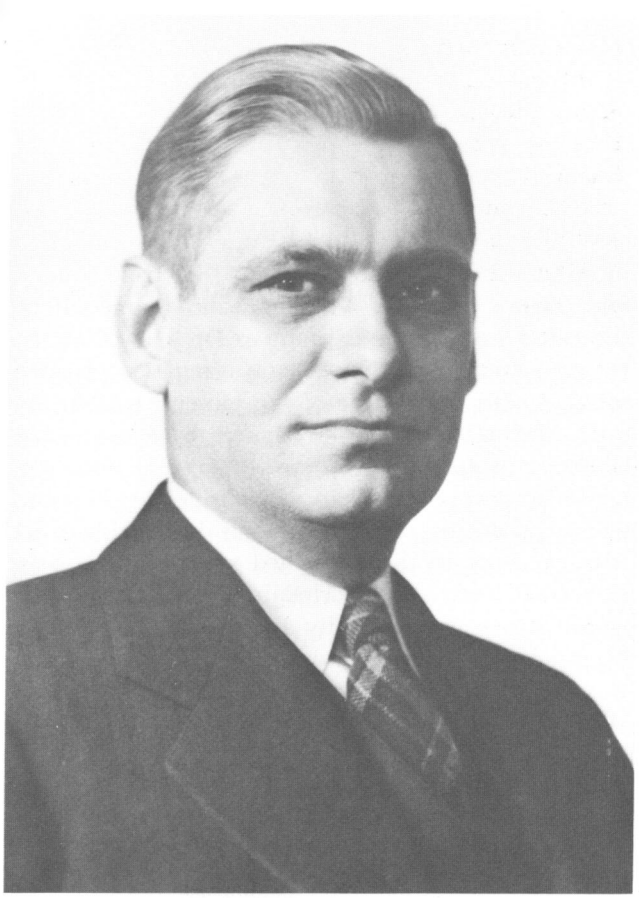

FIGURE 2.—William F. Foshag (1894–1956).

1963. Throughout this time, however, the divisions of Physical and Chemical Geology, and of Mineralogy actually functioned essentially as a single unit, although they appear as separate units on the table of organization until 1942. Merrill was effectively curator of both divisions until his death in 1929. He was succeeded as head curator of the Department of Geology by Dr. R. S. Bassler, a paleontologist, and Dr. W. F. Foshag (Figure 2) was appointed curator of both divisions. Dr. Bassler retired in 1948, and Foshag succeeded him as head curator, a position he held until his death in 1956. Dr. G. A. Cooper, also a paleontologist, then became head curator, and Dr. G. S. Switzer, curator of mineralogy, an arrangement that continued until the eventual formation of separate departments of Paleobiology and Mineral Sciences.

Functions of the Department

With this introduction, it is convenient to describe the operations of the different segments of the department under the headings of mineralogy, petrology, meteorites, and gems and precious stones.

Mineralogy

William S. Yeates, the first appointee specifically in mineralogy, graduated M.A. in 1881 from Emory and Henry College, Virginia, and immediately thereafter became an assistant to Dr. Hawes. After Hawes' death in 1882, Yeates remained as the salaried officer in charge of the mineral collections until May 1893, when he resigned to become state geologist of Georgia. He was apparently more an administrative officer than a scientific investigator, and his work at the Smithsonian Institution contributed little to the published record. Yeates was succeeded for a short period by O. C. Farrington, whose career is essentially linked with the Field Museum of Natural History in Chicago, where he was curator of geology from 1894 to 1930. In 1894 Wirt Tassin became assistant curator, with F. W. Clarke continuing as honorary curator.

Tassin worked in the Division of Mineralogy from 1894 to May 1909, when he resigned to go into private business. He left an interesting and informative manuscript account of the history of the division up to 1906:

FIGURE 3.—Joseph E. Pouge (1887–1971).

> In 1883 Mr. F. W. Clarke was appointed honorary curator. This marks the real beginning of the present Division of Mineralogy. To Mr. Clarke more than any other is due the present standing of the collection. His appreciation of good minerals, his knowledge of their value, his enthusiasm, his widespread acquaintance and his position on the Geological Survey and on exposition boards has been of incalculable value to the collection. In fact it would be almost impossible to say too much concerning the value of his influence in securing fine specimens.

Tassin gave an account of the growth of the mineral collections from 1859 to 1906. The total number grew slowly from 793 in 1859 to 3551 in 1880, and then increased rapidly, evidently due to the reorganization, reaching 45,291 in 1895; growth then leveled off, the total in 1906 being 48,987. While Tassin evidently devoted much of his work to his curatorial and exhibition responsibilities, he also did some research. His name is associated with Dr. Merrill's in the investigation of several meteorites, the first such research in the Institution since that of J. Lawrence Smith half a century earlier.

Tassin was succeeded in 1909 by Dr. Joseph E. Pogue (Figure 3), of whom Merrill (c.1925) remarked: "For the first time in the history of the Department the collections were administered by a

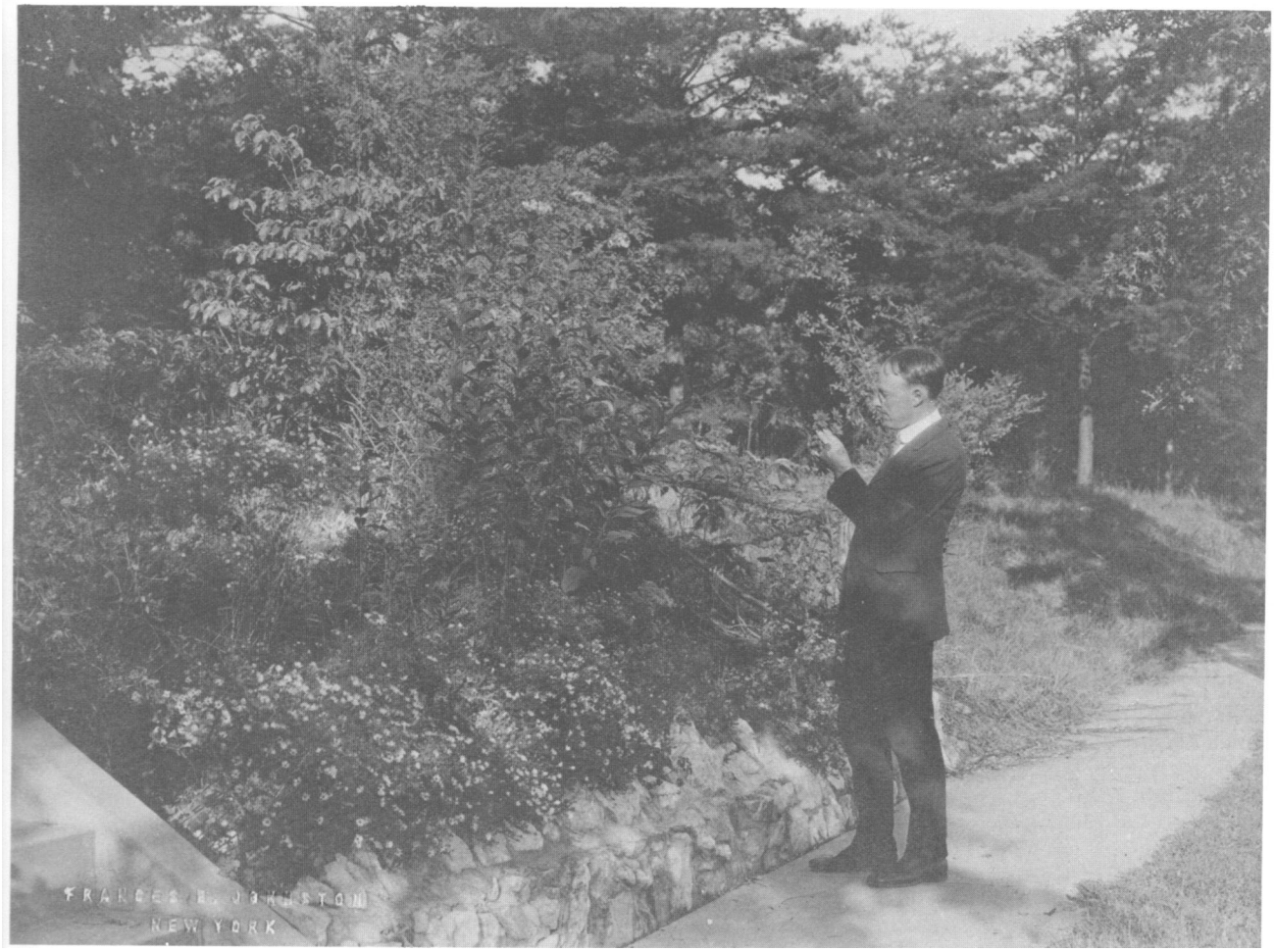

FIGURE 4. Edgar T. Wherry (1885–). Photograph taken in his garden in Chevy Chase, D. C., about 1917.

trained mineralogist." Pogue worked as assistant curator of the Division of Mineralogy until October 1913, when he resigned to join the U.S. Geological Survey. Much of his time must have been occupied in moving the collections and exhibits into the present Natural History Building, which was opened in 1910. During his term in office Dr. Pogue visited many European museums, studying collections and displays. He also published several papers involving original research, among them a monograph on turquoise published by the National Academy of Sciences in 1915.

Pogue was followed by Dr. Edgar T. Wherry (Figure 4), who carried on the work of the division along the lines laid down by his predecessors, but who was able to devote more time to research. He published a number of papers, including one in 1917 giving the name "merrillite" to a new calcium phosphate mineral that Dr. Merrill had recognized as a meteoritic constituent in 1915. He was one of the founders of the *American Mineralogist* and its first managing editor (1916–1921), and president of the Mineralogical Society of America in 1923. He resigned from the Smithsonian Institution in August 1917 to join the Bureau of Chemistry of the Department of Agriculture.

When contacted in April 1972, Dr. Wherry was kind enough to provide the following reminiscences:

> In 1913 I was teaching mineralogy at Lehigh University, Bethlehem, Pennsylvania, and spending summers as field assistant to Professor Florence Bascom of Bryn Mawr College in the preparation of geologic folios of quadrangles in southeastern Pennsylvania, for the U. S. Geological Survey. I was also collecting the minerals of the state, and writing articles about them. Finding these activities somewhat overtaxing I was glad to accept an invitation from Dr. George

P. Merrill, head curator of Geology at the Smithsonian, to join his staff as assistant curator of Mineralogy and Petrology.

Some years before this position had been held by a Mr. Wirt Tassin, who had arranged the mineral collection as a sort of textbook, accompanying each specimen with an elaborate descriptive label, the study of which would take far more time than most visitors could spare. When he retired, his place was taken by Joseph Pogue, who rearranged the collection in accordance with standard classifications, replacing the textual labels with simple ones bearing name, composition, and locality. He resigned to go into business, and I was taken on to complete his reorganization of the collection.

My duties included answering correspondence about minerals, including especially requests for identification of specimens submitted, usually with reference to their potential commercial value. Sometimes my reports would be questioned, but to make me feel at ease, the Smithsonian office showed me a bit of pertinent correspondence: this comprised a report on a specimen made by Dr. Merrill, a response from the sender questioning its correctness, and the marginal annotation addressed by Merrill to the Secretary of the Smithsonian Institution, "If what this man says is true, Merrill ought to be fired."

The most worth-while specimen I received was a bit of clay, and instead of an inquiry as to its value, the question was: "Is this of igneous or sedimentary origin?" Finding it to be free from quartz grains, which make up the large bulk of ordinary sediments, I guessed that it represented altered volcanic ash. I was promptly contacted by a patent-lawyer, who explained that his client held a patent on the use of igneous material for water-softening, and wished to claim royalties from the organization marketing this clay for that purpose, if it was indeed of igneous origin. I was accordingly invited to go to South Dakota where the material occurred, and study it fully. I was thereby enabled to establish the nature of "bentonite" as representing altered volcanic ash, which has had important geological applications.

In the course of that trip I stopped off at several notable mineral localities, and collected multiple specimens of such things as geodes, and lead-zinc ore-minerals. These were packed in barrels, which could then be shipped under government frank, and sent back for adding to the educational collections which the Smithsonian Institution was distributing to schools.

In those days the whole field of mineralogy was handled by one man, and I never had a technical assistant or understudy. Records were kept by a pleasantly efficient secretary, Miss Margaret W. Moody. She had scratched with a diamond point a catalog number on the back of every gem-stone; and when I resigned, it was her duty to check the gems against the catalog, to see that I had not lost any of them. It was pleasant to hear that only one ruby appeared to be missing, but that turned out to have been transferred to a special exhibit of North Carolina specimens.

Dr. Wherry was succeeded as assistant curator by William F. Foshag, and at about the same time Earl V. Shannon was appointed assistant curator in the Division of Physical and Chemical Geology, Merrill being curator of that division as well as head curator of the Department of Geology. Shannon was an accomplished analyst and a keen mineralogist, and an extremely diligent worker. Between 1919 and 1929 he published over 80 papers, many of them short notes but also some lengthy ones, including a 483-page monograph on the minerals of Idaho. Tragically he suffered a mental breakdown in 1929 and left the Institution. He was succeeded by Edward P. Henderson, who served for over 35 years until his retirement in 1966, and is still active in the department as a research associate.

In 1926 the mineral collection was enormously enriched by two remarkable bequests, which raised it from comparatively undistinguished stature to one of the world's great mineral collections. These were the Roebling and Canfield bequests.

Colonel Washington A. Roebling (the Colonel was a Civil War veteran) was a civil engineer and the builder of the Brooklyn Bridge. During the latter work he suffered "cassion disease," with permanent impairment of his health. This caused him to turn his attention to mineral collecting. He sought not only beautifully developed specimens but also those that were rare—indeed his aim was to secure a representative of every known mineral, however insignificant and uninteresting in appearance. In this he was eminently successful, the collection on his death lacking only about a dozen of the accepted mineral species at that time. His impaired health made travel and field collecting impossible for him, but he had ample financial means, and corresponded vigorously with mineralogists and mineral dealers throughout the world. He died on 28 July 1926, leaving his collection of 16,000 carefully selected specimens to the Smithsonian Institution. His son, John A. Roebling, generously established an endowment fund of $150,000, the income to be used for the acquisition of additional material. This endowment has provided for the continued growth of the Roebling collection.

The Canfield collection really comprises three collections. The nucleus was formed by Mahlon Dickerson of Dover, New Jersey, who began collecting in the early part of the nineteenth century. This collection passed to his nephew, Frederick Canfield, and to it were added many fine specimens collected at Franklin and Sterling Hill between 1840 and 1866. This collection, comprising some

1600 specimens, was displayed in the family mansion near Dover, where it remained until it was transferred to Washington in 1926. Frederick A. Canfield, son of Frederick Canfield, who inherited the collection, preferred to leave it intact and begin a new one of his own. This, at the time of his death on 3 July 1926, totaled some 7500 specimens. Frederick A. Canfield was educated as a geologist and mining engineer at Rutgers and Columbia Universities. In the practice of his profession he had the opportunity to travel and acquire many fine specimens at first hand. He also subsidized workmen in the railway tunnels and quarries of northern New Jersey, and in that way obtained many choice specimens of the trap rock minerals. His professional connection with the Franklin and Sterling Hill mines enabled him to keep pace with the new and rare minerals constantly found there. He also obtained many fine suites of specimens from outstanding mineral localities. With the bequest of the mineral collections Mr. Canfield also provided an endowment of $50,000 for future accessions.

Dr. Merrill died on 15 August 1929 and was succeeded as head curator of the Department of Geology by Dr. R. S. Bassler. Dr. Foshag was appointed curator of both the Division of Mineralogy and Petrology, and the Division of Physical and Chemical Geology, in effect combining the two divisions, although on the table of organization the Division of Physical and Chemical Geology survived until 1942. Dr. Foshag was born on Long Island in 1894, but his family moved to California and he graduated from the University of California in 1919. In 1917 and 1918 he served as chemist for the Riverside Portland Cement Company at the famous mineral locality of Crestmore, which probably effectively started his career in mineralogy. During his service with the Smithsonian Institution he examined many famous mineral localities in the United States and Mexico. During World War II he spent most of his time in the latter country in cooperative work with the Mexican authorities in the development of mineral deposits. During that time, in 1944, the new volcano Paricutin erupted, and he began a long-continued study of its eruptive processes and products, a study terminated by his death. His Mexican work also led him to an interest in Latin American archeology and specifically a study of jade objects from Central America. He was successful in pinpointing a source for this jade in Guatemala. His contributions to mineralogy were recognized by the ward of the Roebling Medal of the Mineralogical Society of America in 1953.

Dr. Foshag died on 21 May 1956 and was succeeded as curator of the Division of Mineralogy and Petrology by Dr. George S. Switzer, who had joined the museum as associate curator in the division in April 1948. In August 1957 Paul E. Desautels was appointed associate curator in the division, and later in the same year Roy S. Clarke, Jr., was appointed chemist. These men, together with Dr. Henderson and Dr. Switzer, comprised the professional staff when the division was reformed as the Department of Mineral Sciences in 1963.

Petrology

Systematic petrology in the Smithsonian Institution can be fairly dated from the appointment of G. W. Hawes as curator of the Department of Geology on 1 January 1881. Hawes was one of the pioneers in the use of the petrographic microscope in the United States, having learned its use during graduate work at Yale University with Professor E. S. Dana, and at the University of Heidelberg with Professor Harry Rosenbusch; he received the Ph.D. degree from the latter university in 1880. At the same time as his appointment to the Smithsonian Institution, Hawes began an investigation of the building-stones of the United States as part of the Tenth Census; the Annual Report for 1881 (Baird, 1882:110) states:

> Dr. Hawes . . . has gathered specimens of stone from every quarry in the United States; and a force of fifteen men, in part detailed from the Census Office, has been occupied all the year in preparing them for study and exhibition. . . . Numerous analyses of building-stones by the chemical and specific gravity methods have been made by Messrs. F. P. Dewey and F. W. Taylor. Since the 1st of June (1881), Mr. Geo. P. Merrill has prepared 1550 microscopic slides of building-stones, to be used in connection with the investigation.

Unfortunately Hawes developed tuberculosis during 1881, and the disease advanced rapidly. In 1882 he went to Colorado in the hope of checking it, but he died in Manitou Springs on 22 June 1882. On his death the petrographic work on the building-stones fell to G. P. Merrill, who noted in his manuscript (c.1925) that he was wholly inexperienced in

this field. He evidently learned quickly and well, however, since he was one of the co-authors of "Reports on the Building-Stones of the United States and Statistics of the Quarry Industry for 1880" (1884), in which he contributed an article on the microscopic structure of the building-stones and eighteen reproductions of photomicrographs.

Merrill continued his petrographic work on building-stones and became an authority on the subject, writing several monographs and books thereon. He served as a special agent in this field for the Twelfth Census (1912). He was consulted frequently by both private and public officials regarding the stone to be used for various structures. He thus served in an advisory capacity in the selection of stone for the Natural History Building, the Old Post Office Building, Constitution Hall, the columns on the west face of the Treasury Building, and numerous others. Perhaps the most momentous question left for his decision was the choice of stone for the Lincoln Memorial (Yule marble from Colorado). Probably through his work on building-stones, Merrill became very interested in rock weathering, and wrote extensively on this subject, culminating in his book, *A Treatise on Rocks, Rock Weathering, and Soils.* He also authored *The Nonmetallic Minerals: Their Occurrence and Uses.*

After the turn of the century, Merrill's interest turned to meteorites, and for the remainder of his life his research work was concentrated in this field. The petrological collections continued to grow, largely through accessions of material from the U. S. Geological Survey illustrating regional monographs and bulletins. In 1916, however, Joseph P. Iddings was appointed honorary curator of petrology, and after his death in 1920 Whitman Cross succeeded to this honorary position and held it until his death in 1949. These appointments brought two of the authors of the CIPW system of igneous rock classification into the Smithsonian Institution; a third, Henry S. Washington, was at the Geophysical Laboratory of the Carnegie Institution of Washington and many of his collections were eventually given to the Smithsonian Institution. During his period as honorary curator, Cross developed a collection of some 2000 igneous rocks comprising most of the types established by the CIPW system. Each rock has a thin section accompanying it, with a meticulous description on a file card; many are chemically analyzed. This is probably the most comprehensive systematic collection of igneous rocks in existence.

After the death of Cross active curatorial and research work in petrology was largely discontinued, because of inadequate staffing. This situation was remedied by the establishment of a Division of Petrology within the newly organized Department of Mineral Sciences in 1963, and the appointment of Dr. William G. Melson in 1964 to direct it.

METEORITES

As mentioned earlier, the original Smithson bequest included his cabinet of minerals, which contained "a valuable suite of meteoric stones, which appear to be suites of most of the important meteorites which have fallen in Europe during several centuries" (Goode, 1897:305). Some of these were analyzed by J. Lawrence Smith in the chemical laboratory of the Institution in 1853–54. Unfortunately, these meteorites were evidently lost along with the rest of Smithson's cabinet in the fire of 1865.

The number of falls actually represented in the collection at the first date mentioned (1880) cannot with absolute certainty be given owing to the imperfection of the record, but it was small; seven localities were represented: Imilac and Vaca Muerta, Chile; Marietta (New Concord), Ohio; Parnallee, India; Searsmont, Maine; and Cold Bokkeveld, South Africa. The Tucson iron which should have formed the chief attraction was not catalogued, though brought, through the influence of Dr. B. J. D. Irwin, to Washington in 1863. The Casas Grandes iron which came to Washington from the Philadelphia Centennial should also have received attention (Merrill, c.1925).

The collection grew rapidly, evidently largely through the work of Dr. F. W. Clarke, who was appointed honorary curator in the Department of Mineralogy in December 1883. In 1889 he published a catalog of the meteorite collection as of October 1888, in which he lists 128 distinct falls and finds; in addition, there were 217 meteorites in the Shepard collection, which was deposited in the museum by Shepard's son in 1886 (and ultimately bequeathed to the Smithsonian Institution in 1915). There was considerable duplication between the two collections and many of the specimens in both collections were fragments. Nevertheless, the building-up of the meteorite collection by Clarke, almost entirely by exchanges, was a notable contribution at this early time.

In 1888 Merrill published his first paper on meteorites, and was an active researcher in the field until his death in 1929, publishing over eighty papers on meteorites. The collection continued to grow. In 1902, Tassin brought the Clarke catalog up to date. For the purposes of this catalog the Shepard meteorites were listed along with the museum's collection. The combined collections contained 348 distinct falls and finds. In 1916 Merrill published a "Handbook and Descriptive Catalogue of Meteorite Collections in the United States National Museum". The combined collections at that time contained 412 independent falls and finds. The meteorite collection has continued to grow steadily and may now be the world's largest and most comprehensive from the standpoint of the number of meteorites represented.

The tradition of meteorite research begun by Merrill has continued. Dr. Foshag wrote a number of papers on meteorites during his curatorship, and his presidential address (1940) to the Mineralogical Society of America was entitled "Problems in the Study of Meteorites." Meteorite research within the Institution, however, became the major interest of Dr. Edward P. Henderson. Beginning in 1934 and continuing throughout his curatorship and after his retirement, he had published over thirty papers on meteorites. Many of these were written in collaboration with Stuart H. Perry (1874–1957), a Michigan newspaper publisher. Perry graduated in 1894 from the University of Michigan, where he studied chemistry, geology, and zoology. Fossils were his first love, but around 1930 his scientific interests became directed towards the study of meteorites. He was a vigorous collector, being aided in this respect by adequate private means. In 1944, the Smithsonian published Perry's "Metallography of Meteoritic Iron," which for many years has been the standard reference in this field. He also compiled and privately published nine albums of photomicrographs of iron meteorites (166 in all), of which six sets were produced. Through the years that Perry was studying and collecting meteorites he generously shared his knowledge and specimens with others. Although he presented specimens to many institutions, and privately assisted others in their studies of meteorites, he was sincerely interested in the growth of the national collection and presented what he considered to be his most important specimens to the Smithsonian Institution. During his life Perry donated 192 meteorites in this way.

After J. Lawrence Smith's death in 1883, his widow endowed the Lawrence Smith Medal, to be awarded by the National Academy of Sciences for "original investigation of meteoric bodies." This medal was awarded to George P. Merrill in 1922, Stuart H. Perry in 1945, and Edward P. Henderson in 1970.

Gems and Precious Stones

This collection owes its beginning to an exhibit made by F. W. Clarke and paid for ($2500) by funds appropriated for the New Orleans Exposition of 1884. The same collection was displayed at the Cincinnati Exposition the following year, after which it was returned to Washington and placed on exhibition in the museum. A detailed description of this collection was published by G. F. Kunz in 1889. In 1891 the collection was greatly augmented by purchases from the estate of Dr. Joseph Leidy of Philadelphia, and was exhibited at the Columbian Exposition in Chicago in 1893. In 1894, Mrs. Frances Lea Chamberlain gave the museum a collection of precious stones that had been made by her father, Dr. Isaac Lea. Later, in 1897, her husband, Dr. L. T. Chamberlain, was appointed honorary curator of the collection and added a large number of desirable specimens. On his death in 1913 he bequeathed a sum of money, the income from which is used for its further increase.

The growth of the gem collection is documented by the 1900 "Descriptive Catalogue" by Wirt Tassin and in the 1922 "Handbook and Descriptive Catalogue" by G. P. Merrill. A recent popular account is *Gems in the Smithsonian* by Paul E. Desautels.

Literature Cited

Baird, S. F.
1882. Report of the Secretary. *Annual Report of the Board of Regents of the Smithsonian Institution for the Year 1881,* 839 pages.

Clarke, F. W.
1889. The Meteorite Collection in the U.S. National Museum: A Catalogue of Meteorites Represented November 1, 1886. *Annual Report of the Smithsonian Institution for 1886,* 2:255–265.

Desautels, P. E.
1972. *Gems in the Smithsonian.* Washington, D.C.: Smithsonian Institution Press.

Endlich, F. M.
1874. Mineralogical Collection. *Annual Report of the Board of Regents of the Smithsonian Institution for the Year 1873,* pages 51–53.
1880. List of Species and Varieties of Minerals in the National Museum of the United States in 1879. *Proceedings of the United States National Museum,* 3:333–335.

Goode, G. B.
1897. *The Smithsonian Institution, 1846–1896.* Washington, D.C.

Henry, J.
1854. Report of the Secretary. *Ninth Annual Report of the Board of Regents of the Smithsonian Institution,* 463 pages.
1862. Report of the Secretary. *Annual Report of the Board of Regents of the Smithsonian Institution for the Year 1861,* 463 pages.
1873. Report of the Secretary. *Annual Report of the Board of Regents of the Smithsonian Institution for the Year 1872,* 456 pages.

Kunz, G. F.
1889. Gem Collection of the U.S. National Museum. *Annual Report of the Smithsonian Institution for 1886,* 2:267–275.

Merrill, George P.
1879. *A Treatise on Rocks, Rock Weathering, and Soils.* 1st edition, 411 pages. New York: MacMillian and Co. [2nd edition, 400 pages, published in 1906.]
1884. Reports on the Building-Stones of the United States and Statistics of the Quarry Industry for 1880. *U.S. Tenth Census,* 10:1–410.
1888. On the San Emigdio Meteorite. *Proceedings of the United States National Museum,* 11:161–167.
1904. *The Nonmetallic Minerals: Their Occurrence and Uses.* 414 pages. New York: John Wiley and Sons.
1916. Handbook and Descriptive Catalogue of Meteorite Collections in the United States National Museum. *United States National Museum Bulletin,* 94:1–206.
1922. Handbook and Descriptive Catalogue of the Collections of Gems and Precious Stones in the United States National Museum. *United States National Museum Bulletin,* 118:1–225.
[c. 1925.] [History of the Department of Geology.] Manuscript, files of the Department of Mineral Sciences, National Museum of Natural History, Smithsonian Institution.

Perry, S. H.
1944. Metallography of Meteoritic Iron. *United States National Museum Bulletin,* 184:1–206.

Pogue, J. E.
1915. The Turquoise: A Study of Its History, Mineralogy, Geology, Ethnology, Archaeology, Mythology, Folklore, and Technology. *Memoirs of the National Academy of Sciences,* 12 (2, 3d memoir), 162 pages, 22 plates.

Shannon, E. V.
1926. The Minerals of Idaho, *United States National Museum Bulletin,* 131:1–483.

Smith, J. L.
1853.–1854. Re-examination of American Minerals. *American Journal of Science,* 15:207–215; 16:41–53, 365–373; 18:372–381.
1855. Memoir on Meteorites. *American Journal of Science,* 19:153–163, 322–343.

Smithson, J.
1803. A Chemical Analysis of Some Calamines. *Philosophical Transactions of the Royal Society* (London), 93:12–28.

Tassin, W.
1900. Descriptive Catalogue of the Collection of Gems in the United States National Museum. *Annual Report of the Smithsonian Institution for 1900,* pages 473–670.

Tassin, W.
1906. [The Mineral Collections, 1859–1906.] Manuscript, files of the Department of Mineral Sciences, National Museum of Natural History, Smithsonian Institution.

Wherry, E. T.
1917. Merrillite, Meteoritic Calcium Phosphate. *American Mineralogist,* 2:119.

New Data on Some Mercury Minerals from Terlingua, Texas

Roland C. Rouse

ABSTRACT

An X-ray study has been performed on the three mercury minerals eglestonite, mosesite, and kleinite. Previous work is reviewed and, where necessary, corrected in the light of new data. Eglestonite is cubic, Ia3d, with $a=16.04$ Å and has the formula Hg_4Cl_2O. Mosesite and kleinite are mercury nitrogen chloride sulfates. Mosesite is cubic with $a=28.62$ Å and kleinite, hexagonal with $a=40.60$ and $c=11.16$ Å. Although the chemical formulas of their supercells are still uncertain, their subcell formulas correspond essentially to the chloride salts of Millon's base ($Hg_2NOH\cdot H_2O$).

Introduction

The mercury deposit at Terlingua, Brewster County, Texas, is known mineralogically for its suite of secondary mercury minerals. It is, in fact, the type locality for six of them including terlinguaite ($Hg_4O_2Cl_2$), eglestonite (Hg_4Cl_2O), and the mercury nitrogen chloride sulfates mosesite and kleinite. These minerals are known from but a few localities and one investigator (Lipscomb, 1957) in a review of the crystal chemistry of mercury found it quite remarkable that kleinite and mosesite should occur at all in nature. The latter two are of particular interest as they are thought to be stuffed derivatives of the high tridymite and high cristobalite structures, respectively. They contain NHg_4 tetrahedra, which play the same structural role as SiO_4 tetrahedra do in silicates.

There exists one definitive study of the whole group, that of Hillebrand and Schaller (1909). Subsequent investigators have compiled a large body of chemical, optical, and crystallographic data, but their results have often been ambiguous or contradictory. An accurate determination of the crystal structure has been made only for terlinguaite and since this has resolved most of the problems associated with this mineral, it was not included in the present study. The terlinguaite structure (Aurivillius and Folkmarson, 1968) is interesting from a crystal chemical viewpoint as it contains mercury in two valence states. Some of the mercury atoms are divalent and form the characteristic linear O–Hg–O groups (Grdenić, 1965). Others are arranged in equilateral triangular clusters in which each mercury has a formal oxidation number of $+4/3$. The Hg–Hg distances in the cluster are shorter than those in solid mercury indicating intermetallic bonding, and terlinguaite is therefore a metal cluster compound.

Roland C. Rouse, Department of Geology and Mineralogy, The University of Michigan, Ann Arbor, Michigan 48104.

Experimental Methods

The study of eglestonite, mosesite, and kleinite is rendered difficult by their tendency to occur as multiple crystals, whether as twins, parallel growths or random intergrowths. In the case of kleinite this seems to be invariably the case. The specimens used in this study were from Terlingua and Huahuaxtla, Mexico, and were obtained from the U. S. National Museum collections. As reported by previous workers, eglestonite is photosensitive, its color changing rapidly from yellow to brown to black. The color change produced no obvious changes in the x-ray diffraction patterns, but this matter was not investigated systematically.

Unit cell parameters were determined from precession photographs and verified by the cone-axis or rotating crystal methods. Space groups were determined from precession and Weissenberg photographs taken with $MoK\alpha$ and $CuK\alpha$ radiations,

respectively. The cell parameters were refined from powder data by the method of least-squares using the program of Appleman and Evans. In the case of mosesite and kleinite the data were obtained from a powder diffractometer utilizing monochromatized CuKα radiation and quartz as an internal standard. Since there was not enough eglestonite available for this procedure, it was necessary to use 16 reflections between 102° and 165° 2θ measured from a Debye-Scherrer photograph. The powder patterns in Tables 1, 2, and 3 were likewise measured from shrinkage-corrected Debye-Scherrer photographs taken with a 114.6 mm diameter camera and filtered CuKα radiation. Intensities were estimated visually.

Minerals Studied

EGLESTONITE

Eglestonite was first described by Moses (1903) as a cubic mineral having the formula $Hg_6Cl_3O_2$. Hillebrand and Schaller (1909:145, 147) confirmed the cubic symmetry but found the formula to be Hg_4Cl_2O on the basis of three chemical analyses. The crystal class was determined to be m3m from the presence of the hexoctahedron as a common form.

The crystal structure of eglestonite is of some interest due to the presence of the binary ion Hg_2^{+2}. Two structures have been proposed, both by the same investigator. Hedlik (1948) found eglestonite to be cubic, Pm3n, with $a=16.07$ Å. She went on to propose a structure containing the mercurous ion and having Hillebrand and Schaller's chemical formula. However, in Hedlik (1950) there appeared a revised structure based on a cell having $a=8.03$ Å and symmetry Im3m. The formula was also changed to Hg_6Cl_4O, which is not in accord with the existing chemical analyses. No explanation was offered for the revisions and since both structures were derived with powder and rotating crystal data, neither can be considered reliable. To compound the confusion, Wolfe (cited in Palache, et al., 1951:51) reported the cell parameter $a=16.03$ Å and a probable space group Ia3d for eglestonite.

The present study has confirmed Wolfe's results. Eglestonite is cubic, Ia3d, with a refined parameter $a=16.0398 \pm 0.0003$ Å. There is also a very prominent subcell having $A=a/2=8.02$ Å and symmetry Im3m. That the 16.04 Å cell is the correct one is confirmed by powder data (Table 1), which can only be indexed fully on the larger cell. The unit cell contents calculated from the average of Hillebrande's analyses are $Hg_{94.11}$ $Cl_{49.16}$ $O_{23.76}$. From a consideration of the available equipoints in

TABLE 1.—*Powder pattern of eglestonite*

I	d_{obs}	d_{calc}	hkl
10	6.549	6.548	211
40	4.006	4.010	400
100	3.271	3.274	422
<1	3.142	3.146	510, 431
7	2.925	2.928	521
7	2.832	2.835	440
10	2.599	2.602	611, 532
50	2.529	2.536	620
5	2.471	2.475	541
10	2.313	2.315	444
5	2.265	2.268	543, 710, 550
<1	2.179	2.183	721, 633, 552
<1	2.135	2.143	642
1	2.034	2.037	651, 732
1	2.003	2.005	800
80	1.887	1.890	660, 822
1	1.858	1.865	831, 750, 743
<1	1.811	1.816	752
3	1.788	1.793	840
20	1.707	1.710	664
1	1.687	1.691	851, 930, 754
10	1.633	1.637	844
<1	1.617	1.620	941, 853, 770
1	1.586	1.588	10 • 1 • 1, 772
1	1.554	1.558	943
5	1.526	1.529	10 • 3 • 1, 952
5	1.499	1.502	871
<1	1.475	1.477	961, 10 • 3 • 3
5	1.461	1.464	10 • 4 • 2
1	1.384	1.386	11 • 3 • 2, 10 • 5 • 3, 972
5	1.373	1.375	10 • 6 • 0, 866
10	1.334	1.337	12 • 0 • 0, 884
<1	1.308	1.310	10 • 7 • 1, 11 • 5 • 2
<1	1.290	1.293	12 • 3 • 1, 983
5	1.266	1.268	12 • 4 • 0
3	1.237	1.237	10 • 8 • 2
<1	1.215	1.216	13 • 2 • 1, 11 • 7 • 2
5	1.182	1.182	12 • 6 • 2

Plus ca. 65 more lines to 0.777 Å

Ia3d, the correct formula must be Hg_4Cl_2O with Z=24. These results indicate that Hedlik's revised structure is necessarily wrong since it is based on the subcell rather than the true cell and gives a formula inconsistent with the chemical analyses. Preliminary work on a redetermination of the eglestonite structure is underway and a complete study is planned.

Mosesite

Mosesite was described by Canfield, et al. (1910) as a new mercury-ammonium compound containing chloride, sulfate, and water. Although cubic in morphology, it was weakly birefringent but became isotropic when heated to ~186°C. From this they concluded that mosesite exists in high and low temperature polymorphic forms with the inversion temperature being 186°C. This, of course, is not necessarily the case as many cubic materials show a weak, anomalous birefringence. In a study of mosesite from the Fitting district of Nevada, Bird (1932) found on the basis of powder data that mosesite is cubic with a face-centered lattice and $a=9.57$ Å.

A restudy of mosesite was performed by Switzer, et al. (1953), who obtained the first complete chemical analysis of the mineral. Noting the strong similarity of its powder pattern and chemistry to those of Millon's base ($Hg_2NOH•2H_2O$), they derived a formula $Hg_2N(Cl,SO_4,MoO_4,CO_3)•H_2O$ (Z=8) for material from Huahuaxtla Mexico. Mosesite is, therefore, the chloride salt of Millon's base with lesser amounts of other large anions. The structure of $Hg_2NOH•H_2O$ was determined by Lipscomb (1951) to be cubic, $F\bar{4}3m$, with $a=9.58$ Å. It is a stuffed derivative of the high cristobalite structure with a 3-dimensional framework of linked NHg_4 tetrahedra. The OH^- and H_2O occupy the large open channels in the framework. This explains the presence of large complex anions in the mosesite formula. Switzer, et al. (1953) also proposed a structure for mosesite analogous to that of Millon's base. The structure is cubic, $F\bar{4}3m$, with $a=9.524$ Å, which is consistent with the powder pattern.

The author has reexamined the mosesite crystals from Huahuaxtla, Mexico, analyzed by Fahey (in Switzer, et al., 1953). Although the X-ray study of this material is not yet complete, several important results can be reported. Weissenberg photographs confirm the cubic symmetry, but the space group has not yet been determined with certainty. A rotating crystal photograph shows that mosesite has a supercell with $a=28.8$ Å, three times the value previously reported. The refined value is $a=28.618 \pm 0.002$ Å. The subcell has $A=a/3=9.54$ Å. There is also a second subcell, defined by the strong reflections, which has $A'=a/12=2.38$Å.

TABLE 2.—*Powder pattern of mosesite*

I	d_{obs}	d_{calc}	*hkl*
75	5.512	5.508	333, 511
10	3.375	3.373	660, 822
90	2.877	2.876	933, 771, 755
100	2.756	2.754	666, 10•2•2
40	2.382	2.385	12•0•0
40	2.186	2.188	993, 13•1•1
25	1.834	1.836	999, 15•3•3
		1.832	12•10•0
35	1.685	1.686	12•12•0
		1.683	17•0•0
25	1.610	1.612	17•5•1
		1.607	14•11•0
20	1.454	1.455	19•5•1
		1.453	18•8•0
30	1.436		
20	1.375		
20	1.334		
20	1.241		
10	1.192		
10	1.165		
15	1.102		
20	1.093		
15	1.066		
15	1.047		

Plus ca. 16 more lines (mostly broad bands) to 0.787 Å

Powder data for mosesite are presented in Table 2. The pattern is similar to that of Switzer, et al. (1953), except that the d-values and intensities of the reflections are in better agreement with those of $Hg_2NOH•2H_2O$ than are the data of Switzer, et al. This is especially true of the line at 5.512 Å, whose intensity is much greater than reported by those authors. The indexed reflections in Table 2 do obey the presence rule for a face-centered 9.54 Å cell. Powder diffractometer scans, however, show a small peak at 12.87 Å, which can only be indexed as 210 ($d_{calc}=12.80$ Å) of the 28.62 Å supercell. This is in accord with the single crystal results and also seems to require a primitive lattice for mosesite. It is possible that the 9.54 Å subcell is face-centered,

while the supercell is primitive. The substructure corresponds to the structure of Millon's base and the superstructure is perhaps connected with ordering of the several kinds of large interstitial anions in mosesite. The symmetry and lattice type of the supercell is the subject of continuing single crystal studies.

Kleinite

A fourth yellow mercury mineral occurring at Terlingua was mentioned by Moses (1903), but it remained for Sachs (1905) to name it kleinite. Hillebrand and Schaller (1909) found it to be another mercury ammonium compound with chloride and sulfate, but despite many chemical analyses they could not derive a satisfactory formula. They also described in detail the highly anomalous optical properties of kleinite. Although the mineral is morphologically hexagonal, basal sections are strongly birefringent. Above about 130°C, however, kleinite becomes uniaxial and, as in the case of mosesite, this was ascribed to polymorphism. They also noted that birefringent basal sections would not extinguish under crossed polars. This was explained by assuming each crystal to be composed of a group of parallel biaxial plates stacked along *c*. During further heating experiments, Canfield, et al. (1910) made the interesting observation that kleinite becomes isotropic above 186°C.

In an x-ray investigation Heritsch (1949) found that all kleinite crystals are composed of several individuals and that heating above the supposed inversion temperature does not change this. His crystals were all hexagonal, probably $P6_3/mmc$, with $a=13.56$ and $c=11.13$ Å. There is also a subperiodicity of $a/2=6.78$ Å. A crystal structure was deduced using rotating crystal data. In a later paper Heritsch (1954) noted that mosesite had been shown to be isostructural with Millon's base, which is in turn a high cristobalite derivative. By analogy, he proposed that kleinite is a high tridymite derivative with the formula $(Hg_2N)(Cl,SO_4)\cdot xH_2O$ where $x\sim 1/4$. As with mosesite the structural channels contain the large anions and water molecules.

Nijssen and Lipscomb (1954) came to the same conclusion on the basis of the close relationship between kleinite and Hg_2NBr. They determined the structure of the latter to be a derivative of high tridymite. Hg_2NBr is hexagonal, $P6_3/mmc$, with $a=6.65$ and $c=11.26$ Å, which corresponds to the kleinite subcell. In a later paper, however, Lipscomb (1957) reported evidence that the *a* parameter of kleinite given by Heritsch should be tripled. He further suggested on the basis of some intensity calculations that the channels in the kleinite structure contain mercury atoms as well as anions.

In the present study, the interpretation of the diffraction photographs was greatly hindered by the fact that every crystal examined was multiple. In some cases, however, the volume of one individual was considerably greater than those of the others. It was therefore possible to separate its reciprocal lattice pattern from those of the others and study its symmetry and cell parameters. This approach is not infallible, but its results are supported by the powder data, which are not subject to the uncertainties introduced by the multiplicity of the single crystals.

Rotation photographs around the c-axis are consistent with Hillebrand and Schaller's model of a stacking of parallel plates along *c*. Adjacent individuals, however, seem to be slightly tilted with respect to one another by $\sim 1.5°$ in those crystals examined.

As suggested by Lipscomb (1957), kleinite is hexagonal with *a* three times the value given by Heritsch. The refined cell parameters are $a=40.599\pm 0.005$ and $c=11.155\pm 0.003$ Å. There are two subcells. One, defined by the total pattern of medium plus strong reflections, has $A=a/6=6.77$ and $C=c=11.16$ Å. The other, defined by the strong reflections alone, has $A'=a/12=3.39$ and $C'=c/2=5.58$ Å. An independent check on these parameters is provided by the powder pattern (Table 3). It contains four low-angle reflections (220, 222, 811, and 702), which cannot be indexed on Heritsch's cell but which can be indexed quite satisfactorily on the 40.60 Å cell.

The space group of the supercell could not be determined since the superstructure reflections on the Weissenberg photographs are too few and scattered. However, the 6.77 Å subcell does have symmetry $P6_3mc$, $P\bar{6}2c$, or $P6_3/mmc$. This subcell is the analog of the Hg_2NBr cell.

Using the average chemical analysis of Hillebrand and Schaller (1909), the supercell contents are

$$Hg_{330.47}N_{141.41}Cl_{158.95}S_{24.96}O_{143.91}H_{88.14}.$$

TABLE 3.—*Powder pattern of kleinite*

I	d_{obs}	d_{calc}	hkl
10	10.19	10.15	220
15	5.871	5.860	600
15	5.577	5.577	002
25	5.188	5.188	601
5	4.890	4.888	222
20	4.040	4.040	602
<1	3.850	3.861	811
		3.836	820
1	3.731	3.732	702
10	3.382	3.383	660
5	3.132	3.140	603
		3.127	433
100	2.931	2.930	12 • 0 • 0
70[b]	2.888	2.893	662
		2.890	860
		2.883	752
15	2.831	2.834	12 • 0 • 1
90	2.788	2.789	004
3	2.688	2.693	903
		2.689	224, 960
100	2.592	2.594	12 • 0 • 2
		2.592	504
5	2.518	2.518	604
		2.513	10 • 4 • 2
<1	2.446		
5[vb]	2.306		
10	2.215		
10	2.171		
1	2.084		
10	2.057		
20[vb]	2.019		
3	1.900		
15	1.843		
3	1.772		
3	1.736		
30	1.690		

Plus ca. 40 more lines (mostly broad bands) to 0.781 Å

[b] broad, [vb] very broad

On the basis of the available data it is difficult to derive a satisfactory formula from this. A formula for the 6.77 Å subcell, however, may be derived by analogy to that of Hg_2NBr. The subcell contents are

$$Hg_{9.18}N_{3.93}Cl_{4.42}S_{0.69}O_{4.00}H_{2.45}$$

or very nearly $Hg_9N_4(Cl,SO_4)_5 \cdot H_2O$. This can be rewritten as $4Hg_2NCl \cdot Hg(Cl,SO_4) \cdot H_2O$. Presumably, the $4Hg_2NCl$ represents that part of the substructure analogous to Hg_2NBr (for which $Z=4$), while the remainder represents the contents of the structural channels.

The true symmetry and formula of the superstructure can only be settled by a complete structure determination combined with a new chemical analysis. The former objective, however, may not be attainable due both to the lack of single crystals and the experimental difficulties inherent in treating highly absorbing compounds with very large supercells. The outlook for mosesite is more hopeful, however, and further work is anticipated on this mineral.

Literature Cited

Aurivillius, K., and L. Folkmarson

1968. The Crystal Structure of Terlinguaite $Hg_4O_2Cl_2$. *Acta Chemica Scandinavica,* 22:2529–2540.

Bird, P. H.

1932. A New Occurrence and X-Ray Study of Mosesite. *American Mineralogist,* 17:541–550.

Canfield, F. A., W. F. Hillebrand, and W. T. Schaller

1910. Mosesite, a New Mercury Mineral from Terlingua, Texas. *American Journal of Science,* 4th series, 30:202–208.

Grdenić, D.

1965. The Structural Chemistry of Mercury. *Quarterly Reviews* (London), 19:303–328.

Hedlik, A.

1948. Über die Formel und Struktur von Eglestonit. *Experientia,* 4:66.

1950. Über Formel und Struktur des Mercurooxychlorides Eglestonit. *Tschermaks Mineralogische und Petrographische Mitteilungen, Dritte Folge,* 1:378–389.

Heritsch, H.

1949. Röntgenuntersuchungen an Kleinit. *Tschermaks Mineralogische und Petrographische Mitteilungen, Dritte Folge,* 1:300–312.

1954. Bemerkungen zur Kristallchemischen Konstitution des Kleinites. *Anzeiger der Österreichischen Akademie der Wissenschaften, Mathematisch-Wissenschaftliche Klasse,* 1:1–4.

Hillebrand, W. F., and W. T. Schaller

1909. The Mercury Minerals from Terlingua, Texas. *United States Geological Survey Bulletin,* 405.

Lipscomb, W. N.

1951. The Structure of Millon's Base and Its Salts. *Acta Crystallographica,* 4:156–158.

1957. Recent Studies in the Structural Inorganic Chemistry of Mercury. *Annals of the New York Academy of Sciences,* 65:427–435.

Moses, A. J.

1903. Eglestonite, Terlinguaite and Montroydite, New Mercury Minerals from Terlingua, Texas. *American Journal of Science,* 4th series, 16:253–263.

Nijssen, L., and W. N. Lipscomb
1954. A Hexagonal Modification of a Salt of Millon's Base. *Acta Crystallographica,* 7:103–106.
Palache, C., H. Berman, and C. Frondel
1951. *Dana's System of Mineralogy.* Volume 2, 7th edition. New York: John Wiley and Sons.
Sachs, A.
1905. Der Kleinit, ein Hexagonales Quecksilberoxydchlorid von Terlingua in Texas. *Sitzungberichte der Königlichen Preussischen Akademie der Wissenschaften* (Berlin), 1091–1094.
Switzer, G., W. F. Foshag, K. J. Murata, and J. J. Fahey
1953. Re-examination of Mosesite. *American Mineralogist,* 38:1225–1234.

Dashkesanite: High-Chlorine Amphibole from St. Paul's Rocks, Equatorial Atlantic, and Transcaucasia, U.S.S.R.

Sara S. Jacobson

ABSTRACT

New data are given for dashkesanite, a high-chlorine amphibole, from two localities, Transcaucasia, U.S.S.R., and St. Paul's Rocks, Equatorial Atlantic. Four new analyses (by electron microprobe) of the mineral from Transcaucasia gave a chlorine content ranging from 4.15 to 5.34 percent. The original analysis by Krutov (1936) by wet chemical methods reported Cl=7.24 percent. Five analyses (by microprobe) of dashkesanite from St. Paul's Rocks gave Cl ranging from 6.03 to 6.51 percent. The mineral from both localities is low in SiO_2 and MgO and high in FeO, Cl, and K_2O compared to other hornblende compositions. It is hastingsitic using the classification of Ernst (1968).

Introduction

High-chlorine amphibole was first described by Krutov (1936). He found the mineral in skarn rocks surrounding sheetlike magnetite ore bodies at Dashkesan, Transcaucasia, U.S.S.R. These skarn rocks occur about 1200 meters from the ore body and extend for over 200 meters with an average thickness of 0.60–0.75 meters. The surrounding country rock is described as porphyrites and tuffs with dikes of gabbro porphyrite occuring near the skarn. Krutov (1936) named the mineral "dashkesanite" for the locality.

The mineral was also found by Melson, et al. (1972) in brown hornblende mylonites from St. Paul's Rocks, an ultrabasic intrusion exposed in a series of islets in the equatorial Atlantic. Brown hornblende mylonites are the second most abundant of three rock types found on the islets; peridotite mylonites are the most abundant rock type and clinopyroxene mylonites are the least abundant. All samples examined were collected in 1966 during Cruise 20 of the R. V. *Atlantis II*. Samples from both of these areas were investigated in the present study.

ACKNOWLEDGMENTS.—I wish to thank W. G. Melson for suggesting the project and his help throughout.

Sara S. Jacobson, Department of Geology, University of California, Los Angeles, Los Angeles, California 90024.

Petrography

The specimen from Transcaucasia available for study (USNM 120180) consists of fine- to medium-grained, subhedral to anhedral crystals of dashkesanite; minor chlorite and epidote and a fine-grained material that may be scapolite are also found in the specimen. This specimen of dashkesanite is dark green. In thin section, it shows a strong yellow to blue-green pleochroism. Cleavage is not well developed; rather a basal parting appears to dominate. The mineral has inclined extinction and positive elongation.

Dashkesanite from St. Paul's Rocks was studied in two sections of brown hornblende mylonite, (USNM 110393–13 and 110393–31). Both are from the Southeast Islet. (See Melson, et al., 1972, for map of localities.) The primary assemblage is kaersutitic hornblende, plagioclase, and Fe-Ti oxides. These occur with accessory amounts of dashkesanite, allanite, zircon, scapolite and titanbiotite.

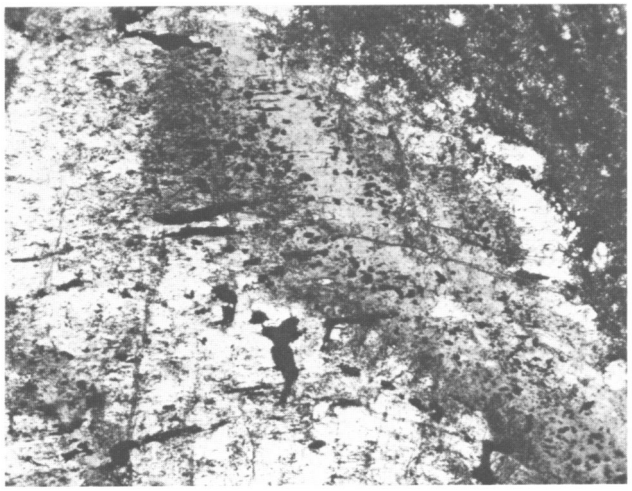

FIGURE 1.—Portion of a hornblende augen in section USNM 110393-13. The diagonal grayish area in the central part of the photo is dashkesanite. Width of field is 1.6 mm × 1.3 mm.

The hornblende forms large rounded augen. Dashkesanite occurs in veins in the augen and as overgrowths on the hornblende augen. It is also found in veins in the fine-grained matrix. It does not occur disseminated in the matrix (Figure 1).

The optical properties of the St. Paul's Rocks dashkesanite are similar to those described for the mineral from the type locality. The dashkesanite forms fine to coarse, anhedral to subhedral masses; good crystal forms are rare. The mineral again shows the distinctive, strong yellow-green to blue-green pleochroism. The dashkesanite is not sheared nor mylonitized.

Analytical Procedure

Analyses of the above samples were done on an ARL EMX electron microprobe using a 15kV acceleration potential, 0.15 μA sample current and a

TABLE 1.—*Amphibole analyses*

Constituent	*1*	*2*	*3*	*4*	*5*	*6*	*7*	*8*	*9*	*10*
SiO_2	36.13	33.90	35.31	33.24	34.92	36.66	35.06	35.76	36.44	36.00
TiO_2	0.30	1.01	0.75	1.14	0.54	0.41	0.80	0.70	0.44	0.59
Al_2O_3	10.22	11.57	11.81	12.21	11.99	11.43	12.27	12.55	11.60	11.85
Fe_2O_3	7.60	–	–	–	–	–	–	–	–	–
FeO	19.99	31.91[a]	30.21[a]	31.76[a]	30.57[a]	26.99[a]	26.71[a]	26.32[a]	27.03[a]	27.99[a]
MgO	3.63	1.81	2.27	1.70	2.27	4.85	4.05	4.87	4.42	3.51
CaO	10.83	11.16	11.34	11.13	11.34	11.69	11.78	11.35	11.35	11.42
Na_2O	1.24	0.74	0.89	0.75	0.80	1.82	1.75	1.77	1.86	1.79
K_2O	2.84	3.34	2.92	3.46	3.47	1.76	1.96	1.76	1.66	1.71
Cl	7.24	4.95	4.15	5.34	5.06	6.10	6.51	6.03	6.20	6.10
H_2O	1.05	–	–	–	–	–	–	–	–	–
	101.93	100.44	99.75	100.73	100.95	101.71	101.39	101.11	101.00	100.96
O=Cl	1.63	1.12	0.94	1.20	1.14	1.38	1.47	1.36	1.40	1.38
Total	100.30	99.32	98.81	99.53	99.81	100.33	99.92	99.75	99.60	99.58
	NUMBER OF IONS ON THE BASIS OF 24 (O, Cl, OH)									
Si	5.934 } 7.91	5.89 } 8.00	6.06 } 8.00	5.77 } 8.00	5.98 } 8.00	6.09 } 8.00	5.91 } 8.00	5.95 } 8.00	6.08 } 8.00	6.05 } 8.00
Al	1.978	2.11	1.94	2.23	2.02	1.91	2.09	2.05	1.92	1.95
Al	–	0.26	0.40	0.27	0.40	0.33	0.35	0.41	0.55	0.40
Ti	0.035	0.13	0.10	0.15	0.07	0.05	0.10	0.09	0.06	0.07
Fe^{+3}	0.940 } 4.67[b]	– } 5.50	– } 5.42	– } 5.47	– } 5.43	– } 5.33	– } 5.23	– } 5.37	– } 5.25	– } 5.29
Mg	0.888	0.47	0.58	0.44	0.58	1.20	1.02	1.21	0.87	0.88
Fe^{+2}	2.747	4.64	4.34	4.61	4.38	3.75	3.76	3.66	3.77	3.94
Na	0.394	0.25	0.33	0.25	0.27	0.59	0.57	0.57	0.60	0.58
Ca	1.906 } 2.90	2.08 } 3.07	2.09 } 3.06	2.07 } 3.09	2.08 } 3.11	2.08 } 3.04	2.13 } 3.12	2.02 } 2.96	2.03 } 2.98	2.06 } 3.01
K	0.596	0.74	0.64	0.77	0.76	0.37	0.42	0.37	0.35	0.37
OH	1.154 } 3.17	–	–	–	–	–	–	–	–	–
Cl	2.016	1.46	1.21	1.57	1.47	1.72	1.86	1.70	1.75	1.74

[a] All Fe calculated as FeO.
[b] Includes Mn 0.06.

Column 1: Krutov's (1936) analysis (includes P_2O_5 0.10, SO_3 0.11, MnO 0.43)

Columns 2–5: Dashkesanite from Transcaucasia. Analyzed on electron microprobe.

Columns 6–10: Dashkesanite from the St. Paul's Rocks. All analyses done on section USNM–110393–31. Analyzed on electron microprobe.

10μm-15μm beam size. The analyses were corrected using the Bence and Albee (1968) correction procedures, and the summations corrected for chlorine equivalents of oxygen. The results are given in Table 1. The ionic proportions were calculated on the basis of 24 anions with H_2O not determined and all Fe assumed to be ferrous. The choice of 24 anions rather than 23 was made because Cl^- rather than OH^- appears to nearly completely fill the A site. Since the occupancy of this site is known and need not be assumed, a normalization on the basis of 24 anions is a justified approximation. The actual number of anions is probably between 23 and 24.

Chemistry

Dashkesanite from the two localities has similar chemistry in some respects. Both are low in SiO_2 and MgO and high in FeO, Cl, and K_2O compared to other hornblende compositions (Leake, 1968; Deer, et al., 1963a:290), while CaO, TiO_2, and Al_2O_3 are consistent with other hornblendes. These hornblendes are hastingsitic, using the classification of Ernst (1968).

There are also chemical differences between the two occurrences. The dashkesanite from the St. Paul's Rocks is higher in SiO_2, Cl, Na_2O, MgO and lower in total Fe and K_2O than the dashkesanite from Transcaucasia. There are also differences between Krutov's original analyses and those done for the present paper. The new analyses show less Cl, SiO_2, and Na_2O, and higher Al_2O_3. These differences may be due to the differences in analytical technique.

The cation sums (Table 1) are high, generally summing over 16. This is probably because for the microprobe analyses all iron is assumed to be ferrous. Krutov's analysis shows a considerable amount of ferric iron, and indicates that from 13 to 14 percent of the ferrous iron reported in the probe analyses may be ferric.

Particularly, the totals for the Y site (Fe + Ti + Mg + octahedral Al) are high, being between 5.23 and 5.50. Leake (1968:249) postulates that good analyses would have sums between 4.75 and 5.25 for this site. Recalculating the ionic proportions assuming all iron as ferric iron reduces the sum for this site by approximately 0.70 and reduces the cation total by approximately 1. Depending on the amount of ferric iron present, all the cation proportions are probably less than those reported for the present analyses in which all iron is assumed as ferrous iron.

Discussion

Dashkesanite from the two localities is close in optical characteristics and chemical composition in spite of the differences in the environments in which they are found. In St. Paul's Rocks dashkesanite is a late stage mineral, as shown by the absence of shearing or mylonitization. Melson, et al. (1972:241) include dashkesanite in the neomineral group. These minerals occur as undeformed grains indicating formation by recrystallization and precipitation continuously during or after mylonitization. Melson, et al. (1972:241) speculate the high-chlorine minerals found (dashkesanite, scapolite and chlorapatite) formed either by reaction of primary minerals with a chlorine-rich pore fluid or by direct crystallization from such a pore fluid.

It is possible that the chlorine was derived from sea water during weathering of the brown hornblende mylonites. The dashkesanite does occur with scapolite, however, which is most characteristically formed in upper amphibolite facies rocks (Deer, et al., 1963b:330); this would indicate moderate to high temperatures.

The formation of the dashkesanite may be related to the formation of the brown hornblende mylonites. Of the three rock types present, the brown hornblende mylonites have the largest amount of chlorine in their bulk composition (1.22–1.86% compared with 0.67% in the clinopyroxene-plagioclase mylonite and 0.05–0.20% in the peridotite mylonites [Melson, et al., 1972]). The higher amount of chlorine may account for the observable presence of the dashkesanite and other high chlorine phases in the brown hornblende mylonites. High chlorine content appears to be a characteristic of the strongly undersaturated alkalic rock clan to which the brown hornblende mylonites are chemically related (Melson, pers. comm.).

The dashkesanite in the Trancaucasian rocks formed by contact metamorphism. Krutov (1936) feels that the dashkesanite was formed by reaction of the fluids from the magma, containing large amounts of FeO and Cl, with the surrounding

country rocks described as porphyrites and tuffs. He projects conditions of low temperature and high fluid pressure. Krutov (1936) thinks the source of the fluids are the basic differentiates of the intrusion, which have a high chlorine content. These basic differentiates occur as dikes of gabbro porphyrite near the amphibole skarn.

The differences in chemistry between the two localities of dashkesanite as noted in the preceding section can be accounted for by the differences in environments. There are, however, strong similarities between the two environments. Both occurrences are in silica-undersaturated environments and this would account for the low SiO_2 content of dashkesanite. Although the specific conditions of formation are not known, both occurrences of the mineral appear to be related to the late stage fluids derived from basic and ultrabasic intrusions. Dashkesanite may be present but may not have been recognized in other rocks of similar composition as the Transcaucaian rocks and St. Paul's Rocks. Further observance of this mineral in other silica-undersaturated rocks could add to our knowledge of the geochemistry of chlorine, the concentration of chlorine in such rocks, and the late stage fluids associated with these rocks.

Dashkesanite may also prove interesting crystallographically because the chlorine ion is the largest (1.81 Å) of the ions commonly reported in the A site in amphiboles (OH^-, 0.91–0.105 Å and F^-, 1.33 Å [Bloss, 1971]).

Literature Cited

Bence, A. E., and A. L. Albee

1968. Empirical Correction Factors for the Electron Microanalysis of Silicates and Oxides. *Journal of Geology,* 76:382–403.

Bloss, F. Donald

1971. *Crystallography and Crystal Chemistry.* 545 pages. New York: Holt, Rinehart and Winston, Inc.

Deer, W. A., R. A. Howie, and J. Zussman

1963a. Chain Silicates. Volume 2 of *Rock-Forming Minerals.* 379 pages. New York: John Wiley and Sons.

1963b. Framework Silicates. Volume 4 of *Rock-Forming Minerals.* 435 pages. New York: John Wiley and Sons.

Ernst, W. G.

1968. *Amphiboles.* 125 pages. New York: Springer-Verlag New York, Inc.

Krutov, G. A.

1936. Dashkessanite: A New Chlorine Amphibole of the Hastingsite Group. *Bulletin de l'Academie des Sciences de l'URSS, Classe des Sciences Mathematiques et Naturelles, Serie Geologique,* 341–373. [See also *Mineralogical Abstracts,* 6(1937): 438.]

Leake, B. E.

1968. A Catalog of Analyzed Calciferous and Subcalciferous Amphiboles Together with their Nomenclature and Associated Minerals. *Geological Society of America Special Paper,* 98.

Melson, W. G., S. R. Hart, and G. Thompson

1972. St. Paul's Rocks, Equatorial Atlantic: Petrogenesis, Radiometric Ages and Implications on Sea Floor Spreading. *Geological Society of America Memoir,* 132:241–272.

Note on High-Alumina Basalt Dredged near the Aleutian Trench

William G. Melson

ABSTRACT

High-alumina basalt was dredged from a small seamount in the Adak Fracture Zone near and south of the Aleutian Trench. The basalt, dredged from magnetic anomaly 25 (about 63 million years old) has a composition transitional between basalt from spreading centers and basalt from seamounts. It thus may have been derived from the ancestral East Pacific Rise or from younger off-ridge volcanism. Extensive weathering effects have changed the concentrations of some elements, and obscured the primary igneous composition.

Introduction

Very little is known about the igneous rocks on the floor of the north Pacific Ocean. Samples dredged from this region were transferred to the National Museum of Natural History, Smithsonian Institution, by Dr. Barrett H. Erickson of the U.S. National Oceanographic and Atmospheric Administration. These are the only samples in the Museum's collections from this area, and their description is the subject of this report.

ACKNOWLEDGMENTS.—I am indebted to Dr. Erickson for providing the samples for study; to Mr. Paul Grim, also of the U.S. National Oceanographic and Atmospheric Administration, for helpful discussions and information on the Adak Fracture Zone; to Mr. E. Jarosewich, National Museum of Natural History, Smithsonian Institution, for performing the chemical analyses; and to Dr. S. R. Cann and his associates, University of East Anglia, England, for performing trace element analyses on the samples.

William G. Melson, Department of Mineral Sciences, National Museum of Natural History, Smithsonian Institution, Washington, D. C. 20560.

Specimen Features

Two basalt samples were received, both identical in hand specimen features and weighing 195 gm (USNM 112471) and 400 gm (USNM 112472). Both are angular, and have very thin, black, hydrous iron-manganese oxide coatings on at least one surface. Other surfaces are free of the coatings, indicating that the fragments were broken off larger boulders or outcrops by the dredge. A thin, 5 to 10 mm, reddish altered zone extends inward into the rock from the oxide-encrusted surfaces. The unencrusted surfaces are mottled by small black circular encrustations, probably composed of hydrous iron-manganese oxides, about 1 to 2 mm across, on a yellowish background of altered basalt. The less-altered appearing interior is dark brown, contains scattered large (up to 1 cm across) rounded, multicrystal aggregates of plagioclase (An_{80}), which compose about 3 volume percent of each sample. The groundmass contains abundant plagioclase microlites (average An_{60}–An_{70}), and small granules and sheaflike quench crystals of clinopyroxene. The large plagioclase crystals are altered to white clay minerals on the outer, oxide-encrusted surface. The very fine grain-size of the samples shows that they cooled near quenched surfaces, although neither fresh glass nor palagonitized glass surfaces occur. There are no obvious grain-size gradients across the samples. These features indicate that the samples are from the interior, but probably less than 20 centimeters from a cooling surface, of a

pillow lava or from the contact of a shallow intrusion.

Bottom Exposure Age

The thickness of the hydrous iron-manganese oxide coating on deep-sea rocks is proportional to the length of time of exposure on the sea-floor. The rate of deposition ranges between 1 and 10 mm per million years (Bender et al., 1966; Ku and Broecker, 1967; Somayujulu, 1967). The maximum thickness of 1 mm on these samples thus indicates a bottom exposure age of from 0.1 to 1 million years.

Sample Locality and Oceanic Basement Age

The sample was dredged from a depth of 4714 m on the south side of a small seamount which rises to 3790 m. The locality (49°30.43′ N, 177°32.88′ W) is on magnetic anomaly 25 (Grim and Erickson, 1969; Erickson and Grim, 1969), which has an age estimated at 63 million years according to the magnetic reversals time scale of Heirtzler, et al. (1968). The thin hydrous iron-manganese encrustation shows that the sample has been exposed at the sea floor for a much shorter period of time than this. The inference, then, is that it has only recently been exposed at the sea-floor by faulting or slumping off of overburden, and/or it is a geologically recent eruptive rock.

The unnamed seamount from which the samples were dredged is elongated in an east-northeast direction, and rises 1210 m over a distance of 15 km in this direction. Steepest slopes are perpendicular to this direction, and average about 10°. The bathymetry itself would indicate formation of the feature as an off-ridge submarine volcano. However, the direction of elongation is nearly paralled to the trend of the regional magnetic anomalies. This feature raises the possibility that the seamount was a bathymetrically high ridge formed originally at a spreading center. The composition of the basalt from the seamount, as will be discussed, does not indicate unambiguously which of these possibilities is true.

Composition

The Adak Fracture Zone basalt samples are high-alumina basalt with evidence of significant weathering (Table 1). The ferric to ferrous iron ratio is considerably greater than fresh oceanic basalts, and reflects submarine oxidation. The water content, on the other hand, is higher (2.43 versus 1.08) than most midocean ridge basalts (Table 1). Weathering of deep-sea basalts commonly produces potassium-rich smectite (Melson and Thompson, 1973) which significantly increases the bulk K_2O content of even slightly weathered submarine basalts. Although clay minerals are abundant in the mesostasis, the K_2O content of the sample, 0.37 percent, is barely higher than the average for fresh ocean-floor basalt (0.22, Table 1).

TABLE 1.—*Chemical composition of high-alumina basalt from the Adak Fracture Zone*

Constituent	*1*	*2*	*3*	*4*	*5*
SiO_2	46.80	49.61	0.72	49.84	48.16
Al_2O_3	17.99	16.01	0.85	14.09	18.31
Fe_2O_3	7.52	2.21	0.74	3.06	4.24
FeO	3.52	7.19	1.25	8.61	5.89
MgO	4.48	7.84	0.90	8.52	4.87
CaO	12.14	11.32	0.64	10.41	8.79
Na_2O	2.84	2.76	0.25	2.15	4.05
K_2O	0.37	0.22	0.12	0.38	1.69
H_2O+	1.66	0.63	0.22	–	–
H_2O-	0.77	0.45	0.30	–	–
TiO_2	1.67	1.43	0.29	2.52	2.91
P_2O_5	0.17	0.14	0.07	0.26	0.93
MnO	0.19	0.18	0.04	0.16	0.16
Total	100.12	–	–	–	–
Total FeO*	10.05	11.49	1.27	11.36	9.71
	TRACE ELEMENTS (ppm)				
Rb	7.2	–	–	–	–
Sr	148	123	46	–	–
Y	57	43	12	–	–
Zr	111	100	42	–	–
Nb	0.8	–	–	–	–

* All Fe recalculated as FeO.

Column 1: Using classical methods, E. Jarosewich, analyst; trace elements by X-ray fluorescence by J. R. Cann and coworkers.

Column 2: Average ocean-floor basalt (Cann, 1971), 94 analyses; Fe_2O_3, FeO, H_2O+, H_2O-, and trace element averages (Melson and Thompson, 1971).

Column 3: Standard deviations for column 2.

Column 4: Average of 181 olivine tholeiites and tholeiites from the Hawaiian Islands (MacDonald and Katsura, 1964). Recalculated on an anhydrous basis.

Column 5: Average of 10 samples of alkali basalt from submarine volcanoes and islands of the eastern Pacific Ocean (Engel, et al., 1965). Recalculated on an anhydrous basis.

TABLE 2.—*Trace element composition (ppm) of the Adak Fracture Zone high-alumina basalt compared to other regions* (all data and averages by Dr. J. R. Cann and colleagues; averages from Pearce and Cann, 1971)

Sample	*Ti*	*Rb*	*Sr*	*Y*	*Zr*	*Nb*
Adak Basalt						
USNM 112471 ...	10012	7.2	148	57	111	0.8
USNM 112472 ...	–	9.7	144	49	108	4.2
Average Ocean floor basalt	7760	–	–	27	80	–
Average Island arc andesite	4050	–	–	21	106	–
Average Hawaii basalt	15360	–	–	24	162	–

In this region of the Adak Fracture Zone old oceanic crust formed by sea-floor spreading at the northern extension of the east Pacific rise about 63 million years ago? Or, is the seamount from which it was dredged the product of much younger, off-ridge volcanism? These two modes of origin correlate with distinct differences in chemical composition. A number of elements whose concentrations commonly differ in these two settings were determined in the Adak sample. These include Ti, K, and Zr, which are characteristically higher in volcanic islands and seamounts compared to deep-sea basalts from spreading ridges.

The most striking compositional differences between the Adak Fracture Zone basalt and most ocean-floor basalts, are its high alumina content, low magnesia content, and high total iron to magnesia ratio. These features are probably not a result of weathering. The Zr and Ti contents are transitional between seamount basalt and basalt derived from spreading centers (Table 2). Chemically, it is thus not clear to which category the Adak Fracture Zone basalt belongs.

If actually derived from a spreading center about 63 million years old, its chemically and perhaps even bathymetric corresponding half would be identifiable on the opposite side of the spreading center at magnetic anomaly 25. This test of a sea-floor spreading origin for the basalt cannot be made because the eastern counterpart of the region from which the Adak basalt may have come has long since been subducted beneath North America.

Origin of High-Alumina Content

High-alumina content can be a feature of erupted liquid, or a reflection of an abundance of already present calcic plagioclase phenocrysts. In the Adak high-alumina basalt, the high-alumina content is a reflection of a high-alumina liquid composition. Although large rounded plagioclase crystals occur, they compose on the order of 3 volume percent of the samples, an amount much too small to account for the high-alumina content of the sample. The large, rounded calcic plagioclase crystals are probably cognate, and may reflect convective movements or settling of early forming plagioclase crystals from cooler to hotter portions of the pre-eruption magma chamber.

Literature Cited

Bender, M. L., T. Ku, and W. Broecker
1966. Manganese Nodules: Their Evolution. *Science,* 151: 325–328.

Cann, J. R.
1971. Major Element Variations in Ocean-Floor basalts. *Philosophical Transactions of the Royal Society of London,* A.268:495–505.

Engel, A. E. J., C. G. Engel, and R. G. Havens
1965. Chemical Characteristics of Oceanic Basalts and the Upper Mantle. *Geological Society of America Bulletin,* 76:719–734.

Ericksson, B. H., and P. J. Grim
1969. Profiles of Magnetic Anomalies South of the Aleutian Island Arc. *Geological Society of America Bulletin,* 80:1387–1389.

Grim, P. J., and B. H. Ericksson.
1969. Fracture Zones and Magnetic Anomalies South of the Aleutian Trench. *Journal of Geophysical Research,* 74:1488–1494.

Heirtzler, J. R., G. O. Dickson, E. M. Herron, W. C. Pitman III, and X. Le Pichon
1968. Marine Magnetic Anomalies, Geomagnetic Field Reversals, and Motions of the Ocean Floor and Continents. *Journal of Geophysical Research,* 73: 2119–2136.

Ku, T., and W. S. Broecker
1967. Uranium, Thorium and Protactinium in a Manganese Nodule. *Earth and Planetary Science Letters,* 2:217–320.

MacDonald, G. A., and T. Katsura
1964. Chemical Composition of Hawaiian Lavas. *Journal of Petrology,* 5:82–133.

Melson, W. G., and G. Thompson
1971. Petrology of a Transform Fault Zone and Adjacent Ridge Segments. *Philosophical Transactions of the Royal Society of London,* A.268:423–441.
1973. Glassy Abyssal Basalts, Atlantic Sea Floor near St.

Paul's Rocks: Petrography and Composition of Secondary Clay Minerals. *Geological Society of America Bulletin,* 84:703–716.

Pearce, J. A., and J. R. Cann

1971. Ophiolite Origin Investigated by Discriminant Analysis Using Ti, Zr, and Y. *Earth and Planetary Science Letters,* 12:339–349.

Somayujulu, B. L. K.

1967. Beryllium-10 in a Manganese Nodule. *Science,* 156: 1219–1220.

Composition of Three Glass Phases in an Apollo 15 Basalt Fragment

George S. Switzer

ABSTRACT

The fragment studied contains glass of three distinct types: A: colorless, high silica glass; B: brown, high-iron interstitial glass. Microprobe analyses show high-iron interstitial glass. Microprobe analyses show there has been strong partitioning of certain elements, especially of K into the high-silica glass, and P and Ti into the high-iron glasses. The high-iron glasses are thought to have been formed as immiscible liquids.

Introduction

Some silicate liquids on cooling separate into two or more liquids of markedly different compositions. This process, generation of immiscible liquids, may be an important process in the generation of certain classes of igneous rocks, such as those in the syenitic and granitic families (Roedder, 1951; Philpotts and Philpotts, 1969; Roedder and Weiblen, 1970). Immiscibility has long been known in certain experimentally studied systems (Greig, 1927; Roedder, 1951), but was first documented in natural materials in Apollo 11 basaltic rocks (Roedder and Weiblen, 1970). Here I describe one of the best examples of liquid immiscibility yet reported in lunar samples.

During a study of Apollo 15 soil sample 15272,11 an unusual basalt fragment was encountered that contains glass of three distinct types, which for convenience are designated types A, B, and C: A is a colorless, high-silica glass; B is brown, high-iron blebs immiscible in A; and C is a brown, high-iron interstitial glass.

The sample is an angular, 2.0 mm fragment composed primarily of plagioclase, orthopyroxene, glass, cristobalite, ilmenite, and clinopyroxene, in that order of abundance. The density of the fragment is $> 2.90 < 3.00$. A photomicrograph is shown in Figure 1.

Microprobe analyses and microscopic examination yielded the following data on the principal minerals. Plagioclase crystals up to 0.2×0.8 mm in size have a composition near An_{86}, with slightly more sodic (An_{83}) rims. The orthopyroxene, in crystals up to 0.5 mm, has composition $En_{75}Fs_{25}Wo_2$. A single crystal of clinopyroxene is $En_{34}Fs_{26}Wo_{40}$.

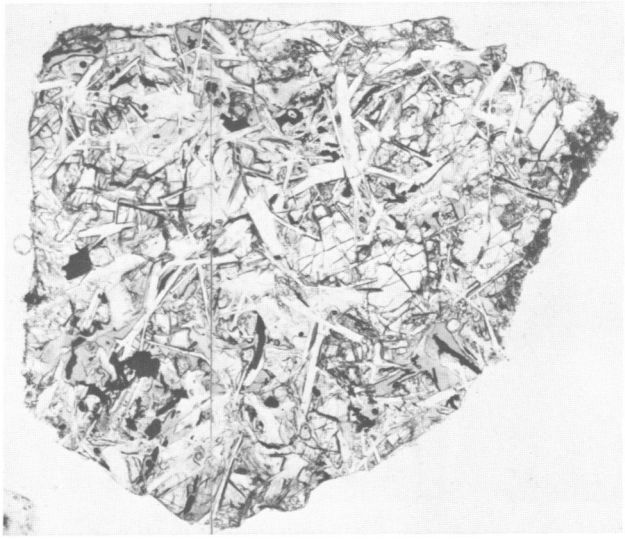

FIGURE 1.—Thin section of basalt fragment from Apollo 15 soil sample 15272,11. Maximum dimension of fragment 2.0 mm. Transmitted light.

George S. Switzer, Department of Mineral Sciences, National Museum of Natural History, Smithsonian Institution, Washington, D.C. 20560.

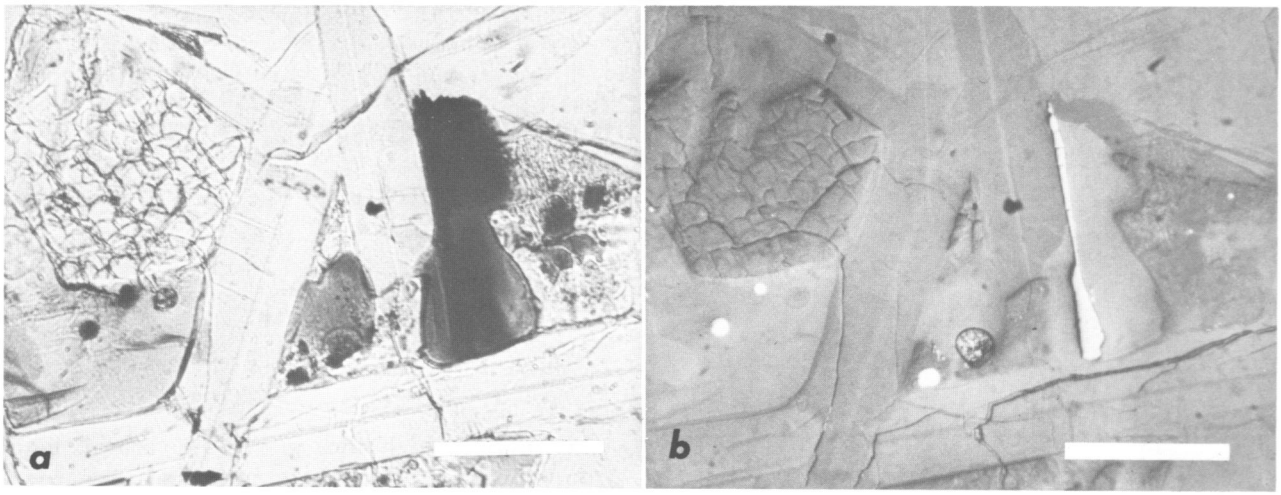

FIGURE 2.—Ilmenite crystal surrounded by interstitial Type C glass except where in contact with plagioclase. Area on left with mosaic structure is cristobalite. Note darkening of glass due to reaction with ilmenite. *a*, Transmitted light. *b*, Reflected light. Length of bar = 0.1 mm.

The cristobalite shows typical mosaic structure. Droplets of iron and possibly some sulfide are scattered throughout the specimen. The ilmenite contains 2.8 percent MgO.

Ilmenite-Glass Reaction

Ilmenite is a prominent phase (about 5 volume percent). Where ilmenite is in contact with Type C glass, the glass is frequently dark brown to opaque, with the depth of color decreasing away from the contact, as though ilmenite has reacted with the glass (Figure 2*a*, *b*). A microprobe step scan for Fe and Ti at 2μm intervals across an ilmenite-glass contact (along A–A′ of Figure 3*a*) yielded the data plotted in Figure 4. There has been some reaction between the two phases, but an apparent more extensive reaction seen in the thin

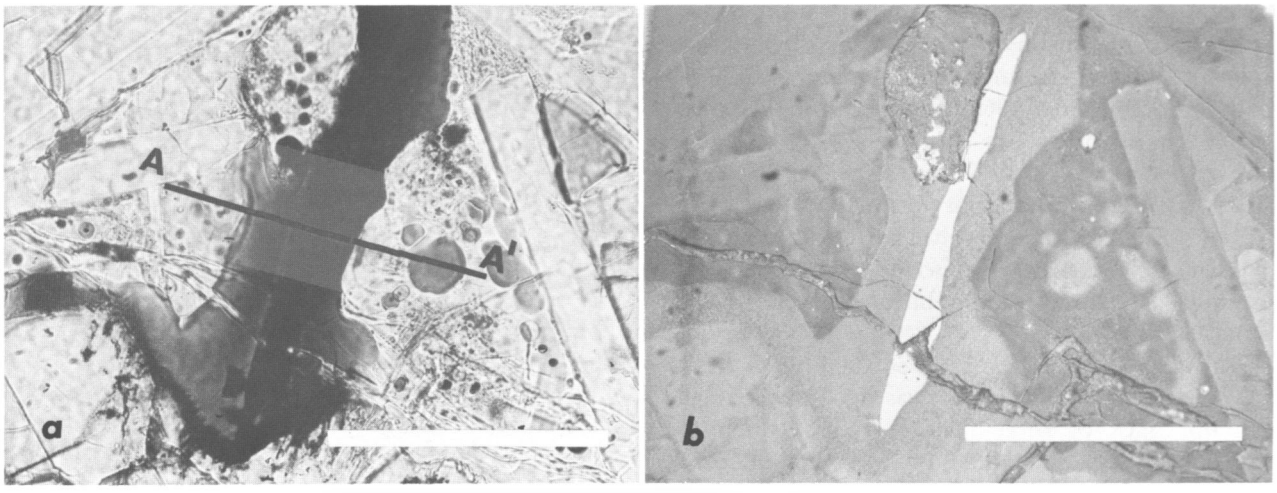

FIGURE 3.—Ilmenite crystal in contact with (to left) Type C interstitial glass, and (to right) with high-silica glass (Type A) with high-iron (Type B) immiscible blebs. A-A′ is line along which step scan analysis was made (see Figure 4). *a*, Transmitted light. *b*, Reflected light. Length of bar = 0.1 mm.

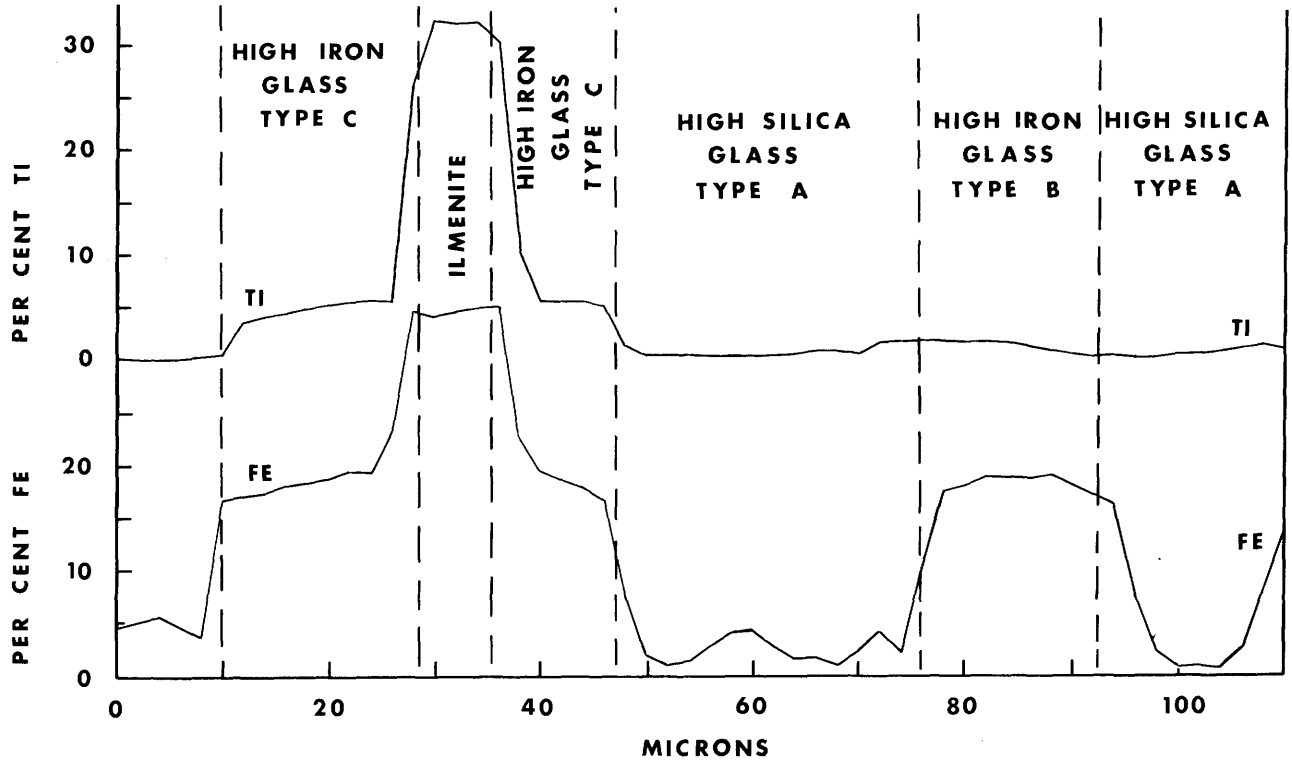

FIGURE 4.—Microprobe step scan for Fe and Ti along A-A′ of Figure 3.

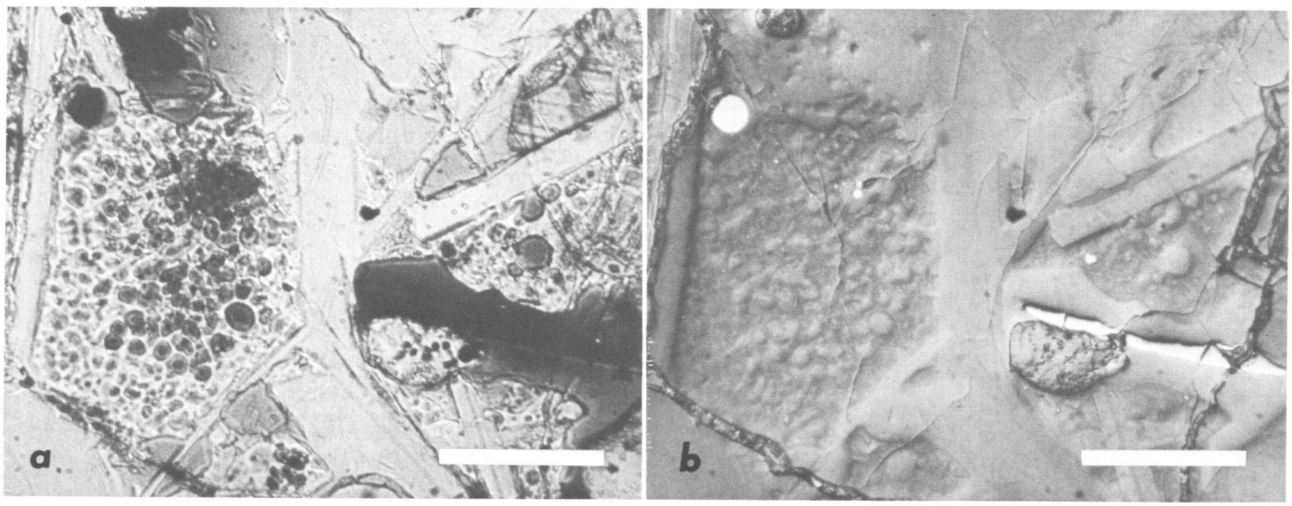

FIGURE 5.—Large area of immiscible glass (left) consisting of high-silica colorless glass (Type A) with blebs of high-iron (Type B) glass. Right half of each photograph is same area as shown in Figure 3. *a*, Transmitted light. *b*, Reflected light. Length of bar = 0.1 mm. Circular, highly-reflective area in upper left is iron.

TABLE 1.—*Composition of glass phases*

Constituent	Apollo 15			Apollo 11 and 12			
	Type A *1*	Type B *2*	Type C *3*	*4*	*5*	*6*	*7*
	ANALYSES						
SiO_2	75.7	53.1	43.4	76.3	75.8	42.2	44.1
Al_2O_3	11.9	8.3	8.0	11.5	11.4	5.4	3.0
FeO	2.7	24.8	24.6	3.0	2.5	32.9	31.2
CaO	1.5	7.1	10.3	1.6	1.8	10.7	10.9
MgO	0.3	0.5	4.7	0.07	0.25	0.79	1.9
K_2O	6.6	1.9	0.8	6.7	6.4	0.41	0.25
Na_2O	1.1	0.4	0.4	0.14	0.35	0.16	0.11
TiO_2	0.5	2.7	6.3	0.68	0.53	4.2	3.8
P_2O_5	0.0	1.1	0.8	0.15	–	0.57	1.2
MnO	0.0	0.2	0.2	0.05	–	0.32	–
BaO	0.3	0.6	0.2	0.62	–	0.0	–
Total	100.6	100.7	99.7	100.81	99.03	97.65	96.46
	NORMS						
Qtz	38.5	14.5	1.3	44.7	43.4	0.5	5.0
Or	39.0	11.2	4.7	39.6	37.8	2.4	1.5
Ab	9.3	3.4	3.4	1.1	3.0	1.4	0.9
An	7.4	15.2	17.7	7.0	8.9	12.8	7.0
Di	–	11.4	24.2	–	–	32.4	34.6
Hy	4.9	36.7	34.4	4.7	4.3	38.9	37.6
Il	1.0	5.1	12.0	1.3	1.0	8.0	7.2
Ap	–	2.6	1.9	0.4	–	1.3	2.8
C	0.2	–	–	1.5	0.6	–	–

Column 1: High-silica immiscible colorless glass.
Column 2: High-iron immiscible brown glass bleb.
Column 3: High-iron brown interstitial glass (average of 2 analyses).
Column 4: High-silica colorless glass from Apollo 12.
Average of 15 analyses (Roedder and Weiblen, 1971).
Column 5: High-silica colorless glass from Apollo 11.
Average of 35 analyses (Roedder and Weiblen, 1971).
Column 6: High-iron brown glass from Apollo 12.
Average of 5 analyses (Roedder and Weiblen, 1971).
Column 7: High-iron brown glass from Apollo 11.
Average of 7 analyses (Roedder and Weiblen, 1971).

section is due to inclined grain boundaries in a section that is approximately 40 μm thick.

The Glass Phases

Microprobe analyses of the three glasses are given in Table 1. The analyses were made using close standards and corrected by use of the ABFAN program of the Geophysical Laboratory (Boyd, et al., 1969). For comparison are given compositions of immiscible glass in Apollo 11 and 12 rocks described by Roedder and Weiblen (1971).

The areas of high-silica glass with immiscible blebs of high-iron glass (Figure 5*a*, *b*) are similar to those described in Apollo 11 and 12 rocks by Roedder and Weiblen (1970, 1971). Comparison of the high-silica glasses (Table 1, columns 1, 4, and 5) shows them to be similar, and characterized (in addition to high-silica), by low iron, calcium, and magnesium, and high potassium.

The correspondence between analyses of the brown immiscible blebs (columns 2, 6, and 7) is not

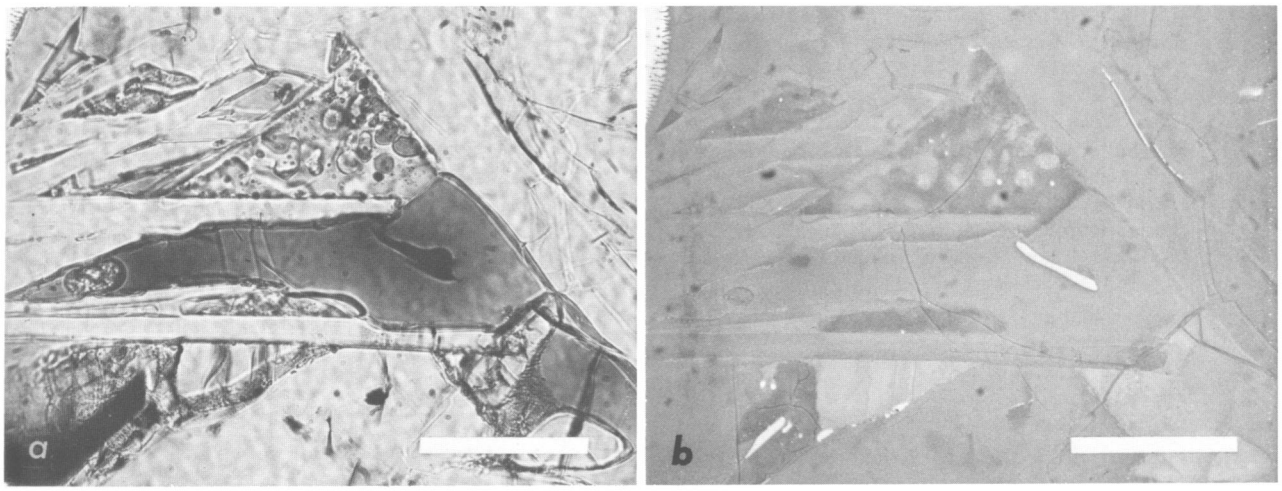

FIGURE 6.—Area of Type C high-iron glass interstitial to plagioclase and surrounding crystal of ilmenite. Triangular area above is high-silica glass (Type A) with high-iron glass blebs (Type B). *a*, Transmitted light. *b*, Reflected light.

as close. However, it should be pointed out that Roedder and Weiblen's analyses of high-iron glasses in Apollo 11 and 12 rocks are averages of seven and five analyses, repectively, with a range in SiO_2 of 36.5–50.2 percent (for Apollo 11), and 40.0–45.0 (for Apollo 12). These authors point out that the high-iron glass in their samples varied somewhat in composition between samples, between blebs, and even within blebs. The new analysis presented here for Apollo 15 is of a single 20μm diameter bleb.

An analysis of the high-iron Type C glass is given in Table 1, column 3. This glass is clear and vitreous and typically interstitial (Figure 6), and quite distinct in this latter feature from the Type B immiscible blebs. It also differs chemically from Type B, as can be seen by comparison of columns 2 and 3 of Table 1.

Discussion

Apollo 15 glass analyses in Table 1 show that there has been strong partitioning of certain elements into one or the other liquid, the same as found by Roedder and Weiblen (1970, 1971) in their studies of immiscible glasses in Apollo 11 and 12 rocks. Of particular interest is the high concentration of K in the high-silica glass and the high concentration of P in the high-iron glasses. The depletion of phosphorus in the high-silica (granitic) fraction is a reverse trend to that in normal fractional crystallization and is thought to be the result of the separation of the liquids by immiscibility (Anderson and Greenland, 1969, and Roedder and Weiblen, 1970, 1971).

Because phosphorus is enriched in both types (B and C) of high-iron glasses described here, one can conclude that both were formed as immiscible liquids. The question then is why one of the two high-iron glasses occurs as blebs in high-silica glass, and the other interstitial to the plagioclase and pyroxene. One possible explanation is that, due to a complex cooling history, initially two immiscible liquids formed, of compositions (A+B) and C. Then on further cooling (A+B) further separated into Type B blebs immiscible in Type A.

Literature Cited

Anderson, A. T., and L. P. Greenland
1969. Phosphorus Fractionation Diagram as a Quantitative Indicator of Crystallization Differentiation of Basaltic Liquids. *Geochimica and Cosmochimica Acta*, 33:493–505.

Boyd, F. R., L. W. Finger, and F. Chayes
1969. Computer Reduction of Electron-probe Data. *Carnegie Institution Year Book 67, Annual Report of the Director, Geophysical Laboratory*, pages 210–215.

Greig, J. W.
1927. Immiscibility in Silicate Melts. *American Journal of Science*, series 5, 13:1–44.

Philpotts, A. R., and J. A. Philpotts
1969. Liquid Immiscibility Between Syenitic and Gabbroic Magmas (Abstract). *Geological Society of America Abstracts 1969,* pages 176–177.

Roedder, E.
1951. Low Temperature Liquid Immiscibility in the System K_2O–FeO–Al_2O_3–SiO_2. *American Mineralogist,* 36:282–286.

Roedder, E., and P. W. Weiblen
1970. Lunar Petrology of Silicate Melt Inclusions, Apollo 11 Rocks. Pages 801–837 *of* volume 1 *in* A. A. Levinson, editor, Proceedings of the Apollo 11 Lunar Science Conference, Houston, Texas, January 5–8, 1970. *Geochimica and Cosmochimica Acta,* supplement 1, volume 34.

1971. Petrology of Silicate Melt Inclusions, Apollo 11 and Apollo 12 and Terrestrial Equivalents. Pages 507–528 *of* volume 1 *in* A. A. Levinson, editor, Proceedings of the Second Lunar Science Conference, Houston, Texas, January 11–14, 1971. *Geochimica and Cosmochimica Acta,* supplement 2.

Petrographic Analysis of Apollo 16 Samples 66083,1 and 67943,1

Brian Mason

ABSTRACT

Two samples of 2–4 mm fines collected on the Apollo 16 mission consist largely of fragments of anorthositic rock and breccias derived therefrom.

Sample 66083,1 was a 0.5 g sample of 2–4 mm fines from a clod of white impact ejecta collected at Station 6 on the southwest wall of a subdued 10 m crater on the lowest "bench" of Stone Mountain, near its base; the astrogeology report (Apollo 16, 1973) says "possibly from South Ray crater, but location generally shadowed from South Ray crater ejecta."

The sample as received contained 12 fragments $>$ 2 mm, with a total weight of 0.433 g, and an average weight of 0.036 g; there was 0.066 g of material $<$ 2 mm. The $>$ 2 mm fragments were density-fractionated in methylene iodide-acetone liquids, with the results as shown in Table 1. Polished thin sections were made of fragments B, C, D, E, F, and of one from 60083,1A (designated as 66083,1AA). Half of fragments AA and F were ground and fused with lithium tetraborate flux, and the resulting glasses analyzed with the microprobe, with the results given in Table 2. A polished thin section (66083,1H) was also prepared from the 0.2–0.4 mm material obtained by sieving from the coarser fragments; this material contained 334 individual particles, which were classified as shown in Table 3.

Brian Mason, Department of Mineral Sciences, National Museum of Natural History, Smithsonian Institution, Washington, D.C. 20560.

There appears to be a continuous sequence between breccia and crystalline rock fragments, and for some fragments the assignment to one class or the other is to some degree arbitrary.

Microprobe analyses of mineral grains gave the following results (number of grains analyzed in parentheses): plagioclase (10): An_{88-97}, mean An_{93}; olivine (4): Fa_{20-25}, mean Fa_{23}; orthopyroxene (6): Wo_{2-4}, Fs_{21-26}, mean Wo_3Fs_{25}; augite (1): $Wo_{41}Fs_{11}En_{48}$. Six glass fragments were also analyzed, with the results as shown in Table 4. Glasses 1, 2, and 3 could be melted regolith from this site; 2 and 3 are very similar to AA in Table 2, while 1 is somewhat more feldspathic. Glass 6 corresponds to a completely melted mare basalt. The interpretation of the compositions of glasses 4 and 5 is not so clear-cut, and they probably represent mixtures of different components.

The petrography of the fragments larger than 2 mm is as follows:

AA. A breccia with a glassy matrix containing about 20–30 percent of crystal fragments. The fragments are predominantly plagioclase (maximum

TABLE 1.—*Density-fractionation results for 66083,1*

Fragment	*Density*	*Number of fragments*	*Grams*
A	<2.70	7	0.208
B	2.72	1	0.030
C	2.85	1	0.042
D	2.90	1	0.029
E	3.03	1	0.025
F	3.07	1	0.099
Total		12	0.433

TABLE 2.—*Analyses and norms of two fragments from 66083,1* (analyst: J. Nelen)

Constituent	*AA*	*F*
	ANALYSES	
SiO_2	44.8	47.3
TiO_2	0.62	0.92
Al_2O_3	25.5	19.2
Cr_2O_3	0.14	0.18
FeO	5.76	9.20
MnO	0.12	0.16
MgO	6.11	9.86
CaO	14.7	11.4
Na_2O	0.52	0.59
K_2O	0.18	0.32
P_2O_5	0.1	0.3
Total	98.6	99.4
	NORMS	
An	66.4	48.8
Ab	4.4	5.0
Or	1.1	1.9
Di	4.7	4.9
Hy	13.5	31.6
Ol	6.6	3.9
Il	1.2	1.8
Ap	0.2	0.7
Cr	0.2	0.3

AA = fragment with D<2.70; F = fragment with D = 3.07.

size 0.3 mm), with minor olivine and orthopyroxene, and some lithic fragments, also mainly plagioclase. Some of the plagioclase fragments show bending of the twin lamellae. This fragment appears to be typical for the material with D <2.70; its analysis (Table 2) is very similar to that of fines

TABLE 3.—*Classification of 334 particles from 66083,1H*

Particles	*Number*	*Percent*
Crystalline rock fragments	126	37.7
Breccia fragments	125	37.4
Glass (clear and devitrified)	36	10.8
Plagioclase fragments	31	9.3
Plagioclase, partly melted	8	2.4
Spherules, glass or devitrified	7	2.1
Metal fragment	1	0.3
Total	334	100.0

TABLE 4.—*Analysis of six glass fragments from 66083,1H*

Constituent	*1*	*2*	*3*	*4*	*5*	*6*
SiO_2	44.0	46.6	44.5	47.7	50.9	45.7
TiO_2	0.54	0.60	0.88	0.53	0.69	3.88
Al_2O_3	31.2	27.8	26.8	20.9	17.5	9.89
FeO	3.58	5.32	5.99	7.08	10.9	20.4
MnO	0.03	0.03	0.03	0.03	0.10	0.15
MgO	3.39	5.87	6.49	12.0	9.45	10.0
CaO	18.0	15.8	14.3	12.0	10.2	7.94
Na_2O	0.26	0.94	0.69	0.62	0.75	0.86
K_2O	0.03	0.06	0.11	0.08	0.11	0.24
Total	101.0	103.0	99.8	100.9	100.6	99.1

from the same location (66081, H. Rose pers. comm.), indicating that it represents partially melted soil.

B. A fragment of partly devitrified glass, with some plagioclase fragments (maximum size 0.1 mm) in one area; one spherule of metal, 0.1 mm diameter, was noted.

C. A fine-grained feldspar-rich rock, made up of a felted aggregate of small plagioclase laths (up to 0.01 mm long) with about 10 percent of interstitial pyroxene and olivine; and minor amounts of opaques (probably ilmenite); occasional larger equidimensional grains of plagioclase (up to 0.1 mm) are also present. The texture suggests a recrystallized breccia, with the larger plagioclase grains being relict fragments from a coarse-grained rock.

D. A breccia consisting of clasts of plagioclase (up to 0.25 mm) and plagioclase-rich rock (up to 2 mm) in a fine-grained microcrystalline feldspathic groundmass; four metal spherules, the largest 0.35 mm in diameter, are present. Microprobe analyses give an average plagioclase composition of An_{90} (range An_{88}–An_{94}); four pyroxene grains show a range of $Wo_{4.3-11.6}$, $Fs_{17.6-22.0}$; one grain of olivine gave Fa_{29}.

E. A fragment consisting of plagioclase clasts (up to 0.3 mm) in a fine-grained groundmass of plagioclase and ferromagnesians (olivine and pigeonite) in subequal amounts, with some opaques (ilmenite and a few metal grains); the texture of the groundmass suggests that it may represent a recrystallized glass. Microprobe analyses of the individual minerals (number of grains analyzed in parentheses) gave plagioclase (9), An_{84}–An_{95}, mean

TABLE 5.—*Density-fractionation results for 67943,1*

Density	*Number of fragments*	*Grams*
<2.70	2	0.061
2.70–2.80	6	0.051
2.80–2.90	5	0.199
2.90–3.00	3	0.049

An_{90}; pigeonite (7), Wo_{8-12}, Fs_{22-24}, mean Wo_9Fs_{23}; olivine (14), Fa_{25-27}, mean Fa_{26}.

F. A crystalline rock made largely of subequal amounts of plagioclase and ferromagnesians (pyroxenes and olivine), with a minor amount of opaque material (mainly ilmenite, but with some prominent metallic spherules up to 0.4 mm in diameter). There are distinct areas of different grain size, suggesting the rock is a recrystallized breccia of lithic and mineral fragments; this is supported by the presence of occasional large (up to 0.4 mm) plagioclase grains, probably porphyroclasts.

Microprobe analyses of the individual minerals gave the following results (number of grains analysed in parentheses): plagioclase (12): An_{90-98}, mean An_{95}; olivine (18): Fa_{38-43}, mean Fa_{41}; orthopyroxene (17): Wo_{3-7}, Fs_{25-32}, mean Wo_4Fs_{28}; pigeonite (6): Wo_{10-12}, Fs_{30-31}, mean $Wo_{11}Fs_{31}$; augite (18): Wo_{34-40}, Fs_{16-20}, mean $Wo_{37}Fs_{17}$; metal (7): Ni 4.7–6.5 percent, mean 5.1 percent, and Co 0.58–0.77 percent, mean 0.67 percent.

The analysis (Table 2) shows that the fragment is of noritic composition, but the texture is hornfelsic rather than igneous, suggesting recrystallization of a norite breccia at high temperatures (perhaps high enough to produce a metal-sulfide melt, represented by the metallic spherules, but not high enough to melt the silicates). The fragment is very similar in composition and texture to 65015, a 1.8 kg rock collected at the adjacent Station 5 and ascribed by the Geology Investigation Team to South Ray crater ejecta.

Sample 67943,1 was a 0.5 g sample of 2–4 mm fines, one of the sieve fractions from 67940, a soil sample collected from the House Rock area on the southeast of North Ray crater (Station 11 of the Apollo 16 traverses).

The sample as received contained 16 fragments >2 mm, with a total weight of 0.453 g, and an average weight of 0.029 g; there was 0.047 g of material <2 mm. The >2 mm fragments were density-fractionated in methylene iodide-acetone liquids, with the results as shown in Table 5. Compared to 66083, another sample of 2–4 mm fines analyzed, this sample shows a smaller density range, and a concentration of material where D=2.70–2.90.

TABLE 6.—*Analyses and norms of three fragments from 67943* (analyst: J. Nelen)

Constituent	*D=2.70–2.80*	*D=2.70–2.80*	*D=2.80–2.90*
	ANALYSES		
SiO_2	44.9	43.4	44.6
TiO_2	0.42	0.35	0.44
Al_2O_3	29.6	29.2	27.9
FeO	3.52	3.58	4.29
MnO	0.05	0.08	0.07
MgO	3.22	3.24	5.43
CaO	16.8	16.4	15.4
Na_2O	0.68	0.60	0.67
K_2O	0.10	0.09	0.15
Total	99.3	96.9	99.0
	NORMS		
An	77.6	76.6	72.4
Ab	5.8	5.1	5.7
Or	0.6	0.6	0.9
Di	4.9	3.9	3.2
Hy	4.8	3.5	6.1
Ol	4.9	6.4	9.5
Il	0.8	0.7	0.8
An	93	93	91
Fa	35.8	36.8	29.8
Pyx	$Ca_{25}Mg_{48}Fe_{27}$	$Ca_{26}Mg_{47}Fe_{27}$	$Ca_{17}Mg_{58}Fe_{25}$

Polished thin sections were made of 11 fragments covering the full density range; for three of them sufficient material remained after sectioning for microprobe analysis after fusion with lithium tetraborate flux, and the results are given in Table 6.

Except for two fragments in the D=2.90–3.00 fraction, the individual fragments could all be classed as brecciated anorthosites; they differed one from another mainly in the amount of glass in the matrix, the lower density fragments having larger amounts of glass. This glass was usually pale brown and isotropic, sometimes showing incipient devitrification. The analyses in Table 6 confirm the anorthositic composition of these fragments; they all show over 80 percent normative plagioclase of

anorthite composition, with minor amounts of olivine and pyroxene.

Of the two non-anorthositic fragments, both with density between 2.90 and 3.00, one was an equigranular plagioclase-rich microgabbro, with individual grains averaging 0.1 mm across. The estimated mineral composition is 65 percent plagioclase (An_{94}), 15 percent olivine (Fa_{19}), 15 percent pigeonite ($Wo_{12}Fs_{23}En_{65}$), and 5 percent opaques (mostly ilmenite). The compositions given for the minerals are averages of microprobe analyses; plagioclase and olivine are very uniform in composition, whereas pigeonite shows minor variability from grain to grain.

The other non-anorthositic fragment appeared to be a composite particle, consisting of a relatively coarse (plagioclase grains up to 0.6 mm) troctolite welded to a fine-grained (maximum grain size 0.1 mm) gabbroic anorthosite. However, the mineralogy of the two parts of the fragment are identical —plagioclase (An_{94}), olivine (Fa_{21}), minor hypersthene (Fa_{19}), and a little opaques—and the fine-grained material may be comminuted and recrystallized troctolite. The boundary between the two parts is quite sharp.

These two non-anorthositic fragments may represent primary igneous rocks from the Apollo 16 site that have escaped the ubiquitous brecciation and recrystallization so characteristic of most of the rocks collected on this mission. Alternatively, they may be exotic fragments transported to the Apollo 16 site from some other region on the Moon.

ACKNOWLEDGMENT.—This research was supported by a grant from the National Aeronautics and Space Administration (NGR 09–015–146).

Literature Cited

Apollo 16 Preliminary Examination Team
1973. The Apollo 16 Lunar Samples. *Science,* 179:23–34.

The Allende Meteorite: Chondrule Composition and the Early Histroy of the Solar System

Andrew L. Graham

ABSTRACT

Fifty chondrules and aggregates from the Allende meteorite (Type III carbonaceous chondrite), have been analyzed for the major elements using a fusion technique and subsequent microprobe analysis of the resulting glass bead. A portion of each sample was retained and made into a polished thin section for mineralogical studies. The major element chemistry suggests that the Ca/Al-rich chondrules and aggregates exhibit compositional changes, whereas the Mg/Fe-rich chondrules do not. There appears to be no simple relationship between these two chondrule groups. Concomitant with a decrease in the ($CaO+Al_2O_3$) content is a decrease in TiO_2 and an increase in Na_2O. This is paralleled by changes in the mineralogy of the chondrules. Although the ($CaO+Al_2O_3$) to TiO_2 relationship is that which has been predicted in terms of a condensing solar nebular model, that of ($CaO+Al_2O_3$) with Na_2O does not conform to this model. Other evidence against the primary nature of the Ca/Al-rich Allende chondrules is cited.

Introduction

The Allende meteorite is a Type III carbonaceous chondrite of the Vigarano subgroup (Clarke, et al., 1970). It is composed of chondrules and microcrystalline aggregates distributed heterogeneously throughout a black, olivine-rich matrix. Some of the chondrules and aggregates contain minerals rarely found in meteorites. These include melilite, magnesian spinel, fassaite, wollastonite, cordierite, hibonite, and grossular (Clarke, et al., 1970; Fuchs, 1969, 1971; Marvin, et al., 1970). From a possible composition of the primitive (that is, undifferentiated), solar nebular gas (e.g., table in Cameron, 1968:127), and making assumptions as to the initial temperature of this gas, the condensation sequence with falling temperature of stable molecules can be calculated. Such calculations (Lord, 1965; Grossman, 1972) indicate that corundum, spinel, and melilite form early in this sequence. It is, therefore, tempting to suggest that the occurrence of these minerals in Type III carbonaceous chondrites is evidence supporting the thermodynamically derived condensation sequence. It is not at present known whether the Ca/Al-rich aggregates and the melilite-bearing chondrules of the Allende and similar meteorites are "bulk primary" condensates or not. Does their bulk composition represent a quasi-equilibrium state, similar to that shown by terrestrial igneous processes, in which the crystalline solids represent one side of an equilibrium solidification sequence, or are these chondrules and aggregates the result of the association of material after the condensation sequence had finished?

The structure and chemistry of the carbonaceous chondrites provide the basis for a strong argument against the metamorphism of these meteorites subsequent to their accretion. This is particularly shown by the wide variation in the Fe/Fe+Mg of the olivines they contain, and by the presence of glass within the chondrules. The bulk chemistry of the chondrules has not, therefore, been changed by metamorphism since the formation of the meteorite. In this work chondrules and aggregates separated from the Allende meteorite have been analyzed for their major elements to see whether there is a sequential relationship in their chemistry. Do they represent particular stages in the condensa-

Andrew L. Graham, Department of Mineralogy, British Museum (Natural History), London S.W. 7, England.

TABLE 1.—*The composition of some chondrules and aggregates from the Allende meteorite*

Constituent	*1*	*2*	*3*	*4*	*5*	*6*	*7*	*8*
SiO_2	43.1	50.9	40.6	32.0	41.5	26.9	35.7	30.9
TiO_2	0.2	0.4	0.2	1.4	1.1	1.3	1.2	1.0
Al_2O_3	5.7	1.2	7.0	27.3	25.8	30.0	24.8	28.1
FeO	8.9	7.6	6.6	4.8	2.2	1.0	0.9	0.3
MgO	38.6	37.9	38.7	12.4	14.8	9.8	7.1	9.8
CaO	3.8	0.9	4.5	21.5	12.7	30.9	29.8	30.3
Na_2O	0.7	0.2	0.5	0.8	1.3	0.2	0.4	0.2
K_2O	0.03	0.03	0.03	0.03	0.03	0.03	0.03	0.03
Cr_2O_3	0.5	0.8	0.7	0.2	0.4	0.05	0.02	0.01
Total	101.53	99.93	98.83	100.43	99.83	100.18	99.95	100.64

Columns 1–3: Mg/Fe-rich chondrules
Columns 4–5: Fine-grained aggregates
Columns 6–8: Coarse-grained Ca/Al-rich chondrules

tion of the nebular gas or are they random associations which have been formed for material produced by this primitive condensation? If the latter is the case then no chemical trends would be expected, while if the former is the case then a sequential chemistry may be shown.

ACKNOWLEDGMENTS.—This work was performed during the tenure of a Smithsonian Research Fellowship. Dr. B. Mason and Dr. R. F. Fudali are thanked for their assistance and also Dr. L. Walter who gave advice on the analytical procedure used. The constructive criticism and suggestions of Dr. A. A. Moss and Dr. R. F. Fudali much improved the manuscript.

Method

Chondrules and aggregates were picked from fractured faces of specimens of the Allende meteorite. The aggregates, which are friable, were removed from the bulk material with a stainless steel needle. Each sample was then crushed in an agate mortar. An aliquot of between 1 and 2 mg was mixed with 2.5 times its weight of a lithium tetraborate/lithium carbonate flux prepared according to the method of Norrish and Hutton (1969). The mixture was fused to a glass bead in a small gold crucible by maintaining it at 960° C for five minutes in a vertical quench furnace. After quenching, the bead was mounted in a lucite disc, polished and analyzed for nine elements in an A.R.L. EMX electron microprobe. United States Geological Survey standards W1, AGV1, DTS1 and the Allende bulk standard were prepared in the same way and used as standards. The homogeneity of the standards and unknowns was checked by performing multiple analyses of the standards and three separate analyses of each unknown. Reproducibility of the whole procedure was checked by making six separate beads of a standard and analyzing each as an unknown. The relative mean deviation of the analyses in this case was ± 3 percent for elements present in the undiluted material at concentrations greater than 0.5 percent by weight. Summation to 100 percent was also used as a test; any analysis that did not total 100 $\pm$ 2 percent was rejected. The values used for the composition of the USGS standards were those given by Flanagan (1969), and those of the Allende bulk standard were given in Clarke, et al. (1970).

Results

The analyses of 50 chondrules and aggregates have been used to plot Figures 1–3 and in Table 1 representative analyses are quoted for eight individual samples. The mineralogy of most of the samples was examined by preparing a thin section from a fragment of each. Analyses 1–3 of Table 1 are of Mg/Fe-rich chondrules. Analyses 4 and 5 are of fine-grained aggregates; these are too fine for microscopic identification of their constituent minerals, but x-ray powder diffractograms show the presence of clinopyroxene, melilite, and spinel.

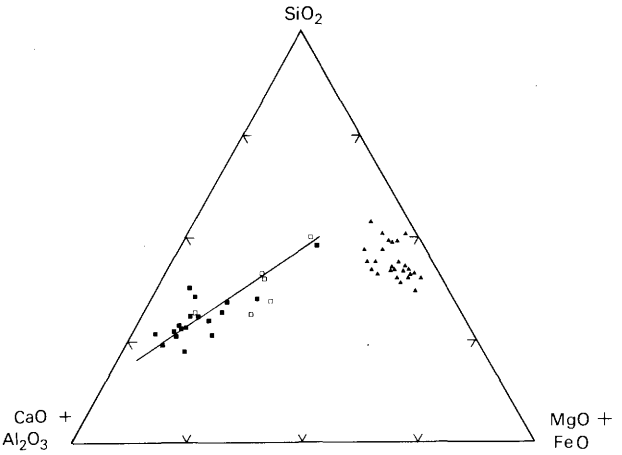

FIGURE 1.—Ternary plot of SiO_2 against $(CaO+Al_2O_3)$ and $(FeO+MgO)$, all in weight percent, for the chondrules and aggregates from the Allende meteorite. The line shown is a possible fractionation trend.

■ well crystallized Ca/Al-rich chondrules
□ finely crystalline aggregates
▲ olivine-rich chondrules

Analyses 6–8 are of coarse-grained chondrules composed of melilite and clinopyroxene with minor spinel. The composition of a melilite and some clinopyroxenes from similar chondrules are given in Clarke, et al. (1970) and in Marvin, et al. (1970).

Figure 1 is a ternary plot of $(CaO+Al_2O_3)$ against SiO_2 and $(MgO+FeO)$ for the data obtained in this work. FeO was combined with MgO as most of the analyses showed less than 5 percent FeO, except for the olivine chondrules in some of which the FeO content rises to 14 percent. From the distribution of points it can be seen that there are two chondrule/aggregate groups. One shows evidence for a development trend, that is to say its composition could be regarded as changing regularly in some manner, but the second shows no such vector properties in the diagram. The former group is made up of the Ca/Al-rich bodies and the latter of chondrules containing olivine and orthopyroxene and, occasionally, glass. The group with a trend in bulk chemistry also shows a corresponding mineralogical development. At the Ca/Al-rich end, the chondrules are composed predominantly of gehlenite with a little spinel and clinopyroxene. Progressing from this extreme towards the $(MgO+FeO)$-SiO_2 join the following trends are observed:

$$\left.\begin{matrix}\text{gehlenite}\\ \text{spinel}\\ \text{minor clinopyroxene}\end{matrix}\right\} \rightarrow \left.\begin{matrix}\text{melilite}\\ \text{clinopyroxene}\\ \text{anorthite}\end{matrix}\right\} \rightarrow \left.\begin{matrix}\text{enstatite}\\ \text{anorthite}\\ \text{olivine}\end{matrix}\right\}$$

This is accompanied by a decrease in the TiO_2 content and an increase in the Na_2O content of the chondrules. The concentration of K_2O is too low to be meaningful with the analytical method used. Figure 2 shows the distribution of TiO_2 contents. The average concentration of TiO_2 in the melilite plus clinopyroxene chondrules is 1.2 percent, and this decreases on moving from the most Ca/Al-rich compositions plotted in Figure 1 towards the SiO_2-$(FeO+MgO)$ join. The olivine chondrules show a uniform TiO_2 content of around 0.2 percent by weight. The changes in the concentration of Na_2O in the same sequence is more complex, as shown in Figure 3. The maximum Na_2O content is observed in those chondrules whose compositions plot in the middle of Figure 1; the $MgO+FeO$-rich chondrules are almost as low in Na_2O as are the gehlenite-rich bodies. Petrographic examination of the thin sections confirms the distinction between the two groups shown in Figure 1. The group richest in CaO and Al_2O_3 contains soda-free melilite and clinopyroxene with spinel and occa-

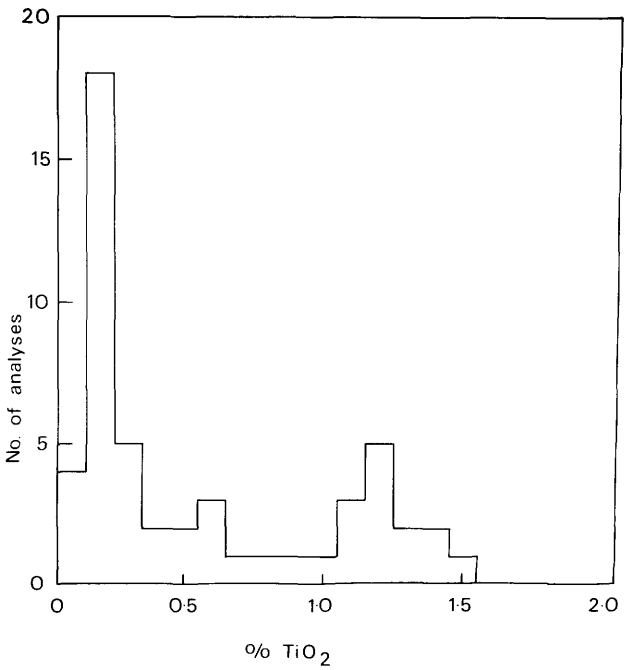

FIGURE 2.—A histogram of TiO_2 concentrations in Allende chondrules and aggregates. The peak at 1.2 percent TiO_2 occurs at the Ca/Al-rich end of the line drawn on Figure 1.

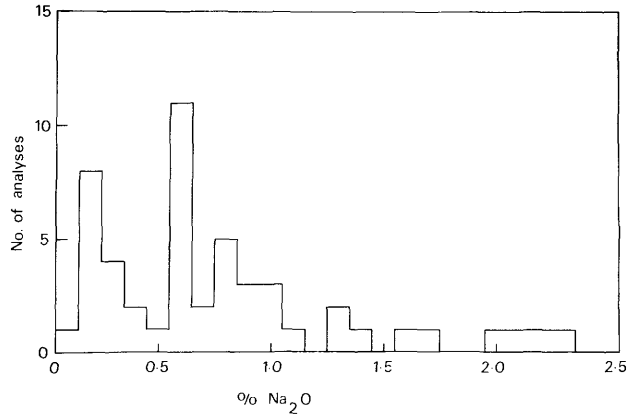

FIGURE 3.—A histogram of Na_2O concentrations in Allende chondrules and aggregates. The peak at about 0.2 percent Na_2O is due to the melilite chondrules and that at 0.6 percent Na_2O to the olivine chondrules.

sionally anorthite while the other group contains olivine and orthopyroxene with occasional glass. The coexistence of olivine and melilite was not seen nor was that of olivine and clinopyroxene. A further interesting observation, not expected from experience with terrestrial samples, is the coexistence of anorthite and melilite. Schairer and Yoder (1969) reported the coexistence of these minerals in experimental runs and commented that this had not, so far, been observed in nature.

Discussion

The distinctive petrographic and chemical differences between the Ca/Al-rich chondrules and aggregates and the Mg/Si-rich chondrules strongly suggest that there was very little brecciation and mixing of chondrule fragments prior to their incorporation in this meteorite. It is, therefore, possible to regard the bulk composition of the Ca/Al-rich chondrules and aggregates as being that of the solid phases of a fractionation sequence and so any trends in their major element chemistry can be interpreted as reflecting changes in the composition of their parent material. Changes in the pressure and temperature of the parent material, the nebular gas of the condensation hypothesis, will have very little effect upon this relationship, since dP/dT for the vapor to solid transition for melilite, enstatite, forsterite, and spinel is almost constant over a pressure range of 10^{-7} to 10^{-2} atmospheres, and has very nearly the same value for all these phases (Grossman, 1972). A further point is that fine-grained aggregates are similar in composition to the more coarsely crystalline Ca/Al-rich chondrules. It is not possible to distinguish between them in terms of those elements used to construct Figure 1. This may, in part, be due to the small number of analyses, data for only six fine-grained aggregates being currently available, but these all plot within the field defined by the analyses of the coarse-grained Ca/Al-rich chondrules. The implication is that either the conditions favoring the crystallization of material from a similar parent were not uniform during the formation of the Ca/Al-rich bodies, or that subsequent recrystallization of the first-formed microcrystalline aggregates produced the coarsely crystalline chondrules. Evidence suggesting that some recrystallization has occurred comes from the Rb/Sr systematics of the Ca/Al-rich bodies. They do not define a single isochron (Gray, et al., 1973), implying that there has been some movement of Rb and/or Sr since their formation. It has been shown, however, that the chondrule olivines show radiation damage whereas the matrix olivines do not (Green, et al., 1971). Since this damage is removed by heating to about 500° K (Green, et al., 1971), the chondrule olivines must have remained below this temperature during and after the accretion of the meteorite. Further, the presence of grossular in some of these aggregates (Clarke, et al., 1970) and of andradite (Fuchs, 1971) implies temperatures of the order of 700° K. Grossular has been synthesized at 800° C from a glass (Yoder, 1954) and at 400° C from a mixture of $3SiO_2$-Al_2O_3-$3CaCO_3$ (Christophe-Michel-Levy, 1956). Thus an upper temperature limit of about 700° K can be given for the postformation history of the Ca/Al-rich bodies of this meteorite, and of about 500° K for the Mg/Fe-rich chondrules. These temperatures are too low to cause the formation of the coarse-grained chondrules from the fine-grained aggregates by recrystallization during or after the accretion of the meteorite.

The changes in the bulk chemistry of the two chondrule types, Ca/Al-rich and Mg/Fe-rich, are such that it is not possible at present to connect them unequivocally into a single fractionation sequence with a common parent. It may be that any sequential change in the Mg/Si ratio of the olivine-rich chondrules that developed as a result of early condensation processes has been modified by sub-

sequent exchange between these chondrules and the residual material prior to the accretion of the Allende meteorite. In particular, the magnesium silicates, enstatite, and forsterite will become more iron-rich by this process, which moves their composition toward the MgO+FeO apex of Figure 1. Plotting this figure on an iron-free basis does not, however, cause the magnesium-rich chondrules to plot on an extension of the line drawn; the distinction between the two groups of chondrules remains.

The alignment of chondrule compositions in the Ca/Al-rich portion of Figure 1 suggests that their bulk compositions were fixed by a fractionation sequence similar to that derived by Grossman (1972) from theoretical considerations of the primitive nebular gas. Fuchs and Blander (1973), however, give a summary of the phenomena that they have observed in Ca/Al-rich chondrules from the Allende meteorite that suggests a liquid precursor for these chondrules, rather than their formation from a vapor by direct condensation. In particular they note the spherical nature of the chondrules and the occurrence of eutectic intergrowths of pyroxene and anorthite and also gehlenite and anorthite. Grossman and Clark (1973) maintain that the formation of any liquid took place after the main condensation sequence, from solids produced in this sequence. This is required by their theory because the calculated condensation sequence predicts the formation of some phases, for example clinopyroxene and anorthite, at temperatures that are below their solidi. The direct condensation hypothesis has difficulty in explaining the observed Mg/Si ratios of the Ca/Al-rich chondrules, which are almost constant during the decrease in ($CaO + Al_2O_3$) content (Figure 1). The direct condensation hypothesis predicts spinel as an early solid phase, subsequent condensates being more siliceous. There should then be a decrease in the Mg/Si ratio of the succeeding chondrules as condensation proceeds. This trend is not observed for the chondrule compositions plotted in Figure 1; actually there is a slight increase in this ratio.

The evidence from the Allende Ca/Al-rich chondrules suggests that, if they are "primary condensates," they have had a more complicated history than simply that of condensation and incorporation into Type III carbonaceous chondrite matrix. How far this has erased evidence of the primitive state of these condensates is not clear. The great heterogeneity of the meteorite is remarkable and it may be that further samples will provide a better means for distinguishing between phenomena that could be produced by the early condensation sequence in the solar nebula, and those that are the result of processes subsequent to this event.

Literature Cited

Cameron, A. G. W.
1968. A New Table of Abundances of the Elements in the Solar System. Pages 125–143 *in* L. H. Ahrens, editor, *Origin and Distribution of the Elements*. New York: Pergamon.

Christophe-Michel-Levy, M.
1956. Reproduction artificielle des granats caliques: grossulaire et andradite. *Société Française de Mineralogie et de Cristallographie Bulletin,* 79:124–128.

Clarke, R. S., Jr., E. Jarosewich, B. Mason, J. Nelen, M. Gomez, and J. R. Hyde
1970. The Allende, Mexico, Meteorite Shower. *Smithsonian Contributions to the Earth Sciences,* 5:1–52.

Flanagan, F. J.
1969. U. S. Geological Survey Standards-II: First Compilation of Data for the New USGS Rocks. *Geochimica et Cosmochimica Acta,* 33:81–120.

Fuchs, L. H.
1969. Occurrence of Cordierite and Aluminous Orthoenstatite in the Allende Meteorite. *American Mineralogist,* 54:1645–1653.
1971. Occurrence of Wollastonite, Rhönite and Andradite in the Allende Meteorite. *American Mineralogist,* 526:2053–2067.

Fuchs, L. H., and Blander, M.
1973. Calcium-Aluminium Rich Inclusions in the Allende Meteorite: Textural and Mineralogical Evidence for a Liquid Origin (abstract). *Transactions of the American Geophysical Union,* 54:345.

Gray, C. A., D. A. Papanastassiou, and G. J. Wasserburg
1973. The Identification of Early Condensates from the Solar Nebula. *Icarus,* 20:213–239.

Green, H. W. II, S. V. Radcliffe, and A. H. Heuer
1971. Allende Meteorite: A High Voltage Electron Petrographic Study. *Science,* 172:936–939.

Grossman, L.
1972. Condensation in the Primitive Solar Nebula. *Geochimica et Cosmochimica Acta,* 36:597–619.

Grossman, L., and S. P. Clark, Jr.,
1973. High Temperature Condensates in Chondrites and the Environment in Which They Formed. *Geochimica et Cosmochimica Acta,* 37:635–650.

Lord, H. C., III
1965. Molecular Equilibria and Condensation in a Solar Nebula and Cool Stellar Atmospheres. *Icarus,* 4: 279–288.

Marvin, U. B., J. A. Wood, and J. S. Dickey, Jr.
1970. Ca-Al-rich Phases in the Allende Meteorite. *Earth and Planetary Science Letters,* 7:346–350.

Norrish, K., and J. T. Hutton
1969. An Accurate X-ray Spectrographic Method for the Analysis of a Wide Range of Geological Samples. *Geochimica et Cosmochimica Acta,* 33:431–454.

Schairer, J. F., and H. S. Yoder, Jr.
1969. Critical Planes and Flow Sheet for a Portion of the System CaO-MgO-Al_2O_3-SiO_2 Having Petrological Significance. *Carnegie Institution Year Book,* 68: 202–214.

Yoder, H. S., Jr.
1954. Garnets and Staurolite. *Carnegie Institution Year Book,* 53:120–121.

The Pulsora Anomaly: A Case against Metamorphic Equilibration in Chondrites

Kurt Fredriksson, Ananda Dube, Eugene Jarosewich, Joseph A. Nelen, and Albert F. Noonan

ABSTRACT

Four Indian H-group chondrites, Andura, Butsura, Pulsora, and Sitathali, with almost identical chemical composition but differing in texture and structure, are described. All have essentially the same and constant ("equilibrated") olivine and pyroxene composition. Pulsora, however, contains lithic fragments, some of which are coarsely crystalline with almost no metal, while others contain skeletal olivine in silica-rich glass. Thus Pulsora could not have been "equilibrated" after the final agglomeration, nor is it necessary to postulate any such "metamorphic" equilibration to explain the texture and mineralogy of other chondrites.

Introduction

Circumstances of fall, morphology, and general classification of the four Indian H-group chondrites, Andura, Butsura, Pulsora, and Sitathali, have been reported by Murthy, et al. (1969), who also referred to some previous work by Coulson (1940). A more detailed description of Sitathali was published by Viswanathan, et al. (1971). Andura and Butsura were grouped together by Murthy, et al., while according to Coulson (using the Rose, Tschermak, Brezina classification) they were respectively Cck, crystalline spherical, and Ci, intermediate chondrites. Pulsora and Sitathali were described by Murthy, et al (1969) as brecciated chondrites with "fine" and "coarse" matrix respectively and as Cib, brecciated intermediate, and Chob, brecciated howarditic chondrites by Coulson (1940). All four belong to the H-group (high iron) as defined by Urey and Craig (1953) and Keil and Fredriksson (1964). According to the subdivision, mainly on degree of "crystallinity," proposed by Van Schmus and Wood (1967), Butsura is H6 and Sitathali H5. Andura and Pulsora have not been classified previously according to this system. However, by applying the criteria of Van Schmus and Wood, Andura is definitely within the H5–H6 range. Pulsora on the other hand shows a variety of features allowing it to be placed in any group from H3 to H6 similarly as the Hedjaz L-group chondrite (Kraut and Fredriksson, 1971).

These four meteorites were selected for detailed comparative studies from a number of meteorites currently being investigated under a joint program of the Geological Survey of India and the Smithsonian Institution, because of their essentially identical chemical composition in spite of gross morphological and textural differences as indicated by the studies referred to above as well as our data.

ACKNOWLEDGMENTS.—We are grateful to the Director General of the Geological Survey of India, Dr. M. K. Roy Chowdhury, as well as his predecessors for encouraging this cooperative work over many years. Mr. R. K. Sundaram and Drs. S. V. P. Iyengar and M. V. N. Murthy, all of the Geological Survey of India, also gave much assistance. For various data reductions we are indebted to the Smithsonian Information Systems Division and B.

Kurt Fredriksson, Eugene Jarosewich, Joseph A. Nelen, and Albert F. Noonan, Department of Mineral Sciences, National Museum of Natural History, Smithsonian Institution, Washington, D. C. 20560. Ananda Dube, Geological Survey of India, Calcutta 13, India.

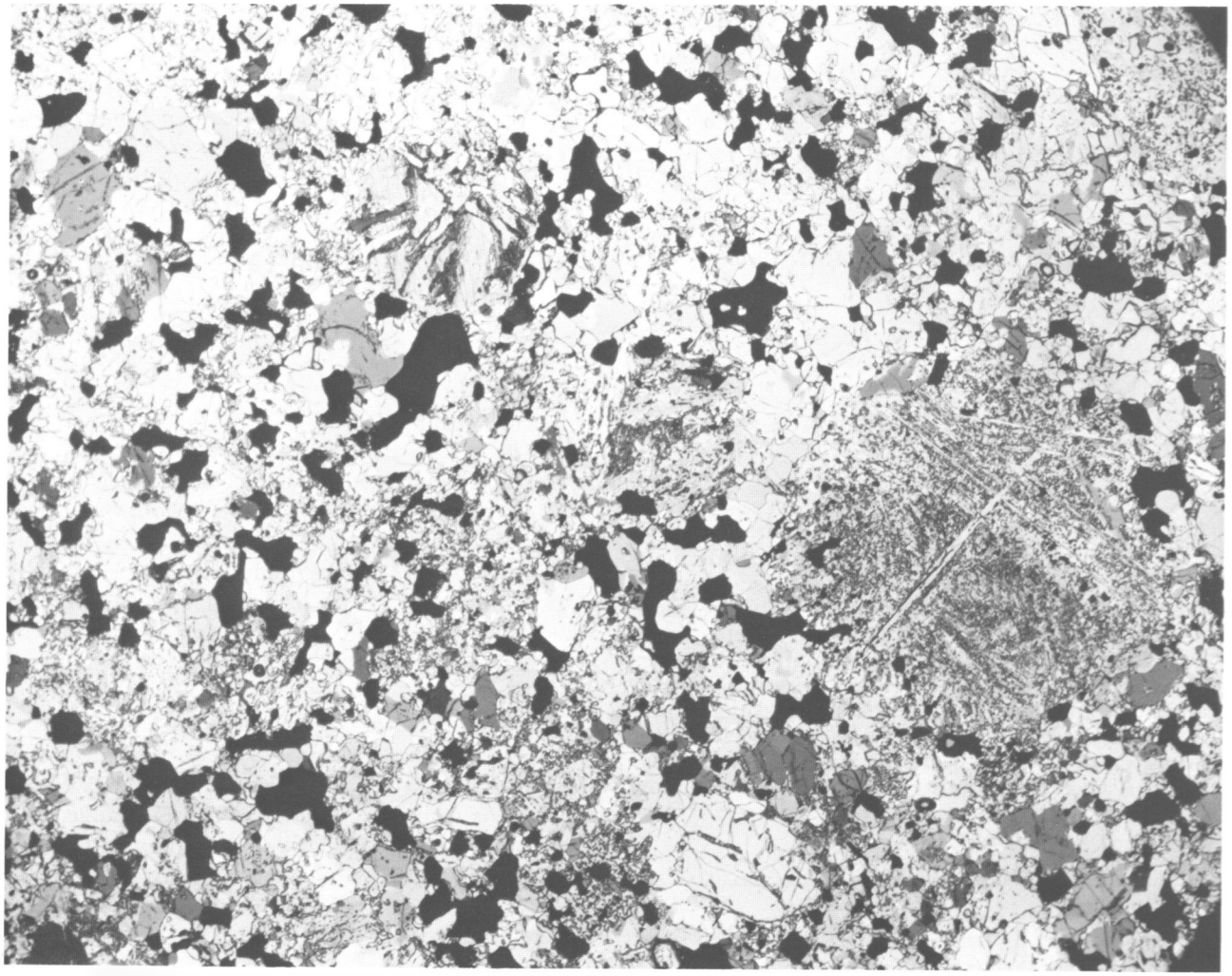

FIGURE 1.—Photomicrograph of thin section of the Andura bronzite-chrondrite (H6). Only one chondrule, right center, is discernible; its boundaries are indistinct. Part of the matrix is relatively coarse and equigranular; other parts, however, are still fine-grained. White to gray are silicates; black, metal and troilite. Length of section 5 mm. Compare with frontispiece (*a*).

J. Fredriksson. This work has been supported in part by grants from the Smithsonian Research Foundation and NASA (NGR 09–015–207).

Mineralogy and Textures

Figures 1–4 and the frontispiece show low magnification photomicrographs of thin sections of the four chondrites. The distinction between Sitathali (H5), Andura (H5–6), and Butsura (H6) with regard to grain size, degree of crystallinity and "integration" between chondrules and matrix (Van Schmus and Wood, 1967) is clearly open to rather subjective judgment. Pulsora has parts similar in texture to the other three, but Figure 5 shows a relatively coarsely crystalline fragment within Pulsora with clear crystals of plagioclase (typical of Type 6), diopside and minor whitlockite. This fragment is also nearly devoid of metal and troilite, like so-called amphoterites, or LL-group chondrites, but its olivine is typical of the H-group (also nearly the same as in the main mass of Pulsora, see Tables 1, 5, and 6) and its texture is achondritic (perhaps a "Grade 7" in the Van Schmus and Wood (1967) 1

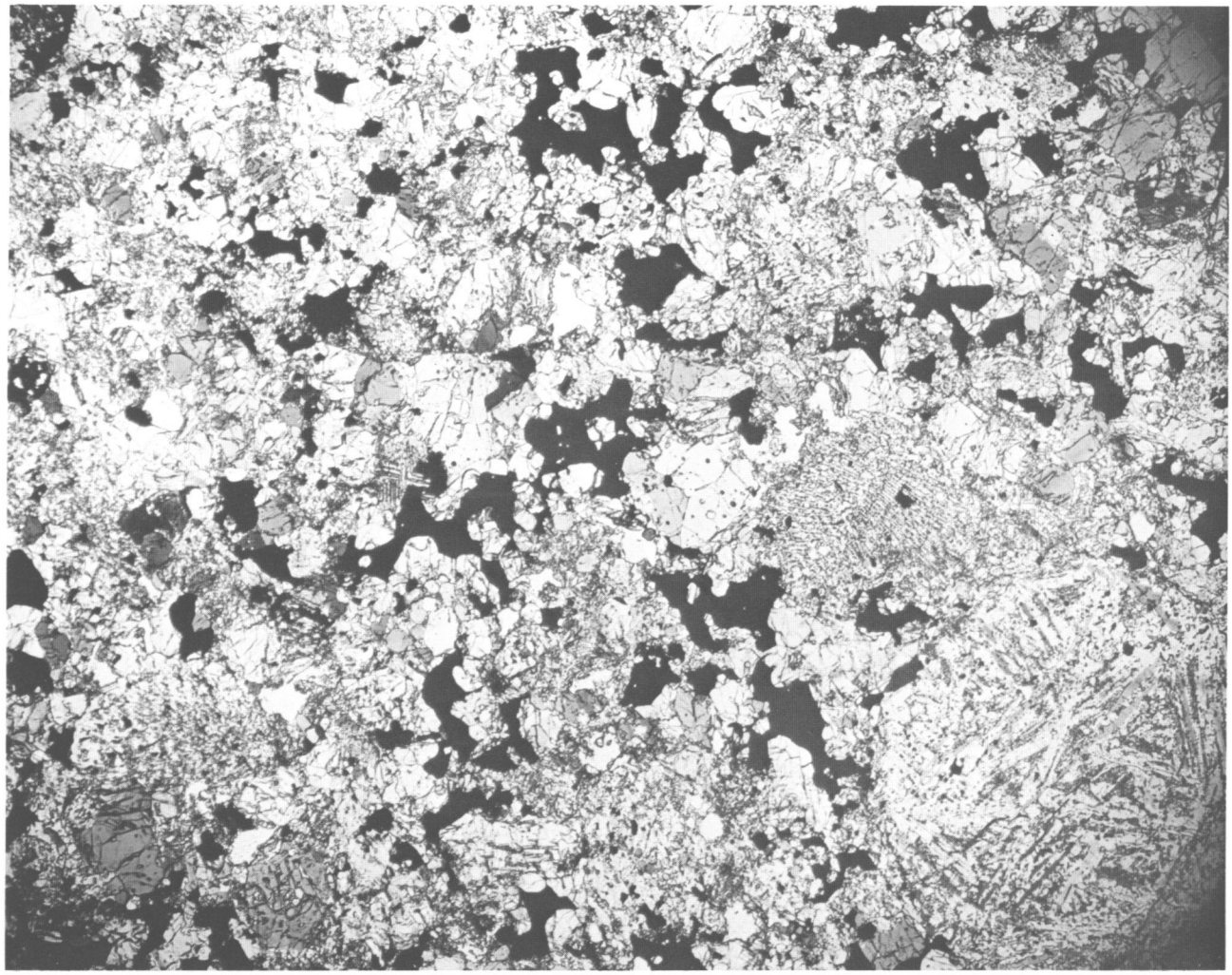

FIGURE 2.—Photomicrograph of thin section of the Butsura bronzite chondrite, classification H5 (towards H6). Chondrules are somewhat more discernible than in Figure 1, while the matrix shows some relatively fine-grained areas. Length of section 5 mm.

to 6 petrographic scale). The Pulsora section shown in Figures 6 and 7, on the other hand, includes a fragment (chondrule?) with skeletal to euhedral olivine in clear glass of the kind usually found only in Type 3 chondrites. The detailed composition and significance of these fragments are discussed further below.

Table 1 summarizes electron probe analyses of the major silicate phases, olivine, low and high calcium pyroxenes and plagioclase in the four meteorites. In addition, the modal composition was determined by point counting by probe analysis of (Fe, Ca, Mg) on a grid 0.3 × 0.3 mm. The calculated weight percentages of these four silicates are also indicated in Table 1. The complete modal analysis is reported in Table 3 and compared to the norm. The technique and the computer program used is described in the Appendix.

The phase compositions in Table 1 are averages from analyses performed at various times with different instruments and we estimate the accuracy to be at the best ±2 percent relative but usually better than ±6 percent.

Olivine: The iron value, which is the most reliable, is no more accurate than ±2 percent of the values given (this is about the best which can be

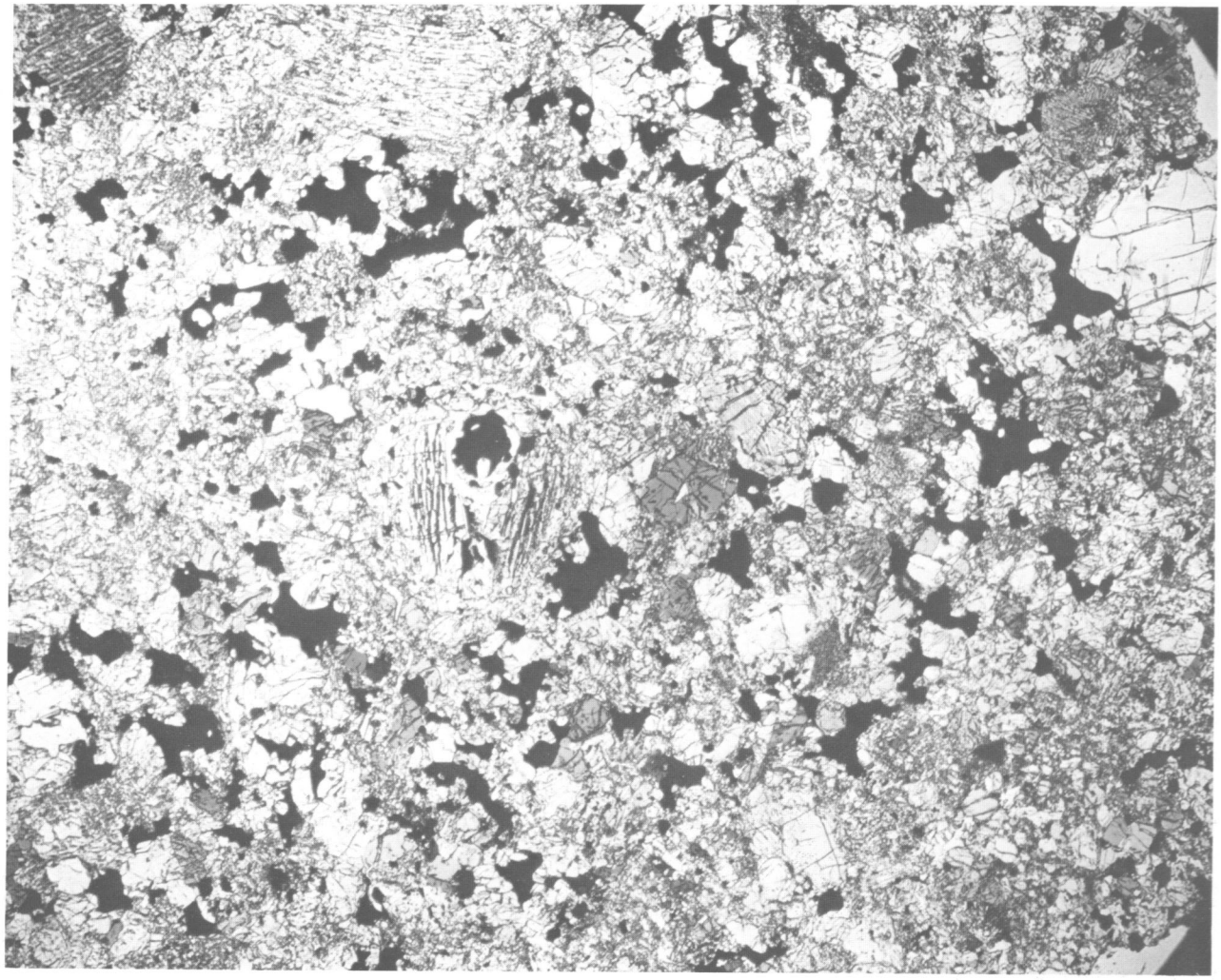

FIGURE 3.—Photomicrograph of thin section of the Sitathali bronzite chondrite (H5). The structure is similar to that shown in Figure 2. Chondrules, e.g., center and top left, are somewhat more abundant and distinct. Length of section 5 mm.

achieved by using a close standard and the Bence and Albee (1968) correction factors); this makes the olivines in all four chondrites essentially identical. The precision, however, while measuring olivine in a single sample is higher (±0.1% FeO), and relative differences in olivine composition in Pulsora are discussed below. Manganese, magnesium, and silicon were also measured but with less accuracy.

Pyroxenes: A calcium-poor orthopyroxene is the most abundant in all four meteorites and has essentially constant composition within each stone but small and probably real differences between the meteorites. Like the olivines they are relatively coarse, well defined and distinguishable in the modal analysis. The less abundant calcium-rich pyroxenes show greater chemical variations (especially in Pulsora), are fine-grained, and occur as inclusions in the other minerals (lamellae in Ca-poor pyroxenes) or intergrown with plagioclase in devitrified areas. Like the plagioclase they are, therefore, hard to distinguish during modal analysis (Appendix) and the average composition given in Table 1 is rather uncertain.

Plagioclase: This phase is almost impossible to identify microscopically (except in a fragment in

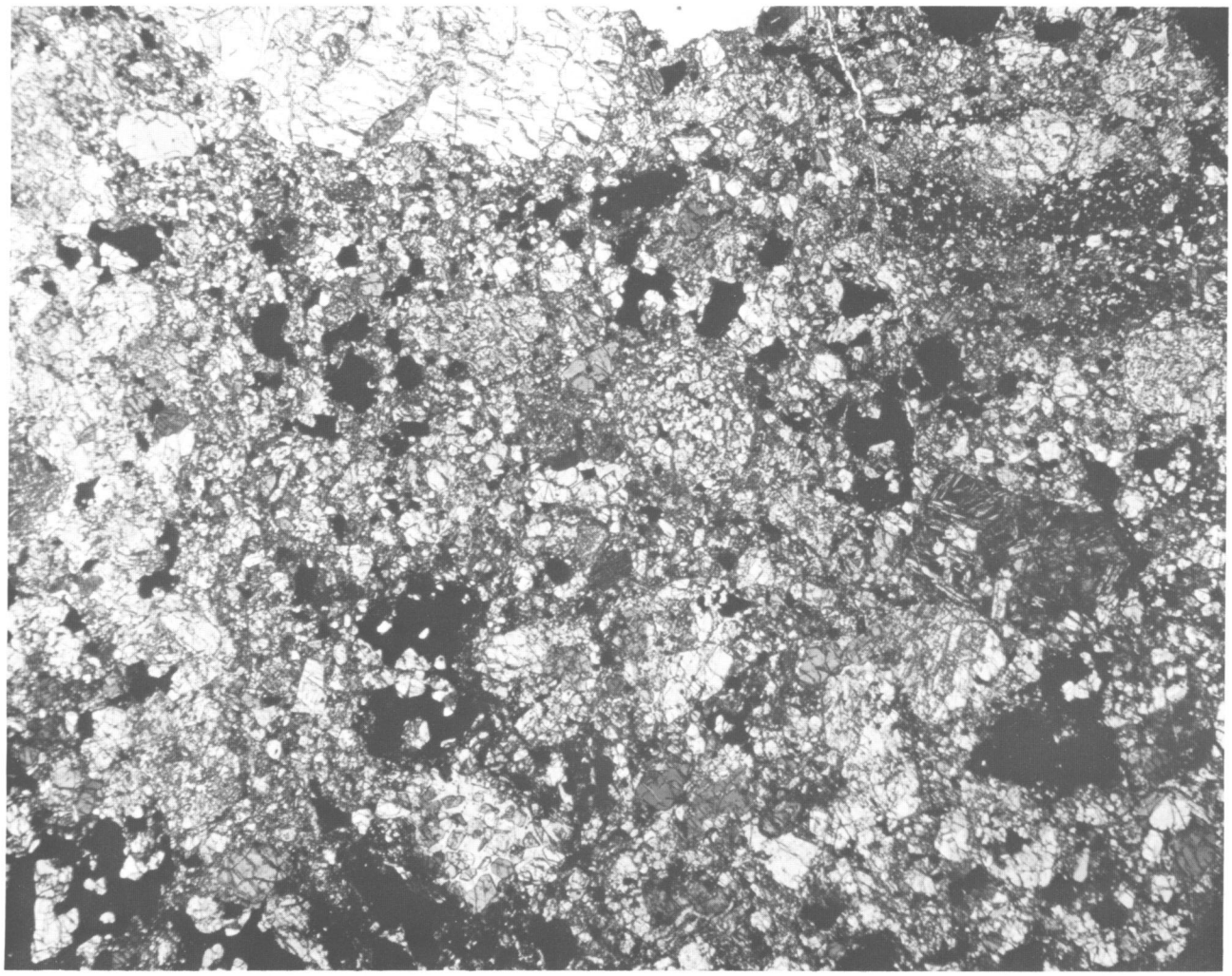

FIGURE 4.—Photomicrograph of thin section of the Pulsora bronzite chondrite. The classification for this section is H4 to H5, but compare also Figures 5 to 8, and frontispiece *(b)*. Chondrules and lithic fragments, e.g., right center, are clearly visible in the mostly fine-grained, gray to opaque matrix. Large, coherent black areas are metal, troilite, and other opaque minerals. Length of section 5 mm.

Pulsora) and almost invariably contains pyroxene crystallites. The reported composition is based on the calcium content obtained in areas where iron and magnesium values approach minimum (~ background). In the modal analyses allowance was made for substantial apparent contents of magnesium and, especially, iron.

Metal, both taenite and kamacite, troilite and whitlockite were identified in our modal analyses and although numerous grains were analysed and counted detailed descriptions are not warranted because they are of average composition and abundance. Also, the absolute abundance of these phases can be estimated more accurately from the bulk chemical analyses. A number of common accessory minerals, e.g., chromite and ilmenite, as well as more exotic ones, like copper and spinels, were also identified (cf. Ramdohr, 1973) but these phases seem to contribute little to the understanding of current models for the origin of chondrites, especially ours involving impact-melting and brecciation.

TABLE 1.—*Abundance and average composition of major silicate phases*

Constituent	*Mode wt.%*	*FeO*	*CaO*	*MgO*	*SiO_2*	*Al_2O_3*	*Na_2O*	*K_2O*	*MnO*
ANDURA									
Olivine	29.0	18.4		42.4	39.6	–	–	–	∿0.2
Pyroxene 1	27.2	11.3	0.8	31.4	56	∿0.1	0.2	–	–
Pyroxene 2	6.0	5	21	18.0	55	0.8	0.5	–	–
Plagioclase	6.1	–	2.4	–	65.6	21.5	10.4	(0.7)	–
BUTSURA									
Olivine	25.5	18.3	–	42.4	39.4	–	–	–	∿0.2
Pyroxene 1	27.8	11.4	0.8	31.1	56.5	–	–	–	–
Pyroxene 2	7.8	5	21	17	56	–	–	–	–
Plagioclase	4.9	–	2.6	–	66	21.7	10.3	(0.7)	–
PULSORA									
Olivine	22.6	18.3	–	42	39.7	–	–	–	∿0.2
Pyroxene 1	26.5	11.0	1.3	30	55	0.3	0.1	–	–
Pyroxene 2	11.3	5	19.6	17.5	54.5	0.7	0.6	–	–
Plagioclase	3.0	–	2.5	–	65.4	21.8	10.4	1.0	–
SITATHALI									
Olivine	28.7	18.0	–	42.3	39.6	–	–	–	∿0.2
Pyroxene 1	24.6	11.2	0.6	31.2	56.5	–	–	–	–
Pyroxene 2	6.7	4.1	21.4	17.6	56	–	–	–	–
Plagioclase	5.3	–	2.5	–	65.8	21.6	10.3	(0.7)	–

Chemical Composition

The analyses reported in Table 2 are almost identical. Only Andura shows less metallic Fe and more FeO. Apparently some of its metal (and/or troilite) has been more susceptible to atmospheric oxidation. This assumption is strongly supported by the fact that the calculated normative fayalite content of the olivine, Fa_{23} (Table 3), is considerably higher than the measured value, Fa_{19} (Table 1), which is the same as in the three other stones. Andura also has a more "rusty" appearance both macroscopically and in thin section. Pulsora and Butsura seem to have higher carbon contents than the other two but the possibility of contamination cannot be entirely disregarded. (The analysis of Sitathali reported by Viswanathan, et al. (1971) is apparently erroneous, especially with regard to the iron content as the authors suspected.)

In Table 3 the normative and modal compositions are compared. The mode was obtained by electron probe analysis as described above and in the Appendix. The composition of the normative minerals agrees closely with the values obtained

TABLE 2.—*Chemical composition* (analysts: J. Nelen, Andura; and E. Jarosewich, Butsura, Pulsora, Sitathali)

Constituent	*Andura*	*Butsura*	*Pulsora*	*Sitathali*
Fe	13.72	16.61	17.23	16.08
Ni	1.62	1.75	1.78	1.79
Co	0.08	0.07	0.10	0.09
FeS	5.57	5.89	4.99	5.76
SiO_2	36.85	36.27	35.97	36.65
TiO_2	0.16	0.12	0.12	0.14
Al_2O_3	1.85	1.98	2.26	2.37
Cr_2O_3	0.53	0.56	0.52	0.43
FeO	12.23	9.65	10.58	9.96
MnO	0.39	0.31	0.29	0.31
MgO	23.42	23.21	22.77	23.45
CaO	1.97	2.00	1.59	1.71
Na_2O	0.91	0.85	0.84	0.87
K_2O	0.12	0.08	0.10	0.10
P_2O_5	0.29	0.31	0.26	0.30
H_2O+	0.19	0.53	0.00	0.10
H_2O-	0.10	0.13	0.10	0.06
C	0.05	0.15	0.14	0.05
Total	100.05	100.47	99.64	100.22
Total Fe	26.74	27.85	28.62	27.48

TABLE 3.—*Normative and modal (weight percent) compositions*

Phase	Andura				Butsura				Pulsora				Sitathali			
	Norm		Mode		Norm		Mode		Norm		Mode		Norm		Mode	
Ni/Fe	15.42		17.1		18.43		16.3		19.11		17.1		17.96		16.1	
FeS	5.57		5.8		5.89		3.6		4.99		4.0		5.76		3.9	
Ap	0.97		0.5		0.74		–		0.60		0.2		0.71		0.2	
Cr	0.85		–		0.90		–		0.83		–		0.68		–	
Il	0.30		*		0.23		–		0.24		–		0.26		–	
Or	0.72				0.44				0.56				0.25			
Ab	7.70	9.0	6.1		7.18	9.0	4.9		7.07	9.7	3.0		7.34	9.8	5.3	
An	0.58				1.36				2.11				2.25			
Wo	2.70		6.0*		2.73		7.8*		1.71		11.3*		1.79		6.7*	
En	17.34	26.7	27.2 †	33.2	20.56	29.6	27.8 †	35.6	20.09	28.7	26.5 †	37.8	20.28	28.5	24.6 †	31.3
Fs	6.71				6.30				6.86				6.38			
Fo	28.52	40.7	29.0		25.90	34.7	25.5		25.47	35.0	22.6		26.52	35.7	28.7	
Fa	12.18				8.75				9.62				9.20			
C	0.05				0.15				0.14				0.05			
Residue			8.4				14.1				15.4				14.4	
Total			100.1				100.0				100.1				99.9	

*Pyroxene 2, see Table 1.
† Pyroxene 1, see Table 1.

by probe analysis (except for the high Fa value in Andura, explained above). Although in the modal analysis only two pyroxenes were distinguished, i.e., those with <1% CaO (Pyroxene 1) and >1% CaO (Pyroxene 2), the average composition calculated according to Table 1 is $Wo_{10}En_{75}Fs_{15}$ while the normative pyroxenes (Table 3) are in the range $Wo_{6-9}En_{72-76}Fs_{18-19}$. The amount of pyroxene in the norm, however, is consistently lower than in the mode while the reverse is true for olivine and plagioclase. Because the "Residue" in the modal analyses is substantial, we have attempted to establish its chemical composition by deducting the elements in the modal minerals as well as normative metal, troilite, chromite, ilmenite, and apatite. In Table 4 these residues are compared with the chemical composition of the bulk silicates obtained by deducting FeO for ilmenite and chromite and CaO for apatite from the chemical analyses in Table 2. It seems clear that the residue is severely deficient in silica but enriched in alumina and alkalies. Since a large part of the residue in these fine-grained rocks must be due to "overlap" between two or more phases, we attempted to remove first olivine, requiring least silica, and secondly pyroxene, having the same composition as in the "bulk" (but different proportions), from the residue. In all the four cases the end result is substantial excess of alumina and FeO, ~1 percent and 0.5 to 1.5 percent, respectively, of the total weight. Alkalies show a similar excess in all cases while calcium appears to be deficient in all but Andura. This calcium deficiency is probably not real but is due to uncertainty in the analysis of the Ca-rich pyroxenes.

Iron and magnesium, as might be expected, are about the same in bulk silicates and residue, again excepting Andura for which the results are distorted because of the oxidation discussed previously. This supports the probability that most of the fine-grained "matrix" is indeed "rock flour" similar in composition to the bulk meteorites. The excess iron may possibly be explained as admixed ultrafine metal and/or troilite. The excess of alumina and alkalies, however, is more puzzling. Three possible interpretations are offered: (1) Our modal and phase analyses are too inaccurate to allow these kinds of calculations. The consistency of the results, however, speaks against this, as well as the fact that if olivine is underestimated and pyroxene overestimated in the mode, which seems most likely, the discrepancies become worse. (2) A small amount of an undiscovered discreet phase(s) is present, e.g., corundum or spinel for alumina, or some silicate

TABLE 4.—*Chemical composition of bulk silicates from chemical analyses and of unidentified fractions residue in the modal analyses*

Constituent	Andura		Butsura		Pulsora		Sitathali	
	Silicate fraction (76% of total)	*Residue (8.4% of total)*	*Silicate fraction (73% of total)*	*Residue (14.1% of total)*	*Silicate fraction (73% of total)*	*Residue (15.4% of total)*	*Silicate fraction (74% of total)*	*Residue (14.4% of total)*
SiO_2	47.8	33.7	49.2	38.0	48.7	38.0	49.0	42.0
Al_2O_3	2.4	5.7	2.7	11.3	3.1	11.9	3.2	13.2
FeO	15.4	38.1	12.7	14.0	13.9	21.8	12.9	15.5
MgO	30.4	18.0	31.5	32.0	30.9	27.0	31.3	25.4
CaO	2.6	0.2	2.7	0.0	2.2	0.0	2.3	0.0
Na_2O	1.2	3.3	1.2	4.5	1.1	3.5	1.2	3.3
K_2O	0.2	1.0	0.1	0.7	0.1	0.6	0.1	0.6

strongly enriched in alumina and alkalies and possibly iron. Our studies have not so far revealed any such exotic minerals though we have searched for all the ones recently described by Ramdohr (1973) and Mason (1972). (3) The fine-grained ground mass does contain a "real matrix" entirely different from the bulk meteorite. This is in accordance with suggestions by Fredriksson and Keil (1964) that some carbonaceous chondrites are mixtures of low and high temperature fractions. Similar mixture models have been pursued in great detail by the Chicago group led by E. Anders in a number of papers, e.g., Anders (1964) and Laul, et al. (1973); (this paper has numerous references), for especially gas-rich and/or unequilibrated chondrites. A study of carbon distribution in some chondrites (Fredriksson and Nelen, 1969) led to the conclusion that also ordinary equilibrated chondrites may have small amounts of a low temperature real matrix and current work (Fredriksson, et al., in prep.) indicates that this matrix is also enriched in some heavy volatiles, e.g., Pb, Zn, and possibly also N and F (Kerridge, pers. comm.). From our present study, however, we can only conclude that if such a matrix is present, its bulk chemistry is still uncertain although Al/Si, Na/Si, and probably Fe/Si are higher than in the bulk silicates of H-group chondrites (as in some carbonaceous chondrites).

The Pulsora Anomaly

It has been demonstrated that Pulsora is chemically and mineralogically almost identical to three other ordinary equilibrated chondrites although its petrographic grade (Van Schmus and Wood, 1967), even on cursory inspection, seems somewhat lower, i.e., 4–5, than the others of 5–6. Detailed studies of a number of thin sections, however, have revealed several unusual lithic fragments that are not conspicuous in hand specimens. Two of these, extremely different from each other and from the bulk, are described in some detail because they have profound implications as to the thermal history of Pulsora and by analogy of other H-group chondrites. The achondritic fragment (Figure 5) referred to previously consists of relatively coarse, equi-

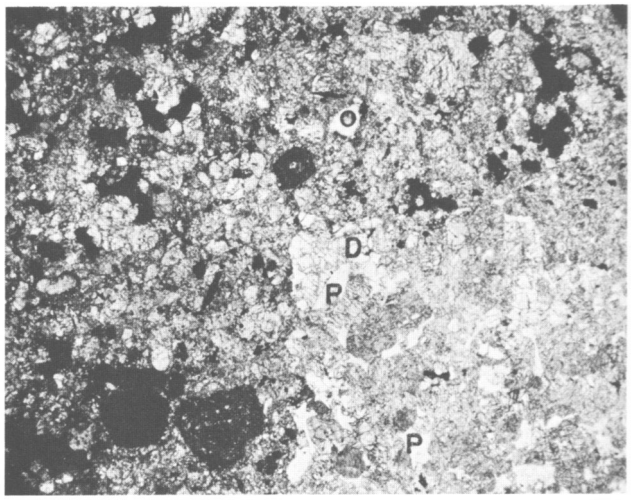

FIGURE 5.—Crystalline "achondritic" (H7?) fragment, lower right quarter, in Pulsora. Diopside (D), plagioclase (P) and whitlockite occur as large clear crystals together with normal olivine and orthopyroxene. Note the scarcity of metal and troilite (black) as compared to the main mass. Length of section 4 mm.

TABLE 5.—*Phase compositions in Pulsora achondritic fragments*

Constituent	*Olivine*	*Pyroxene 1*	*Pyroxene 2*	*Plagioclase*
SiO_2	–	–	–	–
TiO_2	–	–	–	–
Al_2O_3	–	–	1.6	–
FeO	18.0	10.8	5.2	–
MgO	40.5	28.8	17.9	–
CaO	–	2.2	19.0	1.6
Na_2O	–	–	–	–
K_2O	–	–	–	–

granular (in strong contrast with the bulk) olivine, ortho-pyroxene, diopside, plagioclase and apatite, in order of decreasing abundance. The composition of the major silicate phases are given in Tables 5 and 6. Although the accuracy of our iron determinations is no better than ±2 percent relative, we believe that we obtained a precision better than ± 0.1 percent FeO in alternate measurements between fragment and matrix and thus established a small difference in olivine composition, i.e., 18.0 (Table 5) in the fragment and 18.3 (Table 1) in the bulk. The ortho-pyroxene in the fragment (Pyroxene 1) has decidedly higher (2.2%, Table 5) CaO content than in the bulk (1.3%, Table 1) indicating a higher temperature of "equilibration," whereas the plagioclase is somewhat less calcic, An_{5-7} versus An_{10}, in the bulk. In the fragment, troilite and metal are scarce (~0.5%), the latter consisting of about equal amounts of taenite (~45% Ni) and kamacite (~ 5% Ni). In contrast the main mass contains 17 percent metal with only minor amounts of taenite with ~45 percent Ni; its kamacite has ~7 percent Ni. The overall Ni content of the Pulsora metal (Table 2) is 9 percent corresponding to ~95% kamacite and ~5% taenite.

The glassy fragment (Figures 6, 7) consists of euhedral and skeletal crystals of olivine (~65%) displaying normal zoning, in clear glass (~35%) enriched in silica; the composition is given in Table 6. The olivine has somewhat lower average iron content than olivine in the bulk and in other lithic fragments. The variation indicated in Table 6 is mostly due to zoning in the individual crystals, i.e., the cores have almost constant composition with 10–12 percent FeO. The glass is enriched in Si, Al, Ca, and Na and depleted in Mg and Fe. In its overall composition this fragment resembles some glassy chrondrules described from unequilibrated chondrites (e.g., Fredriksson and Reid, 1965) although the iron content of the olivine is unusually high and the glass has > 5 percent normative quartz, also unusual in glassy chondrules. In addition it contains a small, 0.5 mm, metal-sulfide spherule (Figure 8) with ~65 percent kamacite (7.3% Ni), ~35 percent troilite and a eutectic texture. The troilite contains 0.9 percent Ni in sharp contrast to troilite in the main mass of Pulsora, as well as in other ordinary chondrules, which have < 0.05 percent Ni. The texture indicates rapid crystallization and the 0.9 percent Ni content of the troilite would indicate quenching from ~1000° C (Kullerud, 1963) without any appreciable reheating.

This fragment might be a deformed chondrule even if applying the restricted definition proposed by Fredriksson, et al. (1973), but the irregular shape and the fact that other similar but angular fragments were found lead us to believe that it is a

TABLE 6.—*Phase compositions in Pulsora glassy fragments*

Constituent	*Olivine*	*Glass*	*Calculated bulk**
		ANALYSES	
SiO_2	41–39	65	48.5
TiO_2	–	0.4	0.1
Al_2O_3	–	7.8	2.6
FeO	10–15	11.0	12.2
MgO	49–44	6.5	33.7
CaO	–	5.7	1.9
Na_2O	–	2.5	0.8
K_2O	–	0.3	0.1
		NORMS	
Qtz		5.5	–
C		0.3	–
Or		2.3	0.8
Ab		30.6	11.7
An		40.8	6.3
Wo		–	1.9
En		8.7	21.2
Fs		11.2	5.6
Fo		–	40.5
Fa		–	11.8
Il		0.5	0.2

*Modal analysis gave ∿⅔ olivine and ∿⅓ glass of the composition indicated in the two preceding columns. Compare bulk silicates in Table 4.

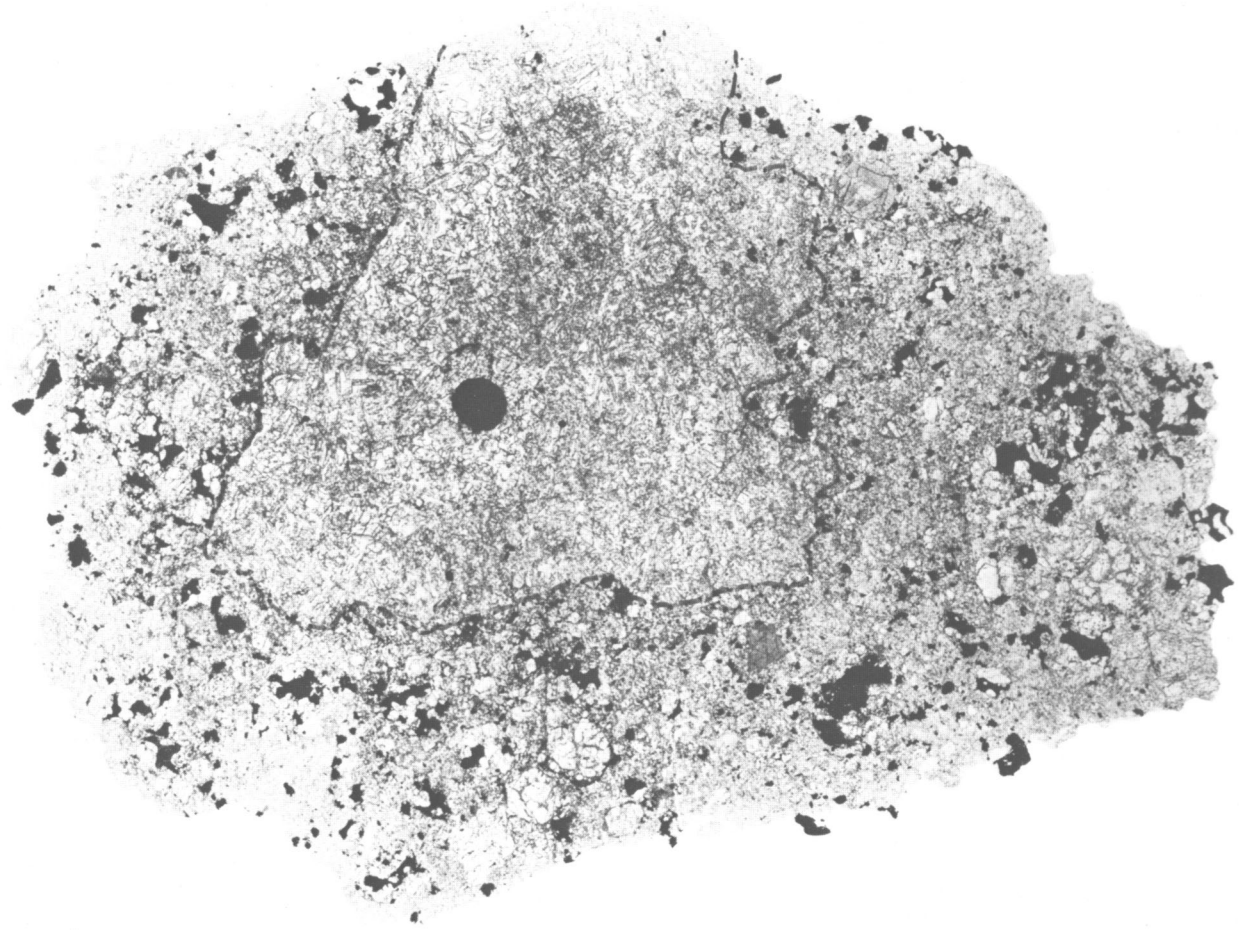

FIGURE 6.—Thin section of Pulsora including a lithic fragment consisting of olivine in a silica-rich glass (outlined by black, dotted line). Compare Figure 7. The black sphere consists of metal and troilite; see Figure 8. Length of section 11 mm.

fragment of a pre-existing rock. In Table 6 we also present the calculated bulk composition of the silicate in this glassy fragment. It is remarkably similar to the composition of the Pulsora bulk silicates as given in Table 4, again indicating a common parent material.

Clearly, the glassy fragments have not been equilibrated within themselves or with the rest of Pulsora either before or after incorporation in the meteorite. The achondritic fragment might have been equilibrated or recrystallized and drained of metal before incorporation in the bulk which then, if metamorphic equilibration is invoked, must have been metamorphosed somewhere else, then broken up and reassembled together with its fragments, most of which have identical olivine and pyroxene composition. Pulsora, or at least its main mass, must have been "metamorphosed" to exactly the same degree as the higher grade Andura, Butsura, and Sitathali, since their chemistry and mineralogy are essentially identical, implying recrystallization at various temperatures and/or length of time without any differentiation. This seems incomprehensible and to explain the chemical similarities between our four chondrites as well as their textural differences it seems necessary to have (1) a common parent material, (2) heating and cooling rapid enough to retain olivine in silica-rich glass and to

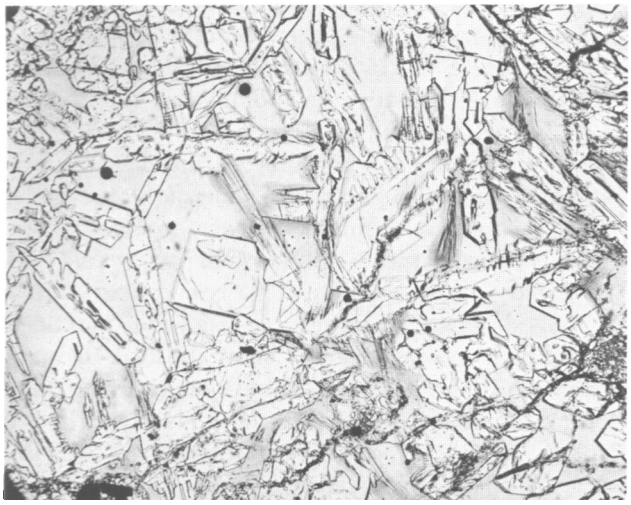

FIGURE 7.—Detail of Figure 6. Skeletal to euhedral zoned olivine (Fa_{13}, center to Fa_{16}, margin) in clear, quartz-normative glass. The bulk composition equals that of the silicates in Pulsora. Length of section 0.9 mm.

prevent chemical differentiation (except for draining of metal), and (3) repetitious brecciation and/or recrystallization processes which again do not cause gross chemical changes and consequently no equilibration.

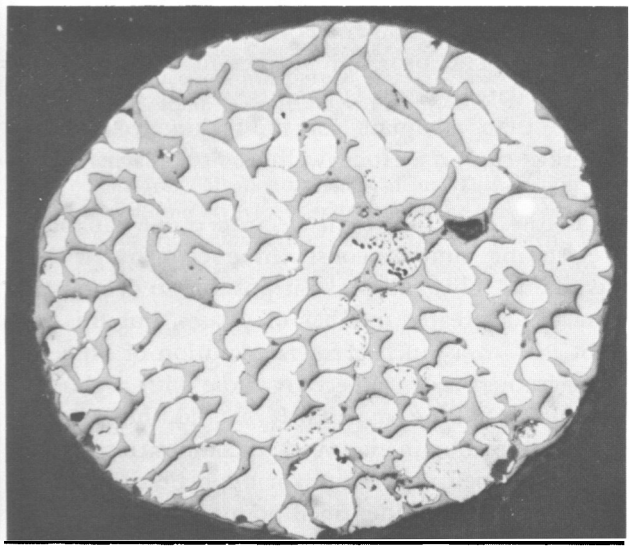

FIGURE 8.—Metal (kamacite, 7% Ni) and troilite spherule in the glassy fragment shown in Figures 6 and 7. The eutectic texture and high (0.9%) Ni content in the troilite indicate quenching from about 1000° C. Diameter 0.5 mm.

Conclusion

We have demonstrated that the Pulsora chondrite, in spite of its constant olivine-pyroxene composition, has never been exposed to thermal metamorphism after agglomeration as has been suggested for most chondrites (e.g., Merrill, 1921; Van Schmus and Wood, 1967; Dodd, 1969). Still, Pulsora, including its greatly variable (H3 to H7) lithic fragments, is practically identical, both chemically and with regard to major phase (and possible matrix) composition, to Andura, Butsura, and Sitathali. These latter three stones may seem to be of a higher average petrographic grade but they do contain, as might be perceived from Figures 1–4, more fine-grained parts similar to the main mass of Pulsora (while Pulsora has high grade fragments). Thus, by analogy, we contend that there is no compelling evidence for the assumption that the three other chondrites here described, or any other ordinary chondrite, ever suffered severe, long term thermal metamorphism, or that the constant olivine-pyroxene compositions were established by such processes. Rather, it seems that rapid, multiple processes acting on a common (at least chemically) parent material may create conditions under which olivine-pyroxene may retain their constant initial composition once established by subliquidus, or even subsolidus, crystallization (Fredriksson, 1963; Kurat, 1967; Blander, et al., 1970). Impacts on moderate sized bodies, $> 10^2$ to $\sim 10^3$ km, seem to be the most plausible and currently most accepted explanation for the contradictions presented by ordinary chondrites. Recent investigations of lunar impact breccias, glasses, and chondrules and the interpretation thereof also seem to corroborate the impact origin of chondrites (Fredriksson, et al., 1973).

Appendix

Modal Analysis with the Electron Probe

Like most chondrites the four stones investigated in this study are fine grained and the minerals are intricately intergrown. Thus modal analysis by point counting under the microscope is practically impossible as illustrated in Figures 1–4 and especiallly in the frontispiece. The proportions of metal, troilite (some oxides) and silicates can be readily estimated (e.g., Keil, 1962) but even estimates of

TABLE 7.—*Identification of phases by number of total counts*

Phase	$FeK\alpha$		$CaK\alpha$		$MgK\alpha$	
	>	<	>	<	>	<
1 Kamacite ...	21000	99000	50	500	20	500
2 Taenite	15000	21000	200	500	20	500
3 Troilite	15800	17500	100	200	20	500
4 Olivine	2500	5000	50	150	4500	10000
5 Pyroxene-1 .	1500	3000	150	600	1500	5000
6 Pyroxene-2 .	500	3000	600	10000	1300	5000
7 Plagioclase .	20	500	500	1500	20	300
8 Apatite	20	400	10000	25000	20	1000
9 "Others" or no fit	–	–	–	–	–	–

Note: Taenite is distinguished from troilite by the $CaK\alpha$ count, i.e., the background, the difference (somewhat uncertain) being caused by the different average atomic number (this adds another variable). In some cases "Taenite 2" was substituted for apatite by changing the criteria for Phase 8 to Fe, >10000 and <15000; Ca. (i.e., background) >200 and <500; and Mg >20 and <500.

the ratio of olivine to pyroxene in Andura (relatively coarse) differed by more than 50 percent between two of us and the amount of residue (unidentified) varied from 18 to 30 percent. In a study of Forest Vale (Noonan, et al., 1972) more rigorous optical criteria were applied which resulted in better olivine/pyroxene ratios but left $\sim$ 45 percent of the points (i.e., > 50% of the silicates) unidentified. We, therefore, decided to resort to point counting by electron probe, simultaneously registering the relative abundance of three elements. Similar techniques have been used before (e.g., Keil, 1962, 1967), but we believe that the procedure used for this study warrants a brief description for three reasons: (1) to illustrate the accuracy (or lack) of some of our calculations, (2) some of the modifications appear to be new and easily adapted to other systems that include computerized data reduction, and (3) the inherent possibility to identify ultrafine interstitial or intergrown minerals, especially if relative abundances of six or more elements are determined simultaneously, as is possible with various modern instruments.

In our study we used an ARL EMX instrument run at 20 kV, and $\sim$ 0.25μA beam ($\sim$ 0.025μA sample) current. The three spectrometers were tuned to $Fek\alpha$, $Cak\alpha$ and $Mgk\alpha$ and intensities recorded in silicate standards were approximately 125 cps (counts per second) per 1 percent Fe, 220 cps/1 percent Ca and 115 cps/1 percent Mg. Counting time was 2 seconds per point and the sample was moved mechanically (manually) under the beam on a 0.3 × 0.3 mm grid during the print out (typewriter and punch cards) time of $\sim$ 3 seconds; thus each point required an average of $\sim$ 6 seconds and a typical thin section $\sim$ 1 cm^2 was analyzed within 1½ hours. No real concentrations were estimated. Rather, phases were identified by number of total counts as established for each run as illustrated in Table 7. Similarly any other phases can be introduced and of course any suitable elements can be substituted for Fe, Ca, Mg to characterize these phases. The developed computer program readily accommodates such changes, i.e., it accommodates eight "fixed" phases, one "unknown" (frequently caused by overlap of different phases) and one "reject," i.e., if all three channels register background or less, the point is not counted but the number of such points is registered and might in special cases be used to identify a special "phase," e.g., holes or pores in a sample, etc. If the counts for each of the three channels are registered on punch card only, the limits as exemplified in the table have to be added, i.e., 48 digit (up to 10^7 counts per channel!) numbers which can be accommodated on 5 IBM cards. (A print out of the current program in Fortran IV is available on request.) The program at present is designed to accomodate up to 750 points, which we consider more than adequate for most thin sections. An average run on a Honeywell 1250 takes a maximum of 2 minutes.

In the near future an electron probe capable of registering simultaneously nine elements will be available. This will make it possible to define more sharply a greater number of phases, but this may not lead to a much greater resolution of phases in fine-grained rocks, especially those with a glassy or crypto-crystalline matrix. It should, however, be possible to obtain the average composition of such a fine-grained matrix and/or apportion (i.e., calculate the norm) unidentified points among the major phases, leaving only small amounts of excess elements or compounds.

Literature Cited

Anders, E.
1964. Origin, Age and Composition of Meteorites. *Space Science Reviews,* 3:583–714.

Bence, A. E., and A. L. Albee
1968. Emperical Correction Factors for the Electron Microanalysis of Silicates and Oxides. *Journal of Geology,* 76:382–403.

Blander, M., K. Keil, L. S. Nelson, and S. R. Skaggs
1970. Heating of Basalts with Carbon Dioxide Laser. *Science,* 170:435–438.

Coulson, A. L.
1940. Catalogue of Indian Meteorites. *Memoirs of the Geological Survey of India,* 75:1–346.

Dodd, R. T.
1969. Metamorphism of the Ordinary Chondrites: A Review. *Geochimica et Cosmochimica Acta,* 33:161–203.

Fredriksson, K.
1963. Chondrules and the Meteorite Parent Bodies. *Transactions of the New York Academy of Sciences,* series 2, 25:756–769.

Fredriksson, K., and K. Keil
1964. The Iron, Magnesium, Calcium and Nickel Distribution in the Murray Carbonaceous Chondrite. *Meteoritics,* 2:201–217.

Fredriksson, K., and J. Nelen
1969. Carbon Distribution in Chondrites. *Meteoritics,* 4:271–272.

Fredriksson, K., A. Noonan, and J. Nelen
1973. Meteoritic, Lunar and Lonar Impact Chondrules. *The Moon,* 7:475–482.

Fredriksson, K., and A. M. Reid
1965. A Chondrule in the Chainpur Meteorite. *Science,* 149:856–860.

Keil, K.
1962. Quantitative-erzmikroskopische Integrationsanalyse der Chondrite. *Chemie der Erde,* 22:281–348.
1967. The Electron Microprobe X-ray Analyzer and Its Application in Mineralogy. *Fortschrittee der Mineralogie,* 44:4–66.

Keil, K., and K. Fredrikkson
1964. The Iron, Magnesium and Calcium Distribution in Coexisting Olivines and Rhombic Pyroxenes in Chondrites. *Journal of Geophysical Research,* 69: 3487–3515.

Kraut, F., and K. Fredriksson
1971. Hedjaz an L-3, L-4, L-5 and L-6 Chondrite. *Meteoritics,* 6:284.

Kullerud, G.
1963. The Fe–Ni–S System. Pages 175–189 in *Annual Report of the Director of the Geophysical Laboratory, 1962–1963.* Carnegie Institution of Washington. [Also as number 1412 in *Papers from the Geophysical Laboratory.*]

Kurat, Gero
1967. Einige Chondren aus dem Meteoriten von Mezo-Madaras. *Geochimica et Cosmochimica Acta,* 31: 1843–1857.

Laul J., C. R. Ganapathy, Edward Anders, and John W. Morgan
1973. Chemical Fractionation in Meteorites–VI: Accretion Temperature of H–, LL–, and E–Chondrites, from Abundance of Volatile Trace Elements, *Geochimica et Cosmochimica Acta,* 37:329–357.

Mason, B.
1972. The Mineralogy of Meteorites. *Meteoritics,* 7:309–326.

Merrill, G. P.
1921. On Metamorphism in Meteorites. *Bulletin of the Geological Society of America,* 32:395–414.

Murthy, M. V. N., S. N. P. Srivastara, and A. Dube
1969. Indian Meteorites. *Memoirs of the Geological Survey of India,* 99:1–192.

Noonan, A. F., K. Fredriksson, and J. Nelen
1972. Forest Vale Meteorite. *Smithsonian Contributions to the Earth Sciences,* 9:57–64.

Ramdohr, P.
1973. *The Opaque Minerals in Stony Meteorites.* 245 pages. Amsterdam: Elsevier Publishing Company.

Urey, H. C., and H. Craig
1953. The Classification of the Stone Meteorites and the Origin of the Meteorites. *Geochimica et Cosmochimica Acta,* 4:36–82.

Van Schmus, W. R., and J. A. Wood
1967. A Chemical and Petrologic Classification for the Chondritic Meteorites. *Geochimica et Cosmochimica Acta,* 31:747–765.

Viswanathan, T. V., N. R. Sen Gupta, D. R. Das Gupta, and S. Banerjee
1971. The Sitathali Meteorite. *Mineralogical Magazine,* 38 (September):335–343.

Impact Survival Conditions for Very Large Meteorites, with Special Reference to the Legendary Chinguetti Meteorite

Robert F. Fudali and Dean R. Chapman

ABSTRACT

Contrary to popular belief, very large meteorites ($>>$ 1000 tons) can be sufficiently slowed by aerodynamic drag to survive impact with the earth's surface provided that they enter the atmosphere at very low angles. This is a stringent requirement and survival probabilities for large, unguided objects are low; but they are not zero. Based on high-velocity impact experiments and published tabulations of the parameters of shallow angle entry trajectories, we estimate the probability of survival for an iron meteorite approximately the size and shape of the legendary Chinguetti meteorite (100 meters x 40 meters x 20–40 meters) to be between 0.1 and 1 percent. Together with a limiting estimate of the flux of such bodies encountering the earth, this leads to an expected survival rate of one per 10^8–10^9 years on the earth's land surface.

Introduction

In 1916, a small (4.5 kg) meteorite was found in the Adrar region of Mauritania (then French West Africa) by a captain in the French army, Gaston Ripert. It was designated the Chinguetti Meteorite, after the nearby oasis of Chinguetti (20° 28′N, 12° 20′W). The meteorite presently resides in the Muséum National d'Histoire Naturelle (Paris).

The fascinating part of the story is that Ripert claimed the meteorite was but the tiniest part of a gigantic mass that he was led to, with the greatest reluctance, by the then chieftain of Chinguetti, Sidi Ahmed Ould Zein. Following is Ripert's description of the find (as originally transcribed by Lacroix, 1924, and cited in Monrod, 1952):

> This specimen was collected about 45 km. to the southwest of Chinguetti and to the west of Aouinet N'Cher. It was lying on top of an enormous metallic mass measuring about 100 m. on one side and about 40 m. in height, which stands up in the middle of dunes covered by a desert plant called 'sba' [sic]. (The mass) is in the form of a compact, unfractured parallelepiped. The visible surface is vertical, standing like a cliff above the sand, which, driven by the wind, has grooved its base to such an extent that its upper edge overhangs; the part worn by eolian erosion is polished like a mirror. The sand has piled up against the opposite face and hides it entirely, a fact that made it impossible to estimate its third dimension. The upper surface of the mass bristles with little needles, which the Arabs have tried to remove; but, because of the malleability of the metal, these were only bent. Some less important blocks (of the same material) are scattered about the neighborhood.

Understandably, this report caused considerable excitement in 1924. If the meteorite existed it would be of enormous mass. Based on dynamical considerations to fix the unreported third dimension we estimate a minimum mass of 500,000 tons and a more likely mass in excess of 1,000,000 tons. Since it would have had to tumble and skid to rest from a high velocity, the most stable attitude was probably achieved during the final stages of deceleration and this would be with the smallest dimension vertical. In the event that the vertical dimension is instead the intermediate dimension it is highly unlikely that the unknown horizontal dimension could

Robert F. Fudali, Department of Mineral Sciences, National Museum of Natural History, Smithsonian Institution, Washington, D. C. 20560. Dean R. Chapman, Thermo- and Gas-Dynamics Division, NASA Ames Research Center, Moffett Field, California 94035.

be significantly smaller than the vertical dimension. We therefore assume that the unknown dimension would be at least 20 meters and more likely in excess of 40 meters.

In addition to the scientific interest, the meteorite would be large enough to generate thoughts of commercial gain. Over the next 14 years there were several, more or less random, attempts made to relocate the original site, without success. Curiously, it was not until 1932 that Ripert was contacted for help in these endeavors and, by then, he apparently retained only a vague notion of the general area of the site. Further, his guide had long since died. In reviewing the problem, Monod (1952) reproduced parts of two letters written by Ripert at about this time. In 1932 Ripert (translated by Brady) wrote, in part, to Dr. Jean Bosler, Director of Le Verrier Observatory in Marseille:

> Unfortunately, 16 years have passed since I had occasion to describe the existence of this meteorite. The times were such that everything else was blotted out by the dramatic events that were occurring in France, and I could not realize at the time all the interest that this meteorite might arouse. I spoke of it incidentally, when I was leaving Mauritania, to one of my friends, M. H. Hubert, a Doctor of Science at Dakar, who did not seem to attach any great importance to its existence.
>
> Moreover, in order to satisfy the urgent demands of my guide I had taken with me neither compass nor any material that would permit me to make notes or any measurements whatsoever; also, I could remain only a very short time, because of the guide's haste to leave the spot; so my observations were extremely cursory. I was able to state that the meteorite formed a sort of cliff, with numerous projecting ridges of sand, lying in an approximately southwest direction, while the northeast side was completely covered by sand. I found there a small fragment, well rounded at the edges, which I turned over to M. Hubert. On one corner (of the large mass), toward the west, I think, sand had carved out fairly thick metallic needles, which I could not loosen or remove. Of the metallic nature of the large mass there could be no doubt at all. Examination of the small specimen given to M. Hubert proves this fact. I tried to detach one of the aforesaid needles by pounding it with the small heavy lump (= the small meteorite). The specimen showed at every point of contact traces of hammer marks, the same condition being true of the needles; and, finally, the surface appearance of the large mass was in no way comparable to that of the blackish polished surface of the rocks that are found on the 'reg' and on the sandstone plateaus of the Adrar. On my return, I wrote down my observations (based on my memory, which was very good at the time), but, since then, I have moved so much from place to place that I do not know where I put those notes. In any case, I told M. Hubert everything that I had seen which was then quite clear in my mind.
>
> As you may imagine, this meteorite, half-covered by sand in 1916, is very likely completely covered now, but, even so, I am astonished that it has not been found by the civilian and military expeditions that have been sent out since 1929 to look for it. It seems likely that they have been blocked by a conspiracy on the part of the natives, who seem anything but anxious that its existence should be known to Europeans. I realized this (fact) when I overheard a conversation among the camel drivers when I was with the Adrar camel corps. I had spoken of (the meteorite) to the head man of Chinguetti, Sidi Ahmed Zein, who at first vigorously denied its existence, and it was only after long conversations (negotiations?) that he consented, in spite of his fears, to lead me secretly to the spot, on condition that I would take nothing with me that might permit me to describe the exact position of the meteorite, or to make notes. Sidi Ahmed died, apparently of poison; and, without wishing to establish any connection between the facts, I cannot now point out anyone who could serve as a guide.

And in 1934 he wrote, in part, to Monod (1952; translated by Brady):

> I know that the general opinion is that the stone (rock) does not exist: that, to some, I am purely and simply an imposter who picked up a metallic specimen on the 'reg' of Mauritania; that, to others, I am a simpleton who mistook an exposure of sandstone, blackened and polished as is so often the case in that country, for an enormous meteorite. I shall do nothing to undeceive them. I care very little for what any of them may think. I know only what I saw, because I saw it, and I could probably have found (the mass) again if I had been directed to do so, when my visual memory and my age still permitted.

Monod in 1934, and one A. Pourquie, in 1938, conducted search expeditions into the Chinguetti region—both with negative results (Monod, 1952). At that point World War II intervened and the matter was not seriously broached again until the early 1950s. In his 1952 paper Monod was still convinced the huge meteorite could very well exist. However, based on his extensive experience in the region, he cautioned:

> Let me add that if the meteorite is actually located among the dunes of Ouarane, 10 hours to the southeast[1] of Chinguetti, the very nature of this terrain is unsuited to easy exploration. It is foolish, of course, to pursue a search (for the meteorite) in a random fashion merely in the hope of making a lucky discovery.

Thus far, this point has been academic as there have been no further efforts to relocate the site. The reason for this neglect is that it is widely believed to be physically impossible for such an enor-

[1] The original report of Lacroix describing the find site as southwest of Chinguetti was subsequently corrected by Ripert to southeast of Chinguetti (Monod, 1952).

mous mass to survive an impact with the earth's surface. This belief is based on simple aerodynamic calculations, which have been generally interpreted as precluding any significant atmospheric braking if the incoming meteoritic mass exceeds a maximum of 100 to 1000 tons. This has been uniformly asserted in several meteoritic texts that have enjoyed wide circulation (e.g., Mason 1962; Hawkins, 1964; Heidi, 1964; Wood, 1968).

With little or no atmospheric braking a meteorite impacts the earth's surface with enough kinetic energy to destroy both itself and a significant portion of the target rock. And there surely is ample evidence—in the form of a number of meteorite impact craters of modest dimensions—that meteorites of mass far less than that estimated for Chinguetti do normally explode upon encountering the earth's surface. But what is not generally appreciated is that this is a normal, rather than an inevitable, result. In this paper we demonstrate that, under special conditions, a Chinguetti-size meteorite could survive a terrestrial impact essentially intact. In the following sections we delineate the conditions necessary for the survival of such a meteorite, and we compute the approximate probability of encountering such conditions. As one might suspect, the conditions are stringent and the concomittant probabilities are small—but they are certainly not zero.

TABLE 1.—*Fate of aluminum projectiles impacting sand targets at high velocities and low incident angles* (NASA Ames Light-Gas Gun Range experiments)

Round	V_t *(km/sec)*	Γ_t	Γ_r	*Fate of projectile*
		(degrees)		
DLG				
209	6.1	2.1	0.9	Essentially intact
211	6.5	4.75	1.1	Two main fragments
221	5.7	7.33	1.15	Three main fragments
215	6.3	15	–	Fragmented into small pieces
233	5.9	30	–	Fragmented into small pieces
VGP				
788	1.9	2.1	1.5	Intact
791	1.8	4.75	3.6	Intact
792	1.9	7.33	2.85	Intact
796	1.8	15	1.32	Essentially intact

TABLE 2.—*Variation of the effective strength of aluminum projectiles as a function of their diameter* (NASA Ames Light-Gas Gun Range experiments)

Projectile diameter (inch)	*Impact velocity for same degree of deformation (km/sec)*	*Corresponding energy for same degree of deformation (ergs)*
1/16	0.8	2×10^{7}
1/4	1.1	2×10^{9}
1/2	1.2	2×10^{10}

The foregoing should in no sense be considered an endorsement for the existence of the legendary Chinguetti meteorite. The primary purposes of this paper is not to demonstrate that it does exist, but that such a large meteorite *can* exist. Clearly this is the absolute minimal requirement necessary if a systematic search for the meteorite is ever seriously contemplated.

ACKNOWLEDGMENTS.—Donald Gault and John Wedekind of the NASA Ames Research Center generously furnished us with the unpublished, experimental high-velocity impact data vital to our study. For this, and for a number of stimulating discussions on all aspects of the study, we express our deep appreciation. We also thank Lionel Levy of the NASA Ames Research Center for the computer-generated trajectories of a large iron meteorite subsequent to ricochet at the earth's surface.

Experimental Data on Impact Survival

There is, of course, no possibility of slowing a Chinguetti-size meteorite to terminal velocity by atmospheric braking alone. In the following section we show that the minimum possible velocity such a body could have upon impact would be 3–4 km/sec, and higher velocities are much more probable. We must therefore consider the possibility of survival only for impact velocities of 3 km/sec and higher.

Some of the hypervelocity impact experiments done at the light-gas gun range of NASA Ames Research Center have a direct bearing on this problem. Most of these impact experiments have been characterized by high angles of impact ($> 30°$). But the few experiments carried out at low incident angles show that, for aluminum projectiles impacting sand targets at velocities between approximately 2 and 6 km/sec, the fate of the projectile is a func-

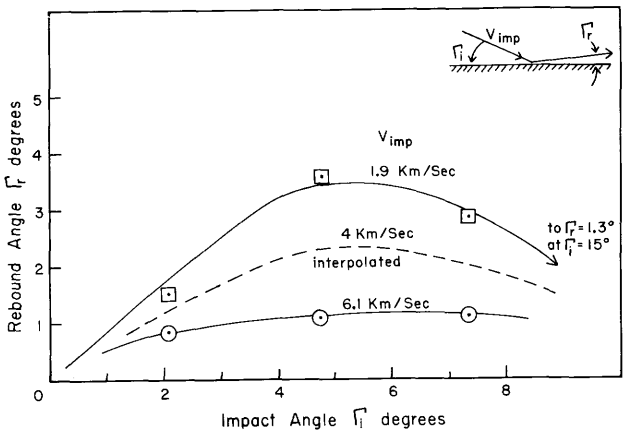

FIGURE 1.—Relationship between impact angle Γ_i, impact velocity V_{imp}, and rebound angle Γ_r. Aluminum projectiles into sand targets.

tion of both velocity *and* incident angle. For a given velocity, as the incident angle is lowered, a value is reached below which the projectile will ricochet intact. The pertinent experimental data are shown in Table 1. Figure 1 plots the angle of ricochet against the angle of incidence for three impact velocities. Note that in all cases the ricochet angle is significantly less than the incident angle.

We have used the data in Table 1 to approximately fix the boundary separating the fragmentation domain from the domain of intact ricochet on plots of impact velocities versus incident angles in Figures 2 and 3. Admittedly the data are scanty and

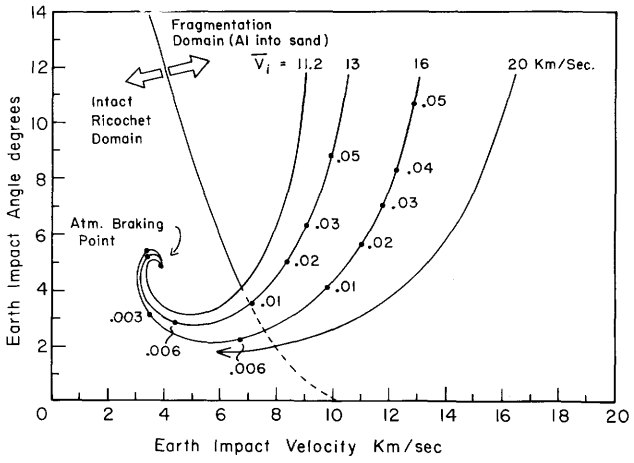

FIGURE 2.—Possible earth impact conditions for shallow angle entry trajectories of an iron meteorite with $\bar{h}=20$m.

there is a rather large uncertainty associated with this boundary placement, especially at higher velocities. However, it seems likely that the boundary, as drawn, is conservative. For a Chinguetti-size, nickel-iron meteorite the true boundary should lie somewhere to the right of the boundary shown in Figures 2 and 3. There are two reasons for this: (1) Nickel-iron has a much greater strength than aluminum, and (2) scaling up from the tiny experimental projectiles to a large meteorite should be favorable for impact survival. Although the shock wave strengths are independent of scale, the deceleration or body forces acting on each element of the projectile vary inversely with the scale of the projectile. We therefore expect a large projectile to

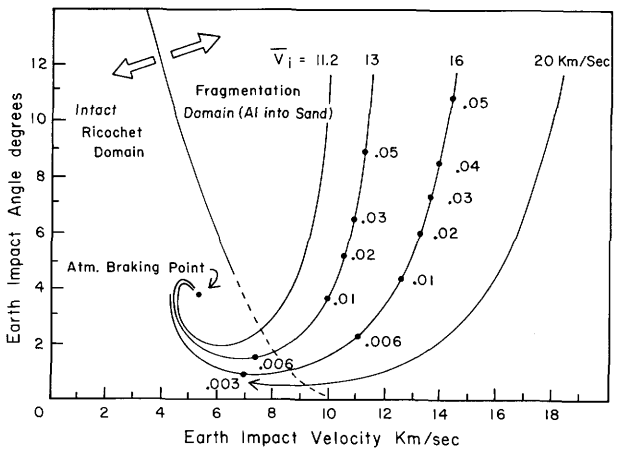

FIGURE 3.—Possible earth impact conditions for shallow angle entry trajectories of an iron meteorite with $\bar{h}=40$m.

effectively behave as if it were stronger than a small projectile. Some experimental confirmation of this expectation is shown in Table 2.

The conditions a projectile experiences subsequent to ricochet are specifically discussed in the following section. Here we merely point out that nothing subsequent to the initial impact can begin to approach this initial event in potential destructiveness. This is because the projectile loses energy during ricochet, and is subject to further atmospheric braking after ricochet.

Possible Impact Conditions

Some years ago, Chapman (1959, 1960) published an analytical method for studying the motion of

extraterrestrial bodies on shallow entry trajectories into the earth's atmosphere. So that these trajectory calculations could be generally applied to any planetary atmosphere and to incoming bodies with any physical properties, the trajectories were described in terms of two dimensionless functions. The conic perigee parameter F_p delineates the conditions at the perigee point of the hypothetical conic trajectory that the incoming body would have had if there were no planetary atmosphere. It characterizes the trajectory prior to atmospheric encounter and is defined as

$$F_P = \frac{\rho_P \sqrt{r_P/\beta}}{2(M/C_D A)} . \quad (1)$$

The trajectory through the atmosphere is characterized by a dependent variable termed the Z function:

$$Z = \frac{\rho \bar{u}}{2(M/C_D A)} \times \frac{r}{\sqrt{r\beta}} \quad (2)$$

where, for both equations ρ=air density, r=radius from the planet's center, β=the atmospheric density decay parameter, M=mass (grams) of the incoming body, A=cross-sectional area normal to the flight path (cm^2), C_D = the atmospheric drag coefficient, $\bar{u}$=the ratio of the horizontal velocity component at any point along the flight path to the circular orbital velocity (8 km/sec), and subscript $_p$ refers to conditions at the conic perigee.

For an incoming body of given F_p, initial velocity, and lift force to drag force ratio (L/D), Z can be determined at all points on its atmospheric trajectory. If Z is known, a number of other pertinent entry motion parameters can be calculated, including the horizontal velocity component and the trajectory angle with respect to the local horizontal. This has been done for a large number of trajectories and the results are assembled in computer-generated tables (Chapman and Kapphahn, 1961). One such table is reproduced herein for illustrative purposes (Table 3).

In order to use these tables for the problem under consideration, we begin by determining $Z/\bar{u}$ at sea level (i.e., at impact) for Chinguetti-size meteorites, using equation 2. This quantity is conveniently given if we use the density of air at set level, ρ_o, for the calculation. For purposes of these calculations the following assumptions and approximations are made: (1) The meteorite is oriented by aerodynamic forces such that the minimum dimension is

TABLE 3.—*Atmospheric behavior of an object entering the earth's atmosphere under the following initial conditions: Initial velocity*=13 km/sec, *Lift/drag*=0, *Conic perigee parameter* F_p=0.466, and *Initial atm. encounter angle*= −5.00° (modified from Chapman and Kapphahn, 1961:155)

$Z/\bar{u}$	$\bar{u}$	Z	G	Γ	S	T
	1.593	.00261	.13	−5.00	.000	0
	1.590	.00986	.47	−4.38	.018	9.2
	1.585	.02070	.99	−3.99	.029	14.9
	1.580	.03074	1.46	−3.77	.036	18.3
	1.575	.04026	1.91	−3.60	.041	20.7
	1.570	.04938	2.33	−3.48	.044	22.6
	1.560	.06667	3.13	−3.28	.050	25.6
	1.550	.08297	3.87	−3.13	.055	27.9
	1.500	.15425	6.96	−2.67	.069	35.5
	1.450	.21384	9.32	−2.38	.078	40.5
	1.400	.26505	11.15	−2.18	.085	44.5
	1.350	.30958	12.55	−2.03	.091	47.9
	1.300	.34848	13.61	−1.90	.096	51.0
	1.250	.38253	14.36	−1.80	.100	53.9
	1.200	.41234	14.86	−1.72	.105	56.7
	1.150	.43842	15.14	−1.66	.108	59.4
	1.100	.46123	15.23	−1.61	.112	62.0
	1.050	.48116	15.17	−1.59	.116	64.7
	1.000	.49864	14.97	−1.58	.119	67.4
0.54	.950	.51405	14.66	−1.59	.122	70.1
0.59	.900	.52781	14.26	−1.62	.126	72.9
	.850	.54031	13.79	−1.67	.129	75.8
	.800	.55202	13.26	−1.76	.132	78.8
	.750	.56340	12.69	−1.87	.135	81.9
	.700	.57496	12.09	−2.02	.138	85.2
	.650	.58727	11.47	−2.22	.141	88.6
	.600	.60091	10.84	−2.47	.143	92.3
1.12	.550	.61654	10.20	−2.79	.146	96.1
	.500	.63485	9.55	−3.19	.149	100.2
	.450	.65657	8.90	−3.69	.151	104.6
	.400	.68242	8.24	−4.34	.154	109.4
	.350	.71309	7.55	−5.17	.156	114.5
	.300	.74914	6.82	−6.27	.158	120.2
	.250	.79078	6.04	−7.76	.161	126.5
	.200	.83749	5.18	−9.91	.163	133.8
	.150	.88673	4.21	−13.26	.165	142.6
	.100	.92946	3.13	−19.33	.166	154.2
	.050	.92114	2.00	−33.68	.168	172.1

$\bar{u}$=Horizontal velocity component normalized to circular satellite velocity.

Z=Dimensionless function proportional to density times velocity.

G=Deceleration in earth g's.

Γ=Flight path angle relative to local horizontal in degrees.

S=Circumferential distance traveled.

T=Time elapsed in seconds.

parallel to the flight path. The calculations are carried out for two minimum dimensions, 20 meters and 40 meters. (2) Density of the nickel-iron meteorite is 8 gm/cc. (3) The meteorite has no aerodynamic lift, either positive or negative (i.e., ballistic entry). The lift-to-drag ratio (L/D) is therefore zero. (4) The drag coefficient $C_D \approx 1.5$ over the entire flight path. (5) The variation of atmospheric density with height is exponential and $\sqrt{r\beta} \approx 30$ everywhere in the earth's atmosphere. (6) $r \approx$ radius of the earth $= 6 \times 10^8$ cm. (7) For shallow angle entries, the (normalized) horizontal velocity component, $\bar{u}$, approximately equals the meteorite's entire velocity.

Now $M/A = 8\bar{h}$ gm/cm^2, where $\bar{h}$ is the average depth of the meteorites (in cm) in the direction parallel to the flight path. Therefore $M/C_D A = 5.3\bar{h}$ gm/cm^2. Also $\rho_0 = 0.0012$ gm/cm^3. Substituting in equation (2) we have:

$$(Z\bar{u})_o = \frac{0.0012 \text{ gm/cm}^3 \times (6 \times 10^8 \text{ cm})}{10.6 \times 30 \times \bar{h} \text{ gm/cm}^2}$$

$$= \frac{2264}{\bar{h}} \quad \text{dimensionless,} \qquad (3)$$

$$\text{for } \bar{h} = 40 \text{ m} = 4 \times 10^3 \text{ cm}, (Z/\bar{u})_0 = 0.57, \qquad (4)$$

$$\text{for } \bar{h} = 20 \text{ m} = 2 \times 10^3 \text{ cm}, (Z/\bar{u})_0 = 1.14. \qquad (5)$$

Table 3 displays the trajectory parameters of a body with zero lift, entering the earth's atmosphere at an initial velocity of 13 km/sec and an initial angle of $-5.00°$ (the negative sign merely denoting that the body is descending). From this table we see that a meteorite characterized by $(Z/\bar{u})_0 = 0.57$ would impact the earth's surface at a velocity of 7.4 km/sec and an angle of $-1.65°$, 75 seconds after first encountering the atmosphere. If $(Z/\bar{u})_0 = 1.14$, the meteorite would impact at 4.4 km/sec and $-2.8°$, 96 seconds after first encountering the atmosphere. It might at first seem paradoxical that the impact angle can be less than the initial entry angle since the trajectory must always steepen (in an absolute sense) due to the combined effects of gravity and aerodynamic deceleration. However, this may indeed be the case for an impact angle *measured with respect to the local horizontal* since the earth's surface curves away from the trajectory path. Both sets of parameters define points within the intact ricochet domain as delineated in Figures 2 and 3. Using the complete tables of Chapman and Kapphahn (1961), a number of such points can be plotted, generating the family of lines shown in Figures 2 and 3. Each line contains all the impact velocities and angles (of interest here) for a single initial encounter velocity. Lines corresponding to encounter velocities of 11.2, 13, 16, and 20 km/sec are plotted. An encounter velocity of 11.2 km/sec (escape velocity) is, of course, the lower limit for an incoming meteorite and we consider velocities between 13 and 16 km/sec to be the most likely range for large iron meteorites. Clearly, at least for all encounter velocities less than 20 km/sec, a significant portion of the generated lines lie in the intact ricochet domain.

TABLE 4.—*Computer-generated trajectory parameters and conditions at second impact for an iron meteorite of* $\bar{h}$*=40 meters ricocheting with velocities* V_1 *and angle* Γ_1

V_1 (km/sec)	Γ_1 (degrees)	Range (km)	Max. height (km)	V_2 (km/sec)	Γ_2 (degrees)
5.3	1.3	161	1.1	3.9	−1.8
4.5	1.9	153	1.4	3.4	−2.4
4.5	1.5	125	0.9	3.5	−1.9
5.0	1.0	114	0.6	4.0	−1.3
6.0	0.5	106	0.3	4.8	−0.7
6.0	0.8	152	0.6	4.4	−1.1
7.0	0.5	172	0.5	4.9	−0.8
7.0	0.7	211	0.9	4.6	−1.2
8.0	0.4	233	0.7	5.0	−0.9
8.0	0.7	306	1.5	4.5	−1.6

For all impact velocities below about 8 km/sec, the associated impact angle is less than $\sim 5°$ for a meteorite of $\bar{h} = 20$ m and less than $\sim 4°$ for a meteorite of $\bar{h} = 40$ m. Combining these data, with those shown in Figure 1, we see that the only possible rebound angles are less than 3° and most are less than 2°. We have used these rebound angles to compute the after-ricochet trajectories of a meteorite of $\bar{h} = 40$ m, and the conditions at second impact. The computer-generated results are shown in Table 4. In all cases there is a significant reduction in velocity at second impact and, in every case but one, the second impact angle is less than 2°. The velocities at second impact would actually be somewhat less than those shown since we did not consider any energy (and velocity) loss due to the initial impact and ricochet. Atmospheric decelera-

tion after rebound is most effective for the higher velocity projectiles, so there is not a great deal of difference between the velocities and angles of the various cases at second impact—velocities varying from 3.4 to 5.0 km/sec and impact angles from $-0.6°$ to $-2.4°$. At these lower velocities and very low incident angles we feel that such a meteorite would most likely tumble and skid to rest without ricocheting a second time. Since aluminum projectiles *vertically* impacting sand targets at 2.5 km/sec remain essentially intact (although severely deformed), we expect a nickel-iron meteorite to survive such a skid to rest essentially intact.

Probabilities of Impact Survival

If certain pre-atmospheric trajectories will permit the impact survival of a Chinguetti-size meteorite, then there must be an envelope or entry corridor containing these trajectories. An unguided, extraterrestrial body on a collison course with the earth may or may not encounter this corridor. To a first approximation, the probability of a "favorable" encounter is merely the ratio of the cross-sectional area of the annular ring defining the entry corridor to the cross-sectional area of the earth itself:

$$P \approx \frac{2\pi r \Delta r}{\pi r^2} \approx \frac{2\Delta r,}{r} \qquad (6)$$

where $\triangle r$ is the width of the annular ring and r is the earth's radius. To be sure, the equation is not precise, nor is it strictly the equation of applicability since the earth's gravity field creates an effective capture cross-section and an annular entry corridor both of which are larger than the comparable terms in equation (6). A precise derivation, however, is complex and, considering the approximations and assumptions already made, the increase in precision would be meaningless. The first approximation is at worst within a factor of 2 of a more precise derivation—for a meteorite with the lowest possible geocentric velocity (11.2 km/sec). The approximation improves as geocentric velocities increase.

For an exponential atmosphere, $\triangle r$ between any two pre-atmospheric trajectories can be determined from the ratio of their conic perigee parameters since these parameters vary directly with air density (equation 1). The atmospheric density changes by a factor of 10 for every 16 km change in altitude and the corridor width is simply:

$$\Delta r = \log_{10} (Fp_1/Fp_2) \times 16 \text{ km} \qquad (7)$$

The upper limit to any entry corridor will be a trajectory resulting in just enough atmospheric braking to transfer the incoming body to an unstable elliptical orbit, which will decay and lead to atmospheric entry on a subsequent pass. For all practical purposes this atmospheric entry will be identical to that for a body with circular satellite velocity, regardless of the initial encounter velocity. (Thus all the curves in Figures 2 and 3 degenerate to the same point). Beyond this limiting trajectory the incoming body will swing around the earth on a nonreturn hyperbolic trajectory. The nonreturn boundaries for zero-lift bodies with initial velocities of 13 and 16 km/sec are characterized by F_p's of 0.036 and 0.10, respectively (Chapman, 1960, fig. 14). The lower corridor boundary can be any arbitrarily chosen trajectory whatsoever. For example, Table 3 describes the atmospheric behavior of incoming bodies with initial velocities of 13 km/sec and pre-atmospheric trajectories characterized by $F_p = 0.466$. The ratio $0.466/0.036 = 12.9 = 10^{1.11}$, so

$$\Delta r = 1.11 \times 16 = 17.8 \text{ km} \qquad (8)$$

The concomitant, approximate probability of an unguided, incoming body (with initial velocity of 13 km/sec) encountering this corridor is

$$\frac{2 \times 17.8}{6 \times 10^3} \approx 0.006. \qquad (9)$$

This probability can be related to survival as follows: In Figure 3, the 13 km/sec curve encompasses possible impact velocities and angles for a meteorite of $\bar{h} = 40$ m. Table 3 was used to generate one point on that line—the point labeled .006. For that class of meteorites encountering the earth, characterized by $\bar{h} = 40$ m and $V_i = 13$ km/sec, 0.6 percent will impact at velocities and angles given by the segment of the 13 km/sec curve lying between the .006 point and the atmospheric braking point. All the other numbered points in Figures 2 and 3 were derived in the same way and have the same meaning.

Discussion and Conclusions

From the foregoing sections it should be clear that meteoritic masses very much greater than 1000

tons can survive a terrestrial impact under certain conditions. In fact, mass is not strictly the governing parameter and a meteorite even more massive than the specific Chinguetti-size bodies considered herein could also survive a terrestrial impact, provided the critical parameter—its linear dimension parallel to the atmospheric flight path—remains modest. The probability of survival, however, will decrease with increasing mass because of the need for a meteorite to assume a favorable flight attitude in the atmosphere. If a meteorite has a stable flight attitude, it will be with the minimum dimension oriented parallel to the flight path. For the present study we have assumed that if all dimensions are small enough to permit significant deceleration by the atmosphere, then the meteorite will become oriented in its stable attitude prior to maximum deceleration. This holds for the maximum dimension considered (100 m) on most shallow-angle entry trajectories. As the other dimensions increase beyond this, the pre-atmospheric orientations that will lead to stable atmospheric orientation are reduced and thus the survival probability decreases, although it never goes to zero as long as the minimum dimension is fixed.

With respect to the specific question of the possible existence of the Chinguetti meteorite, we reiterate the fact that the curves, boundaries and probabilities displayed in Figures 2 and 3 are all approximate. Nevertheless, the data are surely precise enough for order of magnitude conclusions. Bearing this in mind we estimate the survival probability of a Chinguetti-size meteorite (whose geocentric velocity lies somewhere between 11.2 and 20 km/sec) to be between 0.1 and 1 percent. Put another way, such a body has between one chance in 100 and one chance in 1000 of surviving a terrestrial impact. Now, based very crudely on the number of more recent, known and probable terrestrial impact craters due to meteorites with kinetic energies similar to the hypothetical Chinguetti body, the upper limit to the encounter frequency of such bodies with the earth's *land* surface cannot exceed one per 10^6 years (over the past few tens of million years). This means that the expected survival (and potentially recoverable) rate can be no higher than one every 10^8 to 10^9 years. Because the complete oxidation (and thus destruction) of large iron meteorites on the earth's surface is accomplished in a time that is short compared to 100 million years, we are led to the following conclusions. First, the Chinguetti meteorite can exist. Second, from a purely statistical aspect, the odds are heavily against its existence. Of course, the specific existence or nonexistence of the Chinguetti meteorite is not purely a statistical problem, since it involves a reported observation. Thus there are only two possible probabilities: Either the observer, Gaston Ripert, was mistaken (or lied), or his report was correct. In the former case, the probability that the Chinguetti meteorite exists is 0. In the latter case, the probability is 1. No other probability calculations are meaningful, nor is it possible to discriminate between 0 and 1 at this point. The combination of survival and weathering rates, however, does tell us, clearly and irrevocably, that if the Chinguetti meteorite does indeed exist, it must be, now and forever in the history of mankind, unique.

Literature Cited

Chapman, D. R.
1959. An Approximate Analytical Method for Studying Entry into Planetary Atmospheres. *NASA Technical Report,* R-11: 44 pages.
1960. An Analysis of the Corridor and Guidance Requirements for Supercircular Entry into Planetary Atmospheres. *NASA Technical Report,* R-55: 47 pages.

Chapman, D. R., and A. K. Kapphahn
1961. Tables of Z Functions for Atmospheric Entry Analysis. *NASA Technical Report,* R-106: 271 pages.

Hawkins, G. S.
1964. *Meteors, Comets and Meteorites.* 134 pages. New York: McGraw Hill.

Heidi, F.
1964. *Meteorites.* 144 pages. Chicago: The University of Chicago Press.

Lacroix, A.
1924. On a New Type of Meteoric Iron Found in the Desert of Adrar in Mauritania. *Comptes Rendus,* 179:303–313.

Mason, B.
1962. *Meteorites.* 274 pages. New York: John Wiley and Sons.

Monod, Th.
1952. Le problème de la météorite de Chinguetti. *Bulletin de la Direction des Mines, Gouvernement Général de l'Afrique Occidentale Francaise,* 15 (2):405–412. [Translated by L. F. Brady, "The Problem of the [French West Africa] Chinguetti Meteorite [CN= 0127,202:]", and published, in 1955, in *Meteoritics,* 1 (3):308–314.]

Wood, J. A.
1968. *Meteorites and the Origin of Planets.* 117 pages. New York: McGraw Hill.

Preliminary Data on Eight Observed-Fall Chondritic Meteorites

Roy S. Clarke, Jr., Eugene Jarosewich,
and Albert F. Noonan

ABSTRACT

Eight observed-fall meteorites, five olivine-bronzite chondrites and three olivine- hypersthene chondrites, have been chemically analyzed and assigned a Van Schmus-Wood petrographic classification. The names, dates of fall, and classification of the meteorites are as follows; Ankober, 7 July 1942, H4; Schenectady, 12 April 1968, H4; Dwaleni, 12 October 1970, H4 dark fraction and H6 light fraction; Kiffa, 23 October 1970, H5; Kabo (Gwarzo), 25 April 1971, H4 dark fraction and H5 light fraction; Tathlith, 5 October 1967, L6; Malakal, 9–15 August 1970, L5; Wethersfield, 8 April 1971, L6.

Introduction

During the past several years we have obtained a number of newly fallen chondritic meteorites. These specimens, or samples from them, have been made available as promptly as possible to investigators engaged in time-dependent studies. Distribution of samples for other purposes has also been made, depending upon availability of specimen material. In an effort to support these outside studies, as well as to fulfill our curatorial responsibilities, we have undertaken preliminary examinations of each meteorite. Typically, this includes obtaining as much information as possible about the circumstances of fall and recovery of the meteorite, performing a bulk chemical analysis, a preliminary petrographic examination, and an electron microprobe examination of the major minerals. Our objective is sound classification, and the data is circulated promptly to those who have need for it. This paper summarizes data on eight observed-fall chondrites.

The meteorites studied are listed by date of fall in Table 1, together with their geographic location, date and time of fall, and the weight of material recovered. Bulk chemical analyses and calculated normative mineral compositions are given in Table 2. In Table 2 the meteorites are listed in order of date of fall within the two major classification groups. The first five meteorites, Ankober, Schenectady, Dwaleni, Kiffa, and Kabo are all olivine-bronzite chondrites (H-group meteorites). The last three meteorites, Tathlith, Malakal, and Wethersfield are olivine-hypersthene chondrites (L-group meteorites).

RELATED LITERATURE.—A number of papers have been published giving cosmic-ray exposure ages and rare gas measurements on meteorites from our list of eight. References are given here, with the names of the meteorites studied, for papers that are not mentioned in our discussion: Bogard, et al. (1973), Tathlith, Malakal, Dwaleni, Kiffa, Wethersfield, and Kabo; Cressy (1970), Tathlith; Fireman and Goebel (1970), Ankober; Fireman and Spannagel (1971), Dwaleni; Reynolds, et al. (1971), Dwaleni; Smith and Firemen (1973), Dwaleni, Kabo, Kiffa, Malakal, and Wethersfield; Tobailem and Lalou (1972), Kiffa; Heimann, Parekh, and Herr (1974), Malakal.

ACKNOWLEDGMENTS.—The Smithsonian Institution's Center for Short-Lived Phenomena has been responsible for obtaining our specimens of the Malakal, Dwaleni, Kiffa, and Kabo meteorites. We are indebted to the Center's director, Robert A. Citron, and to David Squires for their assistance. Joseph A.

Roy S. Clarke, Jr., Eugene Jarosewich, and Albert F. Noonan, Department of Mineral Sciences, National Museum of Natural History, Smithsonian Institution, Washington, D.C. 20560.

TABLE 1.—*Recovery information on eight observed-fall chondrites* (listed by date of fall)

Name	*Location*	*Date*	*Time*	*Recovered Weight*
Ankober, Ethiopia	9°32′N, 39°43′E	7 Jul 42	10:00 a.m. local time	7 kg
Tathlith, Saudi Arabia	19°21′N, 43°44′E (recovery site, both ±3′)	5 Oct 67	5:15–5:30 a.m. local time	∿2 kg
Schenectady, New York	42°51′39″N, 73°57′1″W	12 Apr 68	8:30 p.m. local time	283 g
Malakal, Sudan	9°30′N, 31°45′E	9–15 Aug 70	Not known	>2 kg
Dwaleni, Swaziland	27°12′S, 31°19′E	12 Oct 70	10:30 hours South African time	3.2 kg
Kiffa, Mauritania	16°35′N, 11°21′W	23 Oct 70	About 2:55 p.m. GMT	∿1.5 kg
Wethersfield, Connecticut	41°42′N, 72°39′E	8 Apr 71	2–6 a.m. local time (0700–1100 hrs. GMT)	350 g
Kabo, Nigeria	11°51′N, 8°13′E	25 Apr 71	About 4:30 p.m. local time (15.30 GMT)	>10 kg

Nelen did preliminary electron microprobe examinations on several of these meteorites. A grant from the National Aeronautics and Space Administration provided funds for the purchase of the Ankober and Wethersfield meteorites, and to pay recovery expenses for the Kabo meteorite. Dr. Robert Hutchison, British Museum (Natural History) read the manuscript and provided us with several helpful suggestions.

Meteorite Descriptions

The procedures and techniques used in this study are standard for this type of investigation. Chemical analyses were perfomed following the general procedures described earlier (Jarosewich, 1966). Normative mineral compositions were calculated from the chemical data. Olivine and pyroxene compositions were determined using the electron microprobe. Individual mineral grains were selected, and Fe, Ca, and Mg were determined simultaneously. The number of grains analyzed depended both on the homogeneity of the sample and on their availability in the sections at hand. Olivine compositions are reported as mole percent fayalite (Fa) and pyroxene compositions are mole percent ferrosilite (Fs). A petrographic classification is given for each meteorite following the procedure of Van Schmus and Wood (1967).

In the following sections, brief descriptions of each of the meteorites are given in the order in which they are listed in Table 2.

ANKOBER, BOLEDE, ETHIOPIA

The Ankober meteorite fall of 7 July 1942 was observed and attracted local attention at the time. We first heard of it more than 10 years later, when Professor Guglielmo Sensi (1953) of the Pasteur Institue, Addis Ababa, wrote in behalf of the owner, Ato Assafa Abye. Professor Sensi reported that the meteorite had been incandescent in the air and that it had fallen into a field of whitish clay causing no damage. A more dramatic version of the fall attributed to Ato Assafa Abye reflects the excited state of the local inhabitants: "After having touched the earth, it sank to a depth of about one meter, giving forth steam. The natives of the region dug at the ground to remove it, but it was still burning so much they could not take it immediately. They therefore left it in place, saying that it must be a shell fired by the English." In early 1954 we received a specimen of the meteorite (USNM 2609) and its identification was confirmed by E. P. Henderson. In 1967 Robert Citron, at that time manager of the Smithsonian Institution Astrophysical Observing Station in Ethiopia, obtained the main mass of the meteorite (USNM 3399). The essentially complete individual stone of 6955 g was subsequently deposited in the meteorite collection in Washington.

TABLE 2.—*Analytical data on observed-fall chondrites* (values in weight percent unless otherwise indicated; chemical analyses, Eugene Jarosewich; microprobe Fa-Fs determinations, Albert F. Noonan; classifications according to Van Schmus and Wood, 1967)

Constituent	*Ankober* *USNM 3399* *H4*	*Schenectady* *USNM 5722* *H4*	*Dwaleni* *USNM 5447* *H4,H6*	*Kiffa* *USNM 5490* *H5*	*Kabo* *USNM 5611* *H4,H5*	*Tathlith* *USNM 5448* *L6*	*Malakal* *USNM 5446* *L5*	*Wethersfield* *USNM 5596* *L6*
				ANALYSES				
Fe	13.96*	15.01*	17.23	17.65	17.56	7.61	7.56	7.00
Ni	1.71	1.72	1.75	1.77	1.80	1.14	1.18	1.25
Co	0.10	0.09	0.09	0.09	0.09	0.06	0.05	0.06
FeS	5.29	5.29	5.21	5.62	4.82	6.58	4.30	5.46
SiO_2	35.25	36.20	36.49	36.14	36.54	39.44	40.38	39.42
TiO_2	0.12	0.12	0.12	0.12	0.12	0.14	0.14	0.12
Al_2O_3	2.32	2.25	2.30	2.14	2.15	2.40	2.14	2.26
Cr_2O_3	0.55	0.55	0.51	0.52	0.53	0.52	0.50	0.50
FeO	13.05*	11.77*	9.52	9.15	9.60	13.84	15.32	15.48
MnO	0.32	0.32	0.27	0.31	0.33	0.33	0.28	0.34
MgO	22.86	23.00	23.16	23.26	23.24	24.35	24.88	24.64
CaO	1.72	1.77	1.72	1.77	1.72	1.88	1.85	1.82
Na_2O	0.84	0.83	0.88	0.82	0.82	0.99	0.95	1.05
K_2O	0.12	0.10	0.09	0.10	0.08	0.11	0.10	0.11
P_2O_5	0.33	0.29	0.22	0.22	0.28	0.21	0.17	0.18
H_2O+	0.45	0.69	0.18	0.00	<0.1	<0.1	<0.1	0.00
H_2O-	0.36	0.23	0.03	0.10	0.03	0.11	0.03	0.10
C	0.10	0.12	0.04	0.01	0.01	0.03	0.03	0.01
Total	99.55	100.35	99.81	99.79	99.72	99.74	99.86	99.80
Total Fe	27.47	27.52	28.41	28.33	28.09	22.55	22.30	22.50
				NORMS				
Olivine	43.6	38.7	33.9	33.6	33.1	43.3	45.4	49.0
Orthopyroxene	18.8	23.2	25.8	25.6	27.5	23.6	24.6	19.5
Diopside	3.4	3.8	4.0	4.4	3.8	5.0	5.5	5.4
Albite	7.1	7.0	7.4	6.9	6.9	8.4	8.0	8.9
Anorthite	2.2	2.1	2.1	1.9	2.0	1.8	1.3	1.1
Orthoclase	0.7	0.6	0.5	0.6	0.5	0.6	0.6	0.6
Chromite	0.8	0.8	0.8	0.8	0.8	0.8	0.7	0.7
Ilmenite	0.2	0.2	0.2	0.2	0.2	0.3	0.3	0.2
Apatite	0.8	0.7	0.5	0.5	0.7	0.5	0.4	0.4
Nickel-Iron	15.8	16.8	19.1	19.5	19.4	8.8	8.8	8.3
Troilite	5.3	5.3	5.2	5.6	4.8	6.6	4.3	5.5
				OLIVINE-PYROXENE COMPOSITIONS (mole percent)				
Fa	19	19	20 L 16–19 D	18	19 L 19 D	26	25	25
Fs	17	17	17 L 15–18 D	16	17 L 14–20 D	21	21	21

*Metallic Fe values are low and calculated FeO values are high in the Ankober and Schenectady analyses. This is primarily due to oxidation of the sample prior to analysis. The brown color of the analysis powder and the high total water values are consistent with this interpretation.

L=light fraction, D=dark fraction.

The stone is blocky in shape and about 90 percent of its surface is covered with fusion crust. Late-stage spalling of fusion crust was restricted to edges and corners where the essentially flat surfaces of the meteorite intersect. The stone appears to have tumbled during flight and there is no ob-

vious anterior surface. One of the main surfaces is markedly less smooth than the other surfaces. This suggests a break-up at an early stage during atmospheric passage and the probability that the Ankober fall produced at least two individuals. The fusion crust is brown in color, probably due to oxidation by atmospheric moisture. It is assumed that the stone has been protected from the weather since shortly after its recovery, but we have no certain information on this prior to our obtaining the specimen.

Freshly cut surfaces of Ankober quickly become brown in color due to limonitic staining. Slices are compact and hard, due largely to the metal forming a continuous structural framework. Under low magnification (× 10) cut and broken surfaces are seen to have a surprisingly open structure. Large numbers of submillimeter size cavities are present, into which chondrules, euhedral crystals, and crystal and chondrule fragments protrude. The meteorite has a very uniform texture with no obvious brecciation or veining.

In thin section Ankober is seen to consist of distinct complete and broken chondrules in a matrix of fine-grained silicates and metallic phases. Chondrules do not normally exceed one millimeter in diameter, but a few unusually large ones up to 6 mm across were observed. Minerals present include olivine, bronzite, clinobronzite, taenite, kamacite, and troilite, with minor amounts of chromite, whitlockite, and copper. Forty microprobe analyses indicated a constant silicate composition of Fa_{19} for olivine and Fs_{17} for the low-Ca pyroxene. Abundant clinobronzite occurs both in chondrules and matrix, often with devitrified glass. Ankober is classified as an H4 chondrite.

Schenectady, Schenectady County, New York

The Schenectady meteorite fall of 12 April 1968 produced an individual stone that was recovered following a widely observed fireball. Details of the fall and recovery have been reported by Fleischer, et al. (1970). These authors also classified the meteorite, presented rare gas data, radioactive-ages and cosmic-ray track information. The meteorite is the property of The Schenectady Museum, Schenectady, New York, and it was loaned to us for study in August of 1969.

The physical characteristics of Schenectady are similar to those described for Ankober. Exposure to moisture from the air and during sawing has resulted in limonitic staining. The fusion crust however, is still black. The stone is compact and hard, but under low magnification (× 10) many small cavities can be seen. The openness of the structure, however, is less than that observed in Ankober. The stone has a uniform texture, free of brecciation or veining.

Chondrules are abundant, distinct, and as large as two millimeters in diameter. They are seen in thin section to be in a relatively coarse-grained matrix. The chondrules are composed of olivine, orthobronzite, minor clinobronzite, and devitrified glass. Forty-five microprobe analyses show the principal silicate minerals to be essentially homogeneous, with an olivine composition of Fa_{19} and a pyroxene composition of Fs_{17}. Other minerals identified were taenite, kamacite, troilite, chromite, whitlockite, and copper. The concentration of copper was unusually high with as many as 20 grains found in one polished section. Schenectady is classified as an H4 chondrite.

Dwaleni, Swaziland

Loud explosions accompanied the fall of the Dawleni meteorite near the Swaziland-Transvaal border on 12 October 1970. Three essentially completely fusion-crusted individuals were recovered promptly from a 12 km^2 area centering on the location given in Table 1. The individuals weighing 2.37, 0.51, and 0.35 kg were recovered from 15 to 18 cm below ground level in moist soil. We received two pieces of the 0.35 kg stone (156 g and 10 g) on 3 November 1970. This sample material and information on the fall and recovery were sent to us by J. G. Urie, Acting Director, Geological Survey and Mines Department, Mbabane.

The Dwaleni chondrite is a compact rock with a pronounced light-dark structure (Figure 1). The one surface available to us shows approximately equal areas of light and dark material, with thin dark veins penetrating both types. The light-colored areas are of uniform composition, have sharp outline and are tightly bound to the darker material. Bogard, et al. (1973:2429) have noted that the dark fraction of Dwaleni is unusually rich in rare gases.

Both light and dark materials undoubtedly have similar bulk compositions, but minor differences in

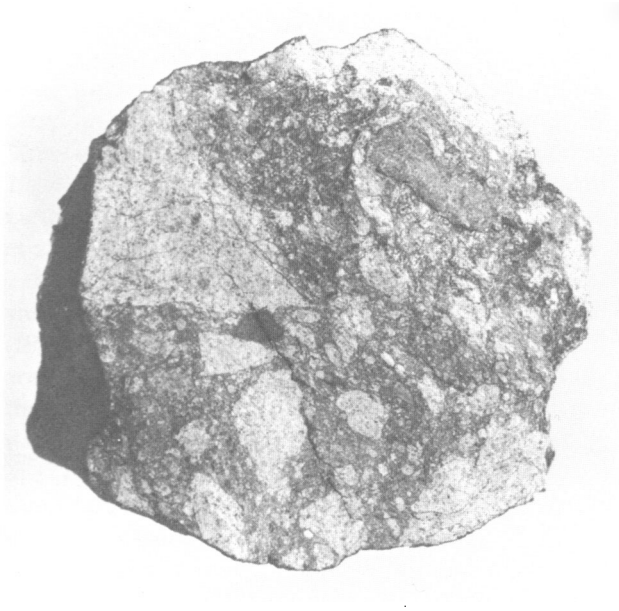

FIGURE 1.—The Dwaleni, Swaziland, chondrite. A broken surface showing light-dark structure and veining. One and a half times actual size.

individual mineral compositions between these two materials were noted. The lighter material contains relatively large crystals of homogeneous olivine, bronzite, and plagioclase. Chondrules are absent or indistinct. Twenty-five grain analyses gave olivine, pyroxene, and plagioclase compositions of Fa_{20}, Fs_{17} and An_{12}. The petrographic classification of this material is H6. The dark material, however, contains olivine and pyroxene of slightly higher magnesium content and of somewhat variable composition. Eighteen grains analyses gave olivine and bronzite compositions of Fa_{16-19} and Fs_{15-18}. Chondrules up to one millimeter in diameter are well defined and contain turbid glass. The petrographic classification of the dark material is H4. Kamacite, taenite, troilite and minor chromite, and copper occur in Dwaleni, mostly in the light-colored fraction.

KIFFA, MAURITANIA

At 2:55 p.m. GMT on 23 October 1970, detonations were heard and a smoke cloud observed in the neighborhood of the town of Kiffa. About 10 a.m. the next morning a meteorite specimen was found by a child 8 km southwest of the town. It had made a shallow hole about 20 cm deep in fine sand. The meteorite shattered into many pieces on landing and less than 1.5 kg was recovered. We received a 36 g piece on 17 February 1971 from M. Henri Gruenwald, Chef de Service Géologique, Direction Des Mines et de la Géologie, Nouakchott. M. Gruenwald was also our source of information on the fall and recovery of the meteorite.

The Kiffa meteorite is a friable gray chondrite with distinct chondrules reaching a maximum diameter of approximately 2 mm. The chondrules can be separated with ease from the fine-grained white matrix, which appears to cement the chondrules and metal phases together. The texture is quite uniform and there are no obvious foreign inclusions. Olivine and bronzite are the principal silicate minerals in both chondrules and matrix. Clinobronzite is rare. Twenty microprobe analyses show chondrule olivine and pyroxene to be constant in composition, the fayalite and ferrosilite value being Fa_{18} and Fs_{16}, respectively. The white matrix is composed, at least in part, of what appears to be comminuted chondrules and devitrified glass. In addition to olivine and bronzite, clinobronzite, kamacite, taenite, troilite, chromite, and whitlockite were identified. Although chondrules are distinct, Kiffa is classified an H5 chondrite principally on the basis of silicate homogeneity and the presence of only minor clinopyroxene.

KABO, GWARZO DISTRICT, KANO STATE, NIGERIA

The name Gwarzo has been used as a synonym for Kabo.

The Kabo meteorite shower of 25 April 1971 attracted considerable local attention, and at least four stones with a total weight of over 10 kg were recovered. We received a 134 g sample on 9 June 1971. Both the sample and a description of the fall and recovery were provided by Professor M. O. Oyawoye, Geology Department, University of Ibadan. A detailed description of this meteorite has been prepared by Hutchison and coworkers (Hutchison, et al., 1973).

Kabo is an ordinary chondrite with a subtle light-dark structure. Bogard, et al. (1973) have shown that its dark fraction contains an enrichment of several trapped rare gases. Veining and distorted metal grains in Kabo seem to be preferentially associated with the dark fraction. Chondrules, which

range up to two millimeters in diameter in both fractions, are well defined in the dark fraction and less well defined in the light fraction. Clinobronzite occurs in both the light and dark fractions.

The minerals identified in Kabo are olivine, bronzite, clinobronzite, kamacite, taenite, troilite, chromite, ilmenite, whitlockite, chlorapatite, and copper. Thirty grain analyses in the dark fraction show pyroxene variability over the composition range Fs_{14-20}. The olivines, however, are essentially homogeneous with a composition of Fa_{19}. Glass occurs as fragments and in chondrules in minor amounts, indicating that the dark fraction is less equilibrated than the light fraction. Thirty olivine and pyroxene grain analyses in the light fraction indicate homogeneous compositions of Fa_{19} and Fs_{17}. The textural and compositional differences result in an H4 classification for the dark fraction and an H5 classification for the light fraction.

Tathlith, Saudi Arabia

The Tathlith meteorite fell early in the morning on 5 October 1967 about 15 km from the village of Tathlith. A single blocky-shaped, fusion-crusted individual was recovered immediately. The exact weight of the stone is not known to us, but estimates based on photographs indicate that it weighed about 2 kg (Figure 2). We received a 205 g slice of Tathlith from Glen F. Brown, Chief, U.S. Geological Survey Field Party, Jiddah, Saudi Arabia on 22 November 1967. It had been identified as a meteorite by Gerhard W. Leo in the U. S. Geological Survey Laboratories in Jiddah. The main mass of the meteorite is believed to be in the possession of the Emir of Abha.

Tathlith is a highly recrystallized gray chondrite of uniform texture. Chondrules range in size up to 3 mm in diameter and are easily discernible on a cut or broken surface. In thin section, however, the chondrules appear relict and intergrown with granular plagioclase and metal. Minerals identified are olivine, hypersthene, clinohypersthene, plagioclase, kamacite, taenite, troilite, chromite, and copper. Twenty grain analyses show the major silicates to be homogeneous with olivine composition of Fa_{26} and hypersthene of Fs_{21}. The plagioclase is also homogeneous with a composition of An_{10}. Small amounts of clinohypersthene, which are probably remnant, occur in some of the larger chondrules. Tathlith is an L6 chondrite.

FIGURE 2.—The Tathlith, Saudi Arabia, meteorite. *a*, Cut surface from which our 205 g specimen was removed. *b*, Meteorite sitting on cut surface. Scale in inches. Photographs by Gerhard W. Leo, U.S. Geological Survey.

Malakal, Upper Nile Province, Sudan

The fall of the Malakal meteorite during the first half of August 1970 into an active military area has been described by Dawoud and Vail (1971). The meteorite fragment that reached Khar-

toum on 15 August 1970, weighed about 2 kg, and photographs of that piece indicate that it is a part of a considerably larger stone. It is not known if other fragments were recovered. We received a 194 g piece and 4.4 g of fragments from Professor J. R. Vail of the University of Khartoum on 3 November 1970. A comprehensive description of the Malakal meteorite has recently been published by El Rabaa, et al. (1974).

Malakal is a unique meteorite from the point of view of its cosmic-ray history. Cressy and Rancitelli (1974) note that cosmic-ray produced ^{26}Al and ^{53}Mn are anomalously high in Malakal. They conclude that the meteorite must have experienced a two-stage irradiation, and that during the earlier stage Malakal was exposed to a cosmic-ray flux several times larger than that incident on other chondrites or that measured by space probes.

Malakal is a moderately veined and brecciated hypersthene chondrite, with the dark and apparently shock-produced vein material also occurring in patches. Kamacite and troilite also appear to have been partially shock melted. Their interfaces with each other are frequently lacy and diffuse, as are their interfaces with surrounding silicates. Abundant spherules of metal or sulfide are observed within the silicates near the metallic phases. Chondrules are present, ranging up to 5 mm in diameter, and the silicate matrix is moderately recrystallized. The minerals identified are olivine, hypersthene, kamacite, taenite, troilite, ilmenite, chromite, and whitlockite. Twenty grain analyses show the major silicates to be homogeneous with olivine composition of Fa_{25} and pyroxene of Fs_{21}. Malakal is classified as an L5 chondrite.

Wethersfield, Hartford County, Connecticut

The Wethersfield meteorite fell into the home of Mr. and Mrs. Paul J. Cassarino during the early morning hours of 8 April 1971. It penetrated a roof of asbestos shingles and three-quarter-inch plywood, then passed through four inches of insulating material and nearly went through a half-inch sheetrock ceiling in a second floor room. Debris on the floor of the room called attention to the presence of a 350 g meteorite precariously suspended in the broken ceiling. Richard E. McCrosky of the Smithsonian Astrophysical Observatory, Cambridge, visited the Cassarino's and obtained the specimen for scientific study and preservation. He also canvassed the surrounding area and made numerous inquiries about the possibility of other pieces having been found. Only the one specimen was recovered, and no observations were reported that would allow fixing the time of fall more precisely.

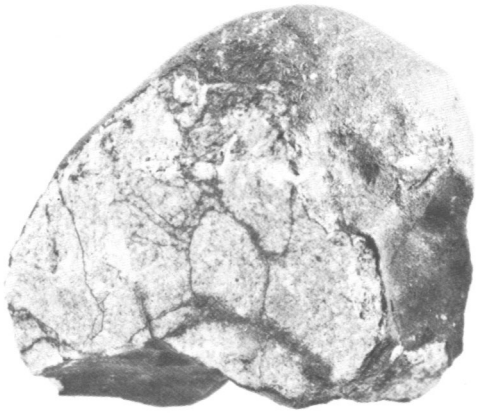

FIGURE 3.—The Wethersfield, Connecticut, chondrite. The bottom left side of the photograph shows posterior fusion crust and spalled areas of crust. The bottom center area shows a broken surface and extensive interior veining.

The meteorite as found was largely covered with a dark fusion crust. Areas where the fusion crust had spalled late in flight covered 10 to 15 percent of the surface. The largest single surface covering nearly half of the specimen, was smooth and rounded and appeared to have been a leading surface during atmospheric flight. The other surfaces were more irregular and the opposite surface appears to have been a posterior surface. Its fusion crust is lighter in color, more vesicular, and it has small areas of the darker anterior fusion crust deposited on it. This area of posterior fusion crust is shown in the central area of Figure 3.

Wethersfield is a gray, highly recrystallized chondrite with black veins and patches of black material (Figure 3). This black material appears to have been produced by shock. Relict chondrules range up to 2 mm in diameter, with a few large ones approaching 5 mm. Fifteen microprobe grain analyses show the silicates to be homogeneous, with an olivine composition of Fa_{25} and hypersthene of Fs_{21}. Other minerals identified were kamacite, taenite, troilite, chromite, and whitlockite. It is classified as an L6 chondrite.

Literature Cited

Bogard, D. D., M. A. Reynolds, and L. A. Simms
1973. Noble Gas Concentrations and Cosmic Ray Exposure Ages of Eight Recently Fallen Chondrites. *Geochimica et Cosmochimica Acta,* 37:2417–2433.

Cressy, Philip J. Jr.
1970. Multiparameter Analysis of Gamma Radiation from the Barwell, St. Séverin and Tathlith Meteorites. *Geochimica et Cosmochimica Acta,* 34:771–779.

Cressy, P. J., Jr., and L. A. Rancitelli
1974. The Unique Cosmic-Ray History of the Malakal Chondrite. *Earth and Planetary Science Letters,* 22: 275–283.

Dawoud, A. S., and J. R. Vail
1971. Malakal Meteorite, Sudan. *Nature: Physical Science,* 229:212–213.

El Rabaa, S. M., A. M. Daminova, M. I. Dyakonova, L. G. Kvasha, L. K. Levskii, and A. V. Fisenko
1974. The Results of the Investigation of the Malakal Chondrite. *Meteoritika,* 33:83–89.

Fireman, E. L., and R. Goebel
1970. Argon 37 and Argon 39 in Recently Fallen Meteorites and Cosmic-Ray Variations. *Journal of Geophysical Research,* 75:2115–2124.

Fireman, Edward L., and Gert Spannagel
1971. Fresh Meteorites in 1970 and the Cosmic-Ray Gradient. *Chemie der Erde,* 30:83–101.

Fleischer, R. L., E. Lifshin, P. B. Price, R. T. Woods, R. W. Carter, and E. L. Fireman
1970. Schenectady Meteorite. *Icarus,* 12:402–406.

Heimann, M., P. P. Parekh, and W. Herr
1974. A Comparative Study on ^{26}Al and ^{53}Mn in Eighteen Chondrites. *Geochimica et Cosmochimica Acta,* 38: 217–234.

Hutchison, R., D. E. Ajakaiye, C. J. Elliott, and F. A. Fry
1973. The Kabo, Nigeria, Meteorite Fall. *Mineralogical Magazine,* 39:340–345.

Jarosewich, E.
1966. Chemical Analyses of Ten Stony Meteorites. *Geochimica et Cosmochimica Acta,* 30:1261–1265.

Reynolds, M. A., D. D. Bogard, and C. M. Polo
1971. Dwaleni—A New Gas-Rich Chondrite (Abstract). *E.O.S.,* 52:269.

Sensi, Guglielmo
1953. [Letter from Professor Sensi to the Smithsonian Institution.] Accession file 202751, Office of the Registrar, Smithsonian Institution.

Smith, S., and E. L. Fireman
1973. Ages of Eight Recently Fallen Meteorites. *Journal of Geophysical Research,* 78:3249–3259.

Tobailem, Jacques, and Claude Lalou
1972. Age d'exposition de la météorite Kiffa. *Comptes Rendus des Séances de L'Académie des Sciences,* Series B, 274 (21):1185–1187.

Van Schmus, W. R., and J. A. Wood
1967. A Chemical-Petrologic Classification for the Chondritic Meteorites. *Geochimica et Cosmochimica Acta,* 31:747–765.

List of Meteorites in the National Museum of Natural History, Smithsonian Institution

Compiled by Brian Mason

ABSTRACT

A brief history of the meteorite collection in the National Museum of Natural History is followed by a list with data of locality, type, and weight of each specimen.

Introduction

Meteorites formed part of the original collections of the Smithsonian Institution. James Smithson's bequest, besides the endowment fund, included (Goode, 1897:305) "a cabinet, which . . . proves to consist of a choice and beautiful collection of minerals, comprising probably eight or ten thousand specimens. . . . The cabinet also contains a valuable suite of meteoric stones, which appear to be suites of most of the important meteorites which have fallen in Europe during several centuries." In 1854 the then Secretary, Joseph Henry (1854:18), recorded: "The laboratory of the Institution during the past year has been used by Professor J. Lawrence Smith in the examination of American minerals. . . . He also made a series of analyses of meteorites, among which were fourteen specimens belonging to the cabinet of James Smithson." Unfortunately, the specific meteorites from the Smithson collection are not identified, and the meteorite collection was apparently destroyed, along with the rest of Smithson's cabinet, in the 1865 fire.

In 1880 G. P. Merrill, in a manuscript report, noted only six meteorites in the catalog: Imilac, Vaca Muerta, New Concord, Parnallee, Searsmont, and Cold Bokkeveld. The Tucson iron, which should have formed the chief attraction, was not cataloged, although brought to Washington in 1863. The Casas Grandes iron was also received around 1880, being transferred to the Smithsonian Institution along with much other material from the Philadelphia Centennial Exhibition. However, the collection grew rapidly during the next decade, largely through the efforts of F. W. Clarke, who was appointed honorary curator in 1883. In 1889 he published a catalog of the meteorite collection as of October 1888, in which he lists 128 distinct falls and finds; in addition, there were 217 meteorites in the Shephard collection, which was deposited in the museum by Shephard's son in 1886 (and ultimately bequeathed to the Smithsonian Institution in 1915). Considerable duplication existed between the two collections, and many of the specimens in both collections were small fragments.

Since that time the meteorite collection has grown steadily. In 1902, W. Tassin brought the Clarke catalog up to date; the Shephard meteorites were listed along with the museum's collection, and the combined collections contained 348 falls and finds. The most recent published catalog is that by G. P. Merrill, "Handbook and Descriptive Catalogue of the Meteorite Collections in the United States National Museum." The collection at that time comprised 412 independent falls and finds. In the Annual Report of the Smithsonian Institution, E. P. Henderson (1948) noted that the collection had grown to 767 meteorites.

The present collection contains representative material of some 1300 meteorites, or about two-thirds of all known meteorites. The current catalog

Brian Mason, Department of Mineral Sciences, National Museum of Natural History, Smithsonian Institution, Washington, D.C. 20560.

in the Department of Mineral Sciences lists over 5700 individual specimens. This collection ranks in size and comprehensiveness with that of the British Museum (Natural History).

ACKNOWLEDGMENTS.—I wish to thank Mr. R. S. Clarke, Jr., and Mr. A. F. Noonan for much assistance in compiling this list, and Dr. W. R. Van Schmus for some unpublished data on the classification of individual chondrites.

Literature Cited

Clarke, F. W.
1889. The Meteorite Collection of the U.S. National Museum: A Catalogue of Meteorites Represented November 1, 1886. *Report of the Smithsonian Institution, 1885–86,* part 2:255–265.

Goode, G. B.
1897. *The Smithsonian Institution, 1846–1896.* Washington.

Henderson, E. P.
1948. American Meteorites and the National Collection. *Annual Report of the Board of Regents of the Smithsonian Institution,* pages 257–268.

Henry, J.
1854. Report of the Secretary. *Ninth Annual Report of the Board of Regents of the Smithsonian Institution.* 463 pages.

Merrill, George P.
1916. Handbook and Descriptive Catalogue of the Meteorite Collections in the United States National Museum. *United States National Museum Bulletin,* 94.

Tassin, W.
1902. Descriptive Catalogue of the Meteorite Collection in the United States National Museum to January 1, 1902. *Report of the United States National Museum for 1900,* pages 671–698.

Abbreviations

CHONDRITES: (Type, where known, is indicated by a following digit)	Enstatite	E
	Bronzite	H
	Hypersthene	L
	Amphoterite	LL
	Carbonaceous	C
ACHONDRITES:	Aubrite	Ae
	Diogenite	Ah
	Chassignite	Ac
	Ureilite	Au
	Angrite	Aa
	Nakhlite	An
	Howardite	Aho
	Eucrite	Aeu
STONY-IRONS:	Pallasite	P
	Mesosiderite	M
	Siderophyre	S
	Lodranite	Lo
IRONS:	Hexahedrite	Hx
	Octahedrite	O
	Coarsest octahedrite	Ogg
	Coarse octahedrite	Og
	Medium octahedrite	Om
	Fine octahedrite	Of
	Finest octahedrite	Off
	Plessitic octahedrite	Opl
	Ataxite	D
	Anomalous	Anom

List

Weights are given in grams unless otherwise indicated;
"s" indicates that only a thin or polished section is present

Name	*Locality*	*Class*	*Weight*	*Name*	*Locality*	*Class*	*Weight*
Aarhus	Denmark	H	s	Adrian	Texas	H4	1090
Abancay	Peru	Of	9.8	Agen	France	H5	163
Abee	Canada	E4	2950	Aggie Creek	Alaska	Om	984
Abernathy	Texas	L6	83	Aguada	Argentina	L6	8.0
Accalana	Australia	L3	14	Ahumada	Mexico	P	834
Achilles	Kansas	H5	546	Ainsworth	Nebraska	Ogg	1635
Achiras	Argentina	L6	6.8	Akpohon	Canada	Om	64
Adams County	Colorado	H5	569	Akron (1961)	Colorado	L6	70
Adargas	Mexico	Om	24	Alais	France	C1	0.6
ad-Dahbubah	Saudi Arabia	H5	40 kg	Alamogordo	New Mexico	H5	905
Adelie Land	Antarctica	L5	69	Alamosa	Colorado	L6	1784
Adhi Kot	Pakistan	E3	22	Albareto	Italy	L4	1.7
Admire	Kansas	P	22 kg	Albin	Wyoming	P	3200

Name	*Locality*	*Class*	*Weight*
Aleppo	Syria	L6	162
Alessandria	Italy	H5	37
Alexander County	North Carolina	Og	12
al-Ghanim (iron)	Saudi Arabia	O?	500
al-Ghanim (stone)	Saudi Arabia	H6	3755
Alfianello	Italy	L6	680
Algoma	Wisconsin	Om	22
Alikatnima	Australia	D	32
Allegan	Michigan	H5	18 kg
Allende	Mexico	C3	380 kg
Al Rais	Saudi Arabia	C2	132
Alt Bela	Czechoslovakia	Om	10
Altonah	Utah	Of	10 kg
Amates	Mexico	Og	14
Ambapur Nagla	India	H5	45
Amherst No. 1	Nebraska	L6	8017
Amherst No. 2	Nebraska	L6	473
Anderson	Ohio	P	48
Andover	Maine	L6	2791
Andura	India	H6	9.0
Angelica	Wisconsin	Om	331
Angers	France	L6	0.7
Angra dos Reis (stone)	Brazil	Aa	8.5
Ankober	Ethiopia	H4	6964
Anoka	Minnesota	Of	132
Anthony	Kansas	H5	8711
Antofagasta	Chile	P	16 kg
Apoala	Mexico	Om	324
Appley Bridge	Great Britain	LL6	545
Arapahoe	Colorado	L5	422
Arcadia	Nebraska	LL6	1676
Archie	Missouri	H6	3760
Arispe	Mexico	Og	178 kg
Arlington	Minnesota	Om	6140
Arltunga	Australia	D	979
Armel	Colorado	L5	301
ar-Rakhbah	Saudi Arabia	O	395
Arriba No. 1	Colorado	L5	1142
Arroyo Aguiar	Argentina	H5	2.9
Artracoona	Australia	L6	375
Asheville	North Carolina	Om	6.2
Ashfork	Arizona	Og	39
Ashmore	Texas	H5	16
ash-Shalfar	Saudi Arabia	H5	935
Assam	India	L5	7
Assisi	Italy	H5	29
as-Su'aydan	Saudi Arabia	H5	5530
Aswan	Egypt	Om	11
Atarra	India	L4	37
Atemajac	Mexico	L6	8
Athens	Alabama	LL6	206
Atlanta	Louisiana	E5	235
Atoka	Oklahoma	L6	432
Atwood	Colorado	L6	161
Auburn	Alabama	Ogg	235
Augustinovka	USSR	Om	99
Aumale	Algeria	L6	81
Aumières	France	L6	16
Aurora	New Mexico	H4	78
Ausson	France	L5	223
Avanhandava	Brazil	H5	162
Babb's Mill (Troost's Iron)	Tennessee	D	133
Bachmut	USSR	L6	9
Bacubirito	Mexico	Off	997
Bahjoi	India	Og	497
Bald Mountain	North Carolina	L4	222
Baldwyn	Mississippi	L6	0.5
Balfour Downs	Australia	Og	911
Bali	Cameroon	C3	154
Ballinger	Texas	Og	459
Ballinoo	Australia	Opl	1415
Bandong	Java	LL6	56
Bansur	India	L6	0.5
Banswal	India	L5	5.7
Baquedano	Chile	Om	864
Barbotan	France	H5	354
Barea	Spain	M	132
Baroti	India	L6	6.6
Barranca Blanca	Chile	Anom	84
Barratta	Australia	L4	4256
Bartlett	Texas	Om	670
Barwell	Great Britain	L5	1463
Barwise	Texas	H5	290
Bath	South Dakota	H4	1086
Bath Furnace	Kentucky	L6	388
Bear Creek	Colorado	Om	275
Beardsley	Kansas	H5	926
Bear Lodge	Wyoming	Om	3265
Beaver Creek	Canada	H4	731
Beddgelert	Great Britain	H5	17
Beenham	New Mexico	L5	4166
Bella Rocca	Mexico	Om	666
Belle Plaine	Kansas	L6	90
Bells	Texas	C2	0.5
Bellsbank	South Africa	Hx	343
Benares	India	LL6	88
Bencubbin	Australia	Anom	7021
Bendego	Brazil	Og	1980
Benld	Illinois	H6	6.3
Bennett County	South Dakota	Hx	8135
Benton	Canada	LL6	225
Bereba	Upper Volta	Aeu	15
Beuste	France	L5	3
Bhola	Bangladesh	L	116
Bholgati	India	Aho	1.6
Bialystok	Poland	Aho	16
Bielokrynitschie	USSR	H4	56
Billings	Missouri	Om	434
Billygoat Donga	Australia	L6	0.6
Binda	Australia	Aho	228
Bingera	Australia	Hx	197
Bir Hadi	Saudi Arabia	H5	525
Bischtübe	USSR	Og	3358
Bishop Canyon	Colorado	Of	226
Bishopville	South Carolina	Ae	630
Bishunpur	India	LL3	42

Name	*Locality*	*Class*	*Weight*
Bitburg	Germany	Of	168
Bjelaja Zerkov	USSR	H6	10
Bjurbole	Finland	L4	3509
Black Moshannon Park	Pennsylvania	L	29
Black Mountain	North Carolina	Og	18
Blackwell	Oklahoma	L5	2362
Blanket	Texas	L6	1790
Blansko	Czechoslovakia	H6	2.3
Blithfield	Canada	E6	129
Bluff	Texas	L5	8585
Bocas	Mexico	L6	2
Bodaibo	USSR	Of	261
Boelus	Nebraska	LL6	675
Boerne	Texas	H6	537
Bogou	Upper Volta	Og	3107
Boguslavka	USSR	Hx	185
Bohumilitz	Czechoslovakia	Og	325
Bolivia	Bolivia	Og	20 kg
Bondoc Peninsula	Philippines	M	28 kg
Bonita Springs	Florida	H5	34 kg
Boogaldi	Australia	Of	79
Bori	India	L6	136
Borkut	USSR	L5	8.4
Bowden	South Africa	H5	6.5
Bowesmont	North Dakota	L6	116
Boxhole	Australia	Om	7346
Brady	Texas	L6	60
Brahin	USSR	P	20
Braunau	Czechoslovakia	Hx	241
Breece	New Mexico	Om	541
Breitscheid	Germany	H5	s
Bremervörde	Germany	H3	33
Brenham	Kansas	P	89 kg
Brewster	Kansas	L6	986
Bridgewater	North Carolina	Om	54
Briggsdale	Colorado	Om	60
Briscoe	Texas	L5	260
Bristol	Tennessee	Of	126
Britstown	South Africa	Opl	19
Broken Bow	Nebraska	H4	283
Brownfield (1937)	Texas	H3	1182
Brownfield (1964)	Texas	H5	168
Bruderheim	Canada	L6	5515
Bruno	Canada	Hx	17
Budulan	USSR	M	97
Bununu	Nigeria	Aho	331
Burdett	Kansas	H5	203
Burgavli	USSR	Og	130
Bur-Gheluai	Somalia	H5	3513
Burkett	Texas	Og	1173
Burlington	New York	Om	1325
Burnabbie	Australia	H5	65
Burrika	Australia	L6	0.6
Buschof	USSR	L6	14
Bushman Land	South Africa	Of	2865
Bushnell	Nebraska	H4	50
Bustee	India	Ae	78
Butler	Missouri	Opl	639
Butsura	India	H6	18
Cabezo de Mayo	Spain	L6	207
Cabin Creek	Arkansas	Om	34
Cacaria	Mexico	Om	165
Cachari	Argentina	Aeu	1650
Cadell	Australia	L6	71
Calico Rock	Arkansas	Hx	539
Calliham	Texas	L6	230
Cambria	New York	Of	351
Campbellsville	Kentucky	Om	9521
Campo del Cielo	Argentina	Og	196 kg
Camp Verde	Arizona	Og	541
Canellas	Spain	H5	6.5
Cangas de Onis	Spain	H5	1103
Canon City	Colorado	H5	55
Canton	Georgia	Om	409
Canyon City	California	Om	284
Canyon Diablo	Arizona	Og	1675 kg
Cape Girardeau	Missouri	H6	4
Cape of Good Hope	South Africa	D	209
Caperr	Argentina	Om	36
Cape York	Greenland	Om	8178
Carbo	Mexico	Om	24 kg
Cardanumbi	Australia	L5	0.6
Carlton	Texas	Of	1486
Caroline	Australia	H5	13
Carraweena	Australia	L3	44
Carthage	Tennessee	Om	1399
Cartoonkana	Australia	L6	s
Casas Grandes	Mexico	Om	1317 kg
Casey County	Kentucky	Og	92
Cashion	Oklahoma	H4	71
Casilda	Argentina	H5	203
Casimiro de Abreu	Brazil	Om	212
Castalia	North Carolina	H5	17
Castine	Maine	L6	0.2
Cavour	South Dakota	H6	9285
Cedar (Kansas)	Kansas	H6	191
Cedar (Texas)	Texas	H4	2181
Cedartown	Georgia	Hx	9940
Cee Vee	Texas	H5	130
Central Missouri	Missouri	Ogg	5072
Cereseto	Italy	H5	65
Chainpur	India	LL3	114
Chamberlin	Texas	H5	98
Chandakapur	India	L5	32
Channing	Texas	H5	1530
Chantonnay	France	L6	371
Charcas	Mexico	Om	182
Charlotte	Tennessee	Of	182
Charsonville	France	H6	83
Chassigny	France	Ac	23
Château-Renard	France	L6	727
Chaves	Portugal	Aho	s
Chebankol	USSR	Og	57
Cherokee Springs	South Carolina	LL6	7885
Chesterville	South Carolina	Hx	103
Chico	New Mexico	L	s
Chico Mountains	Texas	Hx	173
Chicora	Pennsylvania	LL6	272

Name	*Locality*	*Class*	*Weight*
Chihuahua City	Mexico	Anom	363
Chilkoot	Alaska	Om	5524
Chinautla	Guatemala	Of	162
Chinga	USSR	D	1613
Chinguetti	Mauretania	M	409
Chulafinee	Alabama	Om	119
Chupaderos	Mexico	Om	2516
Cincinnati	Ohio	Hx	32
Clareton	Wyoming	L6	208
Clark County	Kentucky	Om	2069
Claytonville	Texas	L5	198
Cleveland	Tennessee	Om	819
Clover Springs	Arizona	M	1041
Clovis No. 1	New Mexico	H3	284 kg
Coahuila	Mexico	Hx	147 kg
Cobija	Chile	H6	202
Cockarrow Creek	Australia	L6	3.2
Cockburn	Australia	L6	1850
Cocklebiddy	Australia	H5	119
Cocunda	Australia	L6	s
Colby	Wisconsin	L6	3906
Cold Bay	Alaska	P	287
Cold Bokkeveld	South Africa	C2	37
Coldwater (iron)	Kansas	O	4768
Coldwater (stone)	Kansas	H5	5472
Colfax	North Carolina	Om	312
Collescipoli	Italy	H5	127
Colomera	Spain	Anom	133
Comanche (iron)	Texas	Og	550
Concho	Texas	L6	138
Cookeville	Tennessee	Og	459
Coolac	Australia	Og	2067
Coolamon	Australia	L6	s
Coolidge	Kansas	C4	203
Coomandook	Australia	H6	11
Coonana	Australia	H4	s
Coon Butte	Arizona	L6	199
Coopertown	Tennessee	Og	1149
Coorara	Australia	L6	7.6
Cope	Colorado	H5	4147
Copiapo	Chile	Anom	174
Cortez	Colorado	H6	54
Cosby's Creek	Tennessee	Og	1375
Costilla Peak	New Mexico	Om	1849
Cotesfield	Nebraska	L6	17
Covert	Kansas	H5	2966
Cowra	Australia	Opl	61
Coya Norte	Chile	Hx	4850
Crab Orchard	Tennessee	M	2047
Cranberry Plains	Virginia	Of	7.9
Cranbourne	Australia	Og	700 kg
Cranganore	India	L6	10
Cratheus	Brazil	Of	42
Credo	Australia	L6	7.4
Crescent	Oklahoma	C2	s
Cronstad	South Africa	H5	12
Cross Roads	North Carolina	H5	6.5
Crumlin	Ireland	L5	35
Cruz del Aire	Mexico	Of	351
Cuernavaca	Mexico	Om	738
Cubertson	Nebraska	H4	12
Cullison	Kansas	H4	2421
Cumberland Falls	Kentucky	Ae	8640
Cumpas	Mexico	Om	2212
Cushing	Oklahoma	H4	519
Cynthiana	Kentucky	L4	643
Dalgaranga	Australia	M	159
Dalgety Downs	Australia	L5	125 kg
Dalhart	Texas	L5	65
Dalton	Georgia	Om	49 kg
Dandapur	India	L6	57
Daniel's Kuil	South Africa	E6	5
Davis Mountains	Texas	Om	117
Dayton	Ohio	Off	24 kg
Deal	New Jersey	L6	3
Deelfontein	South Africa	Og	105
Deep Springs	North Carolina	D	318
Delegate	Australia	Om	202
Del Rio	Texas	D	237
Densmore	Kansas	L6	42 kg
Denton County	Texas	Om	8
Denver	Colorado	L6	208
Deport	Texas	Og	4455
Descubridora	Mexico	Om	6021
Dexter	Texas	Om	212
Dhurmsala	India	LL6	681
Dimboola	Australia	H5	46
Dimitrovgrad	Yugoslavia	Om	219
Dimmitt	Texas	H4	6285
Dingo Pup Donga	Australia	Au	4.0
Dix	Nebraska	L	8905
Djati-Pengilon	Java	H6	464
Dokachi	Bangladesh	H5	16
Doroninsk	USSR	H6	7.5
Dorrigo	Australia	Opl	39
Douar Mghila	Morocco	LL6	0.5
Doyleville	Colorado	H5	17
Drake Creek	Tennessee	L6	152
Dresden (Canada)	Canada	H6	27
Dresden (Kansas)	Kansas	H5	212
Drum Mountains	Utah	Om	522 kg
Duchesne	Utah	Of	2780
Duel Hill (1854)	North Carolina	Of	138
Dungannon	Virginia	Og	1009
Durala	India	L6	59
Duruma	Kenya	L6	1.5
Dwaleni	Swaziland	H6	115
Dwight	Kansas	L6	174
Dyarrl Island	New Guinea	M	8
Eagle Station	Kentucky	P	345
Edjudina	Australia	H4	0.8
Edmonson	Texas	L6	281
Edmonton (Canada)	Canada	Hx	584
Edmonton (Kentucky)	Kentucky	Of	8277
Efremovka	USSR	C3	269
Ehole	Angola	H5	1528

Name	*Locality*	*Class*	*Weight*
Eichstadt	Germany	H5	1
Ekeby	Sweden	H4	18
Elba	Colorado	H5	94
Elbogen	Czechoslovakia	Om	94
El Burro	Mexico	Ogg	34 kg
El Capitan	New Mexico	Om	4831
Elenovka	USSR	L5	219
Eli Elwah	Australia	L6	55
Ellemeet	Holland	Ah	s
Ellerslie	Australia	L5	28
Elm Creek	Kansas	H4	1185
El Perdido	Argentina	H5	39
Elsinora	Australia	H5	87
Elyria	Kansas	Om	234
Emery	South Dakota	M	1002
Emmaville	Australia	Aeu	s
Emmitsburg	Maryland	Om	7
Enigma	Georgia	H4	94
Enon	Ohio	Anom	44
Ensisheim	France	LL6	225
Ergheo	Somalia	L5	1082
Erie	Colorado	L	1275
Erxleben	Germany	H6	31
Essebi	Zaire	C2	61
Estacado	Texas	H6	10 kg
Estherville	Iowa	M	10 kg
Esu	Sudan	H	s
Eustis	Florida	H4	480
Eva	Oklahoma	L5	300
Faith	South Dakota	H5	434
Farley	New Mexico	H5	930
Farmington	Kansas	L5	2620
Farmville	North Carolina	H4	5941
Farnum	Nebraska	L5	150
Faucett	Missouri	H5	6209
Fayetteville	Arkansas	H4	161
Felix	Alabama	C3	1286
Fenbark	Australia	H5	4.0
Filomena	Chile	Hx	20 kg
Finmarken	Norway	P	977
Finney	Texas	L5	277
Fisher	Minnesota	L6	6500
Fleming	Colorado	H3	68
Floyd	New Mexico	H4	256
Föllinge	Sweden	Off	14
Forest City	Iowa	H5	36 kg
Forest Vale	Australia	H4	147
Forksville	Virginia	L6	1995
Forrest	Australia	H5	1.7
Forrest Lakes	Australia	LL5	s
Forsyth	Georgia	L6	9.5
Forsyth County	North Carolina	Hx	1121
Fort Pierre	South Dakota	Om	99
Four Corners	New Mexico	Om	7255
Franceville	Colorado	Om	297
Frankfort (iron)	Kentucky	Om	1638
Frankfort (stone)	Alabama	Aho	4.7
Franklin	Kentucky	H5	207
Freda	North Dakota	D	255
Fremont Butte	Colorado	L4	162
Frenchman Bay	Australia	H3	82
Fukutomi	Japan	L5	9.7
Futtehpur	India	L6	19
Gambat	Pakistan	L6	29
Garland	Utah	Ah	102
Garnett	Kansas	H4	286
Garraf	Spain	L6	53
Geidam	Nigeria	H5	5.5
Georgetown	Colorado	H6	687
Ghubara	Saudi Arabia	L5	9
Gibeon	South-West Africa	Of	263 kg
Gifu	Japan	L6	18
Gilgoin	Australia	H5	4285
Girgenti	Italy	L6	8939
Giroux	Canada	P	2381
Gladstone (iron)	Australia	Og	21 kg
Gladstone (stone)	New Mexico	H6	3250
Glasgow	Kentucky	Om	4047
Glorieta Mountain	New Mexico	Om	11 kg
Gnadenfrei	Germany	H5	0.8
Goalpara	India	Au	163
Gobabeb	Southwest Africa	H4	25
Goodland	Kansas	L4	174
Goose Lake	California	Om	1165 kg
Grady (1933)	New Mexico	L	1768
Grady (1937)	New Mexico	H3	772
Grand Rapids	Michigan	Om	3526
Grant	New Mexico	Om	481 kg
Grant County	Kansas	L6	696
Grassland	Texas	L4	114
Great Bear Lake	Canada	H6	40
Greenbrier County	West Virginia	Om	473
Gressk	USSR	Hx	1935
Gretna	Kansas	L5	32 kg
Grosnaja	USSR	C3	4.7
Grossliebenthal	USSR	L6	49
Grüneberg	Poland	H4	16
Gruver	Texas	H4	1256
Guarena	Spain	H6	416
Guffey	Colorado	D	8200
Guibga	Upper Volta	L5	250
Guidder	Cameroon	LL5	0.4
Gun Creek	Arizona	Om	1204
Gundaring	Australia	Og	237
Gunnadorah	Australia	H5	1.2
Gütersloh	Germany	H4	22
Haig	Australia	Om	450
Hainholz	Germany	M	382
Hale Center No. 1	Texas	L5	188
Hale Center No. 2	Texas	H4	324
Hallingeberg	Sweden	L3	144
Hamilton	Australia	L6	201
Hamlet	Indiana	LL4	1543
Hammond	Wisconsin	Om	293
Hammond Downs	Australia	H4	15 kg

Name	*Locality*	*Class*	*Weight*
Haraiya	India	Aeu	2.2
Hardwick	Minnesota	L4	1091
Harleton	Texas	L6	4400
Harriman	Tennessee	Om	12 kg
Harrison County	Indiana	L6	19
Harrisonville	Missouri	L6	10 kg
Havana	Illinois	Of	12
Haven	Kansas	H6	21
Haverö	Finland	Au	1.8
Haviland	Kansas	H5	84
Hawk Springs	Wyoming	H5	88
Hedeskoga	Sweden	H5	26
Hedjaz	Saudi Arabia	L	107
Helt Township	Indiana	Ogg	135
Henbury	Australia	Om	227 kg
Hendersonville	North Carolina	L5	2695
Hermitage Plains	Australia	L6	130
Hessle	Sweden	H5	1863
Hex River Mountains	South Africa	Hx	582
Hildreth	Nebraska	L5	173
Hill City	Kansas	Of	10 kg
Hoba	South-West Africa	D	4203
Hobbs	New Mexico	H4	224
Hökmark	Sweden	L4	12
Holbrook	Arizona	L6	8454
Holland's Store	Georgia	Hx	54
Holly	Colorado	H4	37
Holyoke	Colorado	H4	222
Homestead	Iowa	L5	5616
Honolulu	Hawaii	L5	32
Hope	Arkansas	Og	885
Hopper	Virginia	Om	25
Horace	Kansas	H5	464
Horse Creek	Colorado	Hx	140
Hraschina	Yugoslavia	Om	1.0
Huckitta	Australia	P	403
Hugoton	Kansas	H5	258
Huizopa	Mexico	Of	2790
Hungen	Germany	H6	21
Hvittis	Finland	E6	190
Ibbenbüren	Germany	Ah	9
Ibitira	Brazil	Aeu	1.6
Ider	Alabama	Om	90 kg
Idutywa	South Africa	H5	50
Ilimaes (pallasite)	Chile	P	155
Ilinskaya Stanitza	USSR	Om	184
Imilac	Chile	P	19 kg
Imperial	California	H4	4
Indarch	USSR	E4	2840
Indianola	Nebraska	L5	225
Indian Valley	Virginia	Hx	489
Indio Rico	Argentina	H6	4.7
Inman	Kansas	L4	14
Ipiringa	Brazil	H6	10
Iquique	Chile	D	168
Iredell	Texas	Ogg	97
Iron Creek	Canada	Om	122
Itapicuru-Mirim	Brazil	H5	9.7
Ivanpah	California	Om	3115
Ivuna	Tanzania	CI	122
Jackalsfontein	South Africa	L6	30
Jackson County	Tennessee	Om	46
Jajh deh Kot Lalu	Pakistan	E6	18
Jamestown	North Dakota	Of	329
Jelica	Yugoslavia	LL6	231
Jenkins	Missouri	Og	55 kg
Jenny's Creek	West Virginia	Og	14
Jerome	Kansas	L4	166
Jhung	Pakistan	L5	22
Joe Wright Mountain	Arkansas	Om	571
Johnson City	Kansas	L6	1955
Johnstown	Colorado	Ah	1028
Jonzac	France	Aeu	0.2
Judesegeri	India	H6	16
Juromenha	Portugal	D	16
Juvinas	France	Aeu	172
Kaalijarv	USSR	Og	4.3
Kaba	Hungary	C3	0.7
Kabo	Nigeria	H5	80
Kainsaz	USSR	C3	26
Kakangari	India	C3?	0.5
Kalaba	Zaire	H4	11
Kaldoonera Hill	Australia	H6	1.4
Kalkaska	Michigan	Om	759
Kamiomi	Japan	H4	5
Kamsagar	India	L6	9.6
Kandahar	Afghanistan	L6	123
Kansas City	Missouri	H5	283
Kapoeta	Sudan	Aho	0.9
Kappakoola	Australia	H6	0.7
Karakol	USSR	LL6	4
Karatu	Tanzania	LL6	57
Karee Kloof	South Africa	Og	27
Karkh	Pakistan	L6	49
Karoonda	Australia	C4	123
Kaufman	Texas	L5	168
Kearney	Nebraska	H5	1008
Keen Mountain	Virginia	Hx	5629
Kelly	Colorado	LL4	3512
Kendall County	Texas	Anom	2044
Kennard	Nebraska	H5	156
Kenton County	Kentucky	Om	2691
Kerilis	France	H5	2.4
Kermichel	France	L6	42
Kernouvé	France	H6	1135
Kesen	Japan	H4	2105
Keyes	Oklahoma	L6	1781
Khairpur	Pakistan	E6	27
Khanpur	India	LL5	30
Kharkov	USSR	L6	26
Khohar	India	L3	92
Khor Temiki	Sudan	Ae	90
Kiel	Germany	L6	6.2
Kielpa	Australia	H5	351

Name	*Locality*	*Class*	*Weight*
Kiffa	Mauritania	H4	25
Killeter	Ireland	H6	2.5
Kimble County	Texas	H6	4130
Kingfisher	Oklahoma	L5	2260
Kingoonya	Australia	L4	2.4
Kingston	New Mexico	Om	333
Kissij	USSR	H5	22
Kittakittaooloo	Australia	H4	10
Klein-Wenden	Germany	H6	67
Klondike	Canada	D	158
Knowles	Oklahoma	Om	58
Knyahinya	USSR	L5	1575
Kodaikanal	India	Off	283
Kopjes Vlei	South Africa	Hx	64
Koraleigh	Australia	L6	s
Krähenberg	Germany	LL5	4.4
Kramer Creek	Colorado	L4	38
Krasnoi-Ugol	USSR	L6	5.5
Krasnoyarsk	USSR	P	910
Kress	Texas	L6	113
Krymka	USSR	LL3	136
Kuleschovka	USSR	L6	11
Kulnine	Australia	L6	170
Kumerina	Australia	Opl	339
Kunashak	USSR	L6	175
Kuttippuram	India	L6	120
Kyancutta	Australia	Om	754
Kybunga	Australia	L5	94
Kyle	Texas	L6	253
Kyushu	Japan	L6	216
La Bécasse	France	L6	81
Laborel	France	H5	17
La Caille	France	Om	107
Ladder Creek	Kansas	L6	5700
Lafayette	Indiana	An	637
La Grange	Kentucky	Of	2168
L'Aigle	France	L6	448
Lakangaon	India	Aeu	10
Lake Bonney	Australia	L6	s
Lake Brown	Australia	L6	0.2
Lake Grace	Australia	L6	335
Lake Labyrinth	Australia	LL6	1085
Lake Murray	Oklahoma	Ogg	80
Laketon	Texas	L6	124
Lakewood	New Mexico	L6	523
La Lande	New Mexico	L5	158
Lancé	France	C3	185
Lançon	France	H6	73
Landes	West Virginia	O	492
Långhalsen	Sweden	L6	76
Lanton	Missouri	Om	558
La Porte	Indiana	Om	1491
La Primitiva	Chile	Hx	93
Las Vegas	Nevada	Og	2791
Laundry East	Australia	H3	1.0
Laundry Rockhole	Australia	H5	3.1
Laundry West	Australia	L4	2.9
Laurens County	South Carolina	Of	12
Lawrence	Kansas	L6	328
Leedey	Oklahoma	L6	97
Leeds	Canada	Og	20
Lenarto	Czechoslovakia	Om	208
Leon	Kansas	H5	17 kg
Leoville	Kansas	C2	482
Le Pressoir	France	L6	3.6
Les Ormes	France	L5	0.3
Lesves	Belgium	L6	1.5
Lexington County	South Carolina	Og	2617
Lick Creek	North Carolina	Hx	9.7
Lillaverke	Sweden	H5	150
Lime Creek	Alabama	D	2.9
Limerick	Ireland	H5	210
Lincoln County	Colorado	L6	71
Linville	North Carolina	D	15
Linwood	Nebraska	Og	33 kg
Lissa	Czechoslovakia	L6	118
Little Piney	Missouri	L5	78
Little River	Kansas	H6	170
Livingston (Montana)	Montana	Om	294
Livingston (Tennessee)	Tennessee	Om	123
Lixna	USSR	H4	58
Locust Grove	Georgia	Hx	2166
Lodran	Pakistan	Lo	13
Logan	Oklahoma	H5	336
Lombard	Montana	Hx	62
Lonaconing	Maryland	Og	24
Long Island	Kansas	L6	2696
Loomis	Nebraska	L6	229
Loop	Texas	L6	149
Loreto	Mexico	Om	89 kg
Los Reyes	Mexico	Om	377
Lost City	Oklahoma	H5	16 kg
Losttown	Georgia	Om	71
Lowicz	Poland	M	82
Loyola	doubtful	L5	1772
Lua	India	L5	25
Lubbock	Texas	L5	390
Lucky Hill	Jamaica	Om	40
Luis Lopez	New Mexico	Om	174
Lumpkin	Georgia	L6	31
Lundsgård	Sweden	L6	97
Luotolax	Finland	Aho	0.5
Lutschaunig's Stone	Chile	L6	73
Macau	Brazil	H5	72
Macibini	South Africa	Aeu	15
Madoc	Canada	Om	11
Madrid	Spain	L6	3.5
Mafra	Brazil	L4	9
Magura	Czechoslovakia	Og	672
Mainz	Germany	L5	2
Malakal	Sudan	L5	160
Malotas	Argentina	H5	206
Malvern	South Africa	Aho	19
Manbhoom	India	LL6	15
Mangwendi	Rhodesia	LL6	17
Mantos Blancos	Chile	Of	356

Name	*Locality*	*Class*	*Weight*
Mapleton	Iowa	Om	3728
Maria Elena (1935)	Chile	Om	11 kg
Marion	Iowa	L6	1717
Marjalahti	Finland	P	452
Marshall County	Kentucky	Om	67
Marsland	Nebraska	H5	244
Mart	Texas	Of	454
Matatiele	South Africa	Og	69
Mauerkirchen	Austria	L6	73
Mayday	Kansas	H	5
Mayodan	North Carolina	Hx	13 kg
Maziba	Uganda	L6	390
Mbosi	Tanzania	Om	779
McKinney	Texas	L4	5208
Mejillones	Chile	Hx	12 kg
Melrose	New Mexico	L5	2782
Menow	Germany	H4	110
Merceditas	Chile	Om	724
Mern	Denmark	L6	220
Mertzon	Texas	Om	3319
Merua	India	H5	197
Mesa Verde Park	Colorado	Om	3439
Messina	Italy	L5	3.4
Metsäkyla	Finland	H4	s
Mezö-Madaras	Romania	L3	335
Miami	Texas	H	1160
Mighei	USSR	C2	620
Milena	Yugoslavia	L6	99
Miller (Arkansas)	Arkansas	H5	53
Miller (Kansas)	Kansas	H	41
Mills	New Mexico	H6	367
Milly Milly	Australia	Om	283
Minas Gerais	Brazil	L	10
Mincy	Missouri	M	308
Misshof	USSR	H5	158
Misteca	Mexico	Og	344
Moab	Utah	O	253
Mocs	Romania	L6	3346
Modoc	Kansas	L6	5623
Mokoia	New Zealand	C3	6.4
Molina	Spain	L5	1189
Molong	Australia	P	864
Monahans	Texas	Opl	913
Monroe	North Carolina	H4	252
Monte Milone	Italy	L	0.6
Monze	Zambia	L6	265
Moonbi	Australia	Om	286
Mooranoppin	Australia	Og	149
Moore County	North Carolina	Aeu	460
Mooresfort	Ireland	H5	161
Moorleah	Australia	L6	s
Morito	Mexico	Om	636
Morland	Kansas	H6	517
Mornans	France	H5	32
Morradal	Norway	D	58
Morrill	Nebraska	Om	87
Morristown	Tennessee	M	1757
Morven	New Zealand	H5	112
Mosca	Colorado	L6	6136
Mosquero	New Mexico	H4	1629
Mossgiel	Australia	L4	560
Moti-ka-nagla	India	H6	77
Motpena	Australia	L6	98
Motta di Conti	Italy	H	2.4
Mount Ayliff	South Africa	Og	95
Mount Browne	Australia	H6	486
Mount Dooling	Australia	Ogg	370
Mount Dyrring	Australia	P	672
Mount Edith	Australia	Om	1577
Mount Egerton	Australia	Ae	3731
Mount Joy	Pennsylvania	Ogg	2833
Mount Magnet	Australia	Opl	100
Mount Morris	Wisconsin	E6?	557
Mount Ouray	Colorado	Om	84
Mount Padbury	Australia	M	8147
Mount Sir Charles	Australia	Of	21
Mount Stirling	Australia	Og	383
Mount Vernon	Kentucky	P	134 kg
Muddoor	India	H5	26
Mulga (North)	Australia	H6	278
Mulga (South)	Australia	H4	0.4
Mundrabilla	Australia	Om	217 kg
Mungindi	Australia	Of	573
Muonionalusta	Sweden	Of	419
Murchison	Australia	C2	30 kg
Murfreesboro	Tennessee	Om	125
Murnpeowie	Australia	Anom	191
Muroc Dry Lake	California	L	43
Murphy	North Carolina	Hx	582
Murray	Kentucky	C2	5830
Muzzaffarpur	India	Opl	5
Nagaria	India	Aeu	s
Nagy-Vazsony	Hungary	Og	36
Nakhla	Egypt	An	644
Nakhon Pathom	Thailand	L6	852
Nanjemoy	Maryland	H6	79
Naoki	India	H6	227
Nàrdoo No. 1	Australia	H5	75
Nardoo No. 2	Australia	L6	109
Narellan	Australia	L6	33
Naretha	Australia	L4	2.7
Narraburra	Australia	Om	321
Näs	Sweden	LL6	17
Nashville (Kansas)	Kansas	L6	23 kg
Nashville (North Carolina)	North Carolina	O	2676
Navajo	Arizona	Ogg	517
Nazareth (iron)	Texas	Om	315
Nedagolla	India	Anom	28
Needles	California	Of	10 kg
Neenach	California	L6	2210
Negrillos	Chile	Hx	15 kg
Nejed	Saudi Arabia	Om	2931
Nejo	Ethiopia	L6	183
Nelson County	Kentucky	Ogg	1207
Nenntmannsdorf	Germany	Ogg	15
Neptune Mountains	Antarctica	Og	997

Name	*Locality*	*Class*	*Weight*
Nerft	USSR	L6	71
Ness County	Kansas	L6	5810
Netschaevo	USSR	Om	267
New Almelo	Kansas	L5	1557
New Baltimore	Pennsylvania	Anom	3216
New Concord	Ohio	L6	8700
New Leipzig	North Dakota	Og	17 kg
Newport	Arkansas	P	222
New Westville	Ohio	Of	3318
Ngawi	Java	LL3	103
N'Goureyma	Mali	Anom	1519
Nikolskoe	USSR	L4	32
N'Kandhla	South Africa	Om	146
Nobleborough	Maine	Aeu	0.1
Nocoleche	Australia	Anom	203
Nogoya	Argentina	C2	4.5
Nora Creina	Australia	L4	8.5
Norcateur ·	Kansas	L6	133
Nordheim	Texas	D	1094
Norfolk	Virginia	Om	110
Norfork	Arkansas	Om	60
Norristown	Georgia	Om	196
North East Reid	Australia	H5	1.9
North Forrest	Australia	H4	3.8
North Haig	Australia	Au	8.2
North Reid	Australia	LL5	4.7
North West Forrest	Australia	E6	11
Norton County	Kansas	Ae	1797
Novo-Urei	USSR	Au	93
Nuevo Laredo	Mexico	Aeu	132
Nulles	Spain	H6	124
Nyirabrany	Hungary	LL5	s
Oak	Australia	L5	0.8
Oakley (iron)	Idaho	Og	111 kg
Oakley (stone)	Kansas	H6	1614
Oberlin	Kansas	LL5	195
Obernkirchen	Germany	Of	302
Ochansk	USSR	H4	1668
Odessa	Texas	Og	128 kg
Oesede	Germany	H5	137
Oesel	USSR	L6	28
Ogallala	Nebraska	Og	118
Ogi	Japan	H6	40
Ojuelos Altos	Spain	L	191
Okano	Japan	Hx	20
Okechobee	Florida	L4	968
Okirai	Japan	H5	31
Olivenza	Spain	LL5	938
Ollague	Bolivia	P	296
Olmedilla de Alarcon	Spain	H	314
Orange River (iron)	South Africa	Om	120
Orgueil	France	Cl	183
Orlovka	USSR	H	127
Ornans	France	C3	3.8
Oro Grande	New Mexico	H5	9.1
Oroville	California	Om	401
Orvinio	Italy	L6	59
Oscuro Mountains	New Mexico	Og	102
Osseo	Canada	Og	37 kg
Otis	Kansas	L6	215
Ottawa	Kansas	LL6	12
Oubari	Libya	L4	151
Ovid	Colorado	H	251
Owens Valley	California	Om	157 kg
Ozona	Texas	H	1658
Ozren	Yugoslavia	Og	17
Pacula	Mexico	L6	44
Palo Blanco Creek	New Mexico	Aeu	s
Pan de Azucar	Chile	Og	101
Pantar	Philippines	H5	112
Para de Minas	Brazil	Of	223
Paragould	Arkansas	LL5	31 kg
Paranaiba	Brazil	L6	322
Parnallee	India	LL3	520
Pasamonte	New Mexico	Aeu	1585
Patos de Minas	Brazil	Hx	827
Patrimonio	Brazil	L	14
Patwar	Pakistan	M	592
Pavlodar	USSR	P	12
Pavlograd	USSR	L6	97
Pavlovka	USSR	Aho	8
Peace River	Canada	L6	551
Peckelsheim	Germany	Ah	2.2
Peck's Spring	Texas	L5	629
Peetz	Colorado	L6	810
Pena Blanca Springs	Texas	Ae	457
Penokee	Kansas	H	3552
Perpeti	Pakistan	L6	35
Perryville	Missouri	Opl	14 kg
Persimmon Creek	North Carolina	Opl	3519
Pervomaisky	USSR	L6	446
Pesyanoe	USSR	Ae	67
Petersburg	Tennessee	Aeu	42
Petropavlovka	USSR	H	118
Pevensey	Australia	LL5	14
Phillips County	Colorado	P	368
Piancaldoli	Italy	L3	s
Pickens County	Georgia	H	67
Piedade do Bargre	Brazil	Om	398
Pierceville (iron)	Kansas	Om?	808
Pierceville (stone)	Kansas	L	183
Pillistfer	USSR	E6	66
Pima County	Arizona	Hx	150
Pine River	Wisconsin	Om	297
Pinnaroo	Australia	M	1132
Pinon	New Mexico	D	1240
Pipe Creek	Texas	H6	312
Pitts	Georgia	Of	1022
Plains	Texas	H5	363
Plainview (1917)	Texas	H5	24 kg
Plantersville	Texas	H6	1862
Pleasanton	Kansas	H5	204
Plymouth	Indiana	Om	619
Pohlitz	Germany	L5	0.1
Ponca Creek	Nebraska	Ogg	29
Portales No. 3	New Mexico	L	156

Name	*Locality*	*Class*	*Weight*
Port Orford	Oregon	P	24
Potter	Nebraska	L6	1930
Prairie Dog Creek	Kansas	H3	314
Prambanan	Java	Off	2.3
Pribram	Czechoslovakia	H5	140
Pricetown	Ohio	L6	3.0
Providence	Kentucky	Om	5492
Puente del Zacate	Mexico	Om	2332
Pulaski County	Georgia	Og	112
Pulsora	India	H5	5.8
Pultusk	Poland	H5	3263
Puquios	Chile	Om	90
Puripica	Chile	Hx	15 kg
Putinga	Brazil	L6	962
Putnam County	Georgia	Of	2736
Quartz Mountain	Nevada	Om	57
Queen's Mercy	South Africa	H6	424
Quenggouk	Burma	H4	35
Quillagua	Chile	Hx	741
Quinn Canyon	Nevada	Om	45
Raco	Argentina	H5	133
Rafrüti	Switzerland	D	22
Rakovka	USSR	L6	23
Ramsdorf	Germany	L6	20
Ranchapur	India	H4	59
Rancho de la Pila	Mexico	Om	54
Rancho de la Presa	Mexico	H	12
Rangala	India	L	26
Ransom	Kansas	H4	295
Ras Tanura	Saudi Arabia	H	5.9
Rawlinna	Australia	H5	2.8
Reager	Kansas	L	37
Red River	Texas	Om	79
Reed City	Michigan	Og	1877
Reid	Australia	H	4.0
Reliegos	Spain	L	26
Renazzo	Italy	C2	26
Rhine Villa	Australia	Og	114
Richardton	North Dakota	H5	5155
Richland	Texas	Hx	1026
Richmond	Virginia	L5	18
Rich Mountain	North Carolina	L6	112
Rifle	Colorado	Og	4367
Rio Loa	Chile	Hx	940
Rio Negro	Brazil	L4	66
Rochester	Indiana	H	53
Rodeo	Mexico	Om	1998
Roebourne	Australia	Om	4018
Rolla (1936)	Kansas	H	414
Rolla (1939)	Kansas	H	10
Rosario	Honduras	Og	190
Rosebud	Texas	H	5
Rose City	Michigan	H5	3587
Rowena	Australia	H6	78
Rowton	Great Britain	Om	32
Roy (1933)	New Mexico	L5	8607
Roy (1934)	New Mexico	L6	4528
Ruff's Mountain	South Carolina	Om	4762
Rupota	Tanzania	L6	975
Rush County	Indiana	H	4020
Rush Creek	Colorado	L6	3170
Russel Gulch	Colorado	Om	72
Sacramento Mountains	New Mexico	Om	6550
St. Caprais-de-Quinsac	France	L	0.4
St. Francois County	Missouri	Og	236
St. Genevieve County	Missouri	Of	1380
St. Germain-du-Pinel	France	H	53
St. Lawrence	Texas	LL6	100
St. Louis	Missouri	H4	2.4
St. Mark's	South Africa	E5	258
St. Mary's County	Maryland	LL3	s
St. Mesmin	France	LL6	86
St. Michel	Finland	L6	231
St. Peter	Kansas	L5	549
Saint-Sauveur	France	E4	7.8
St. Severin	France	LL6	2463
Salaices	Mexico	H4	395
Salina	Utah	Om	221
Saline	Kansas	H5	897
Salla	Finland	L	318
Salles	France	H6	50
Salta	Argentina	P	24 kg
Salt Lake City	Utah	H5	2.5
Salt River	Kentucky	Opl	112
Sams Valley	Oregon	Om	19
San Angelo	Texas	Om	3443
San Cristobal	Chile	D	136
Sanderson	Texas	Om	471
Sandia Mountains	New Mexico	Ogg	1672
Sandtown	Arkansas	Om	100
San Emigdio	California	H4	490
San Francisco Mountains	Arizona	Of	1334
San José	Mexico	H5	142
San Juan Capistrano	California	H6	18
Santa Apolonia	Mexico	Om	5689
Santa Catharina	Brazil	D	11 kg
Santa Cruz	Mexico	C2	s
Santa Isabel	Argentina	L6	29
Santa Luzia	Brazil	Ogg	23 kg
Santa Rosa	Colombia	Anom	5751
Santa Rosalia	Mexico	P	63
Santiago Papasquiero	Mexico	Anom	1176
Sao Jose do Rio Preto	Brazil	L5	7.5
Sao Juliao de Moreira	Portugal	Ogg	2150
Saratov	USSR	L4	513
Sardis	Georgia	Og	800 kg
Sarepta	USSR	Og	254
Savannah	Tennessee	Om	27 kg
Schenectady	New York	H5	30
Schönenberg	Germany	L6	8.8
Schwetz	Poland	Om	165
Scott City	Kansas	H5	228
Scottsville	Kentucky	Hx	1042
Scurry	Texas	H5	26
Seagraves	Texas	H4	13 kg

Name	*Locality*	*Class*	*Weight*
Searsmont	Maine	H5	90
Seeläsgen	Poland	Og	407
Segowlie	India	L6	61
Seguin	Kansas	H	49
Seibert	Colorado	H	131
Seligman	Arizona	Og	147
Selma	Alabama	H4	157
Semarkona	India	LL3	245
Seminole	Texas	H4	457
Sena	Spain	H4	167
Seneca	Kansas	H	265
Seneca Township	Michigan	Of	9372
Seres	Greece	H4	2.0
Serre de Mage	Brazil	Aeu	25
Sevrukovo	USSR	L5	23
Seymour	Missouri	Og	1320
Shalka	India	Ah	88
Shallowater	Texas	Ae	1017
Sharps	Virginia	H3	401
Shaw	Colorado	L6	1596
Shelburne	Canada	L5	735
Shergotty	India	Aeu	270
Shingle Springs	California	D	32
Shrewsbury	Pennsylvania	Om	395
Shytal	Pakistan	L6	27
Siena	Italy	LL5	15
Sierra Gorda	Chile	Hx	17 kg
Sierra Sandon	Chile	Og	72
Signal Mountain	Mexico	Of	41
Sikhote-Alin	USSR	Ogg	4107
Silver Bell	Arizona	Ogg	192
Silver Crown	Wyoming	Og	170
Silverton	Australia	L6	69
Simondium	South Africa	M	9.1
Sindhri	Pakistan	H5	46
Sinnai	Italy	H	17
Sioux County	Nebraska	Aeu	154
Sitathali	India	H5	13
Ski	Norway	L6	1.2
Sleeper Camp	Australia	L6	3.3
Slobodka (1818)	USSR	L4	3.5
Slobodka (1838)	USSR	L	4.0
Smith Center	Kansas	L6	91
Smithland	Kentucky	D	133
Smithonia	Georgia	Hx	590
Smith's Mountain	North Carolina	Om	57
Smithsonian Iron		Ogg	3400
Smithville	Tennessee	Og	3708
Social Circle	Georgia	Of	22 kg
Soko-Banja	Yugoslavia	LL4	337
Somervell County	Texas	P	80
Soper	Oklahoma	Anom	1122
Soroti	Uganda	Off	154
South Bend	Indiana	P	2.8
South Byron	New York	D	465
South Dahna	Arabia	O	142 kg
South Oman	Arabia	E	13
Spearman	Texas	Om	870
Springwater	Canada	P	2647
Ställdalen	Sweden	H5	192
Stannern	Czechoslovakia	Aeu	497
Staunton	Virginia	Og	6101
Stavropol	USSR	L6	52
Steinbach	Germany	S	427
Stonington	Colorado	H	100
Sublette	Kansas	L	62
Success	Arkansas	L6	3503
Suchy Dul	Czechoslovakia	H5	1.8
Sultanpur	India	L6	71
Supuhee	India	H6	89
Susuman	USSR	Om	74
Sutton	Nebraska	H5	305
Suwahib (Buwah)	Saudi Arabia	H3	5
Sweetwater	Texas	H5	1018
Sylacauga	Alabama	H	1682
Tabor	Czechoslovakia	H5	65
Tadjera	Algeria	L5	69
Taiban	New Mexico	L5	438
Tamarugal	Chile	Om	17 kg
Tambo Quemado	Peru	Om	970
Tané	Japan	L5	586
Tanokami Mountain	Japan	Og	91
Tatahouine	Tunisia	Ah	14
Tathlith	Saudi Arabia	L6	246
Tawallah Valley	Australia	D	1267
Tazewell	Tennessee	Off	1642
Tell	Texas	L6	180
Temple	Texas	L	169
Tenham	Australia	L6	5535
Tennasilm	USSR	L4	4838
Ternera	Chile	D	31
Texline	Texas	H5	646
Thiel Mountains	Antarctica	P	28 kg
Thomson	Georgia	L6	217
Thoreau	New Mexico	Og	294
Thule	Greenland	Om	449
Thunda	Australia	Om	209
Thurlow	Canada	Om	403
Tiberrhamine	Algeria	L6	100
Tieraco Creek	Australia	Om	4038
Tieschitz	Czechoslovakia	H3	31
Tilden	Illinois	L6	903
Timochin	USSR	H5	64
Tirupati	India	H	16
Tjabe	Java	H	39
Tjerebon	Java	L5	s
Tlacotepec	Mexico	D	2400
Tobe	Colorado	H4	5454
Tocopilla	Chile	Hx	1467
Toluca	Mexico	Og	109 kg
Tomatlan	Mexico	H6	168
Tombigbee River	Alabama	Hx	3001
Tomhannock Creek	New York	H5	31
Tonganoxie	Kansas	Om	231
Tonk	India	Cl	3
Torrington	Wyoming	H	116
Toubil River	USSR	Om	175

Name	*Locality*	*Class*	*Weight*
Tourinnes-la-Grosse	Belgium	L6	69
Travis County	Texas	H5	1480
Trenton	Wisconsin	Om	391 kg
Trenzano	Italy	H6	285
Treysa	Germany	Om	195
Trifir	Mali	L	3.0
Troup	Texas	L6	114
Tryon	Nebraska	L	2028
Tucson	Arizona	Anom	911 kg
Tulia	Texas	H5	4917
Turtle River	Minnesota	Om	387
Twin City	Georgia	D	3400
Tysnes Island	Norway	H4	104
Uberaba	Brazil	H5	103
Ucera	Venezuela	H5	205
Udei Station	Nigeria	Om	202
Ularring	Australia	L6	1.2
Ulysses	Kansas	H	334
Umm Ruaba	Sudan	L5	64
Union	Chile	Hx	172
Union County	Georgia	Ogg	84
Ute Creek	New Mexico	H4	177
Utrecht	Holland	L6	40
Utzenstorf	Switzerland	H	105
Uwet	Nigeria	Hx	1105
Uwharrie	North Carolina	Om	1287
Vaca Muerta	Chile	M	1449
Valdinizza	Italy	L6	850
Valkeala	Finland	L6	s
Valley Wells	California	L6	11
Vavilovka	USSR	LL6	3.0
Vengerovo	USSR	H5	34
Vera	Argentina	L4	50
Veramin	Iran	M	52
Verkhne Udinsk	USSR	Om	36
Vernon County	Wisconsin	H	9.3
Victoria West	South Africa	Of	34
View Hill	New Zealand	Om	1883
Vigarano	Italy	C3	2051
Vincent	Australia	L5	s
Vishnupur	India	LL6	24
Vouillé	France	L	161
Wabar	Saudi Arabia	Om	299
Waconda	Kansas	L6	1189
Waingaromia	New Zealand	Om	600
Waldo	Kansas	L	94
Waldron Ridge	Tennessee	Og	70
Walker County	Alabama	Hx	291
Wallapai	Arizona	Of	303 kg
Walltown	Kentucky	L	3.7
Walters	Oklahoma	L6	25 kg
Warrenton	Missouri	C3	36
Waterville	Washington	Anom	197
Wathena	Kansas	Hx	429
Weatherford	Oklahoma	Anom	1216
Weaver Mountains	Arizona	D	773
Webb	Australia	L6	3.1
Weekeroo	Australia	Og	11 kg
Weldona	Colorado	H	1070
Welland	Canada	Om	213
Wellington	Texas	H	4224
Wellman	Texas	H5	543
Wessely	Czechoslovakia	H	0.2
Western Arkansas	Arkansas	Of	1672
West Forrest	Australia	H5	2.3
Weston	Connecticut	H4	181
West Reid	Australia	H6	0.8
Weathersfield	Connecticut	L5	290
Whitman	Nebraska	H	21
Wichita County	Texas	Og	2251
Wilbia	Australia	H5	3.8
Wildara	Australia	H5	s
Wiley	Colorado	Opl	189
Willamette	Oregon	Om	2721
Willaroy	Australia	H3	187
Williamstown	Kentucky	Om	1223
Willow Creek	Wyoming	Og	4866
Willowdale	Kansas	H	74
Wilmot	Kansas	H6	133
Wiluna	Australia	H4	284
Wingellina	Australia	H4	s
Winona	Arizona	E6?	224
Witchellina	Australia	H4	156
Wold Cottage	Great Britain	L6	57
Wolf Creek	Australia	Om	350 kg
Wonyulgunna	Australia	Om	577
Woodbine	Illinois	Of	48 kg
Wood's Mountain	North Carolina	Of	1786
Woodward County	Oklahoma	H4	44 kg
Woolgorong	Australia	L6	362
Wynella	Australia	H4	431
Yambo No. 1	Zaire	H	4.0
Yambo No. 2	Zaire	L3	3.2
Yandama	Australia	L6	377
Yanhuitlan	Mexico	Of	1200
Yardymly	USSR	Og	81
Yatoor	India	H5	222
Yayjinna	Australia	L6	14
Yenberrie	Australia	Og	3836
Yonozu	Japan	H4	44
York (iron)	Nebraska	Om	30
Youndegin	Australia	Og	5756
Ysleta	Texas	Anom	19
Yurtuk	USSR	Aho	33
Zaborzika	USSR	L	4.1
Zacatecas (1972)	Mexico	Anom	444
Zacatecas (1969)	Mexico	Om	6600
Zavid	Yugoslavia	L6	234
Zebrak	Czechoslovakia	H5	73
Zhovtnevyi	USSR	H	703
Zomba	Malawi	L6	270
Zsadany	Romania	H	13
Zvonkov	USSR	H	40

Chemical Analyses of Two Microprobe Standards

Eugene Jarosewich

ABSTRACT

Chemical analyses are given for two materials for use as microprobe standards: volcanic glass from the Mid-Atlantic Ridge and hornblende from Arenal Volcano, Costa Rica.

There has been increasing need for well-analyzed microprobe standards because, as with any instrumental method, a standard compositionally similar to an unknown is the most likely to give reliable results. The key requirements for microprobe standards can be found in the literature in general and some are briefly summarized in an earlier paper (Jarosewich, 1972).

The chemical analyses were performed employing analytical methods described by Hillebrand, et al. (1953) and Peck (1964) except for the determination of sodium and potassium. The latter elements were determined by flame photometry. Data for two new microprobe standards follow.

ARENAL HORNBLENDE USNM 111356.—A green hornblende xenocryst from an andesitic basalt scoria was collected by Dr. W. Melson from the September 1968 eruption of Arenal Volcano, Costa Rica. The sample was crushed and sieved and the 60–100 mesh fraction purified using a heavy liquid (D 3.19–3.21) followed by Franz magnetic separation. The purified sample contains less than 0.5 percent grains with adhering groundmass. An electron microprobe check indicates the sample to be homogeneous within the limits of analytical error.

TABLE 1.—*Chemical analyses of two microprobe standards (analyst: E. Jarosewich)*

Constituent	*Arenal Hornblende (USNM 111356)*	*Basaltic Glass Juan de Fuca Ridge (USNM 111240/52)*
SiO_2	41.46	50.81
Al_2O_3	15.47	14.06
Fe_2O_3	5.60	2.23
FeO	6.43	9.83
MgO	14.24	6.71
CaO	11.55	11.12
Na_2O	1.91	2.62
K_2O	0.21	0.19
H_2O+	1.21	n.d.
H_2O-	<0.01	0.02
TiO_2	1.41	1.85
P_2O_5	<0.01	0.17
MnO	0.15	0.22
Total	99.64	99.83
Total Fe	8.91	9.20

n.d.=not determined.

BASALTIC GLASS USNM 111240/52.—This sample was dredged from the median, flat-floored valley of the southern part of the Juan de Fuca Ridge (44° 40′N, 130°30′W, 2195–2220 m). Approximately 2 percent of the sample is composed of inclusions, primarily plagioclase and olivine. Because the average combined chemical composition of these inclusions is similar to the composition of the glass and because they are present in small amount, the bulk chemistry of the sample is essentially the same as

Eugene Jarosewich, Department of Mineral Sciences, National Museum of Natural History, Smithsonian Institution, Washington, D. C. 20560.

the glass. Electron microprobe analyses shows the glass to be extremely homogeneous in major and minor element content.

Literature Cited

Hillebrand, W. F., G. E. F. Lundell, H. A. Bright, and J. I. Hoffman
1953. *Applied Inorganic Analysis.* 2nd edition, 1034 pages. New York: John Wiley and Sons.

Jarosewich, E.
1972. Chemical Analyses of Five Minerals for Microprobe Standards. *Smithsonian Contributions to the Earth Sciences,* 9:83–84.

Peck, L. C.
1964. Systematic Analysis of Silicates. *U. S. Geological Survey Bulletin,* 1170:66.

Preparation of Multiple Microprobe Samples

Grover C. Moreland and Richard Johnson

ABSTRACT

Several microprobe samples may be prepared simultaneously using a new technique described here. With judicious choice of samples the same technique may be used to prepare microprobe standard discs.

A preparation technique has been developed whereby it is possible to prepare several probe samples simultaneously. The basic mount is a plexiglass disc ¼ inch thick cut from a 1-inch rod. Holes of any convenient size are drilled through the disc and the holes numbered with a scriber. As many as 19 samples can be mounted and prepared simultaneously (Figure 1).

A white 3 × 5 inch card is fastened to a hot plate with masking tape; this card provides a visual contrast against which the sample can be easily seen. A carefully cleaned one inch cover glass is placed on the white card, and the sample disc placed on the cover glass. A weight is added to insure good contact between the disc and the cover glass, and the hot plate temperature adjusted to 40° to 45° C (100°–115° F). Rubber cement is now painted around the edge of the coverglass-plexiglass disc sandwich, and the mount is left on the hot plate for 5 to 10 minutes, or until cured as shown by a brown color.

A mixture of epoxide and expoxide hardener is now prepared (Buehler 20–8130 epoxide and 20–8132 hardener or equivalent). A convenient amount is 4.8 gms of epoxide and 0.8 gm of hardener. This mixture is stirred on the 40° to 45° C hot plate until it reaches a watery consistency.

Each sample is now inserted in its appropriately numbered hole. Then using a dissecting needle, place some of the epoxy mixture on the plexiglass disc and with the needle push some of the mixture over the edge of each hole. The epoxy will run down the wall of the hole, hit the cover glass, and rise. This procedure should leave the specimen in contact with the cover glass, with epoxy around and above it, but very little if any beneath it. One can check under a stereomicroscope to see that the sample is resting on the cover glass (i.e., at the bottom of the hole) and that no air bubbles have formed. If these conditions are not met then the samples can be pushed down and air bubbles freed

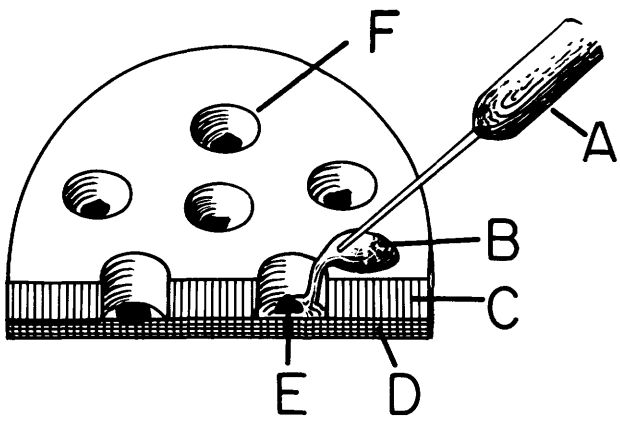

FIGURE 1.—Schematic of plexiglass disc. (A = Dissecting needle, B = epoxy mixture, C = cross-section of plexiglass disc, D = coverglass, E = mineral grain, F = hole drilled in plexiglass disc.)

Grover C. Moreland and Richard Johnson, Department of Mineral Sciences, National Museum of Natural History, Smithsonian Institution, Washington, D. C. 20560.

using a small dissecting needle. One then covers the entire upper (numbered) side of the disc with epoxy, thus insuring that the numbers will not be accidentally obliterated during the subsequent steps of preparation and during later use of the disc.

The epoxy mixture should be allowed to dry on the hot plate for about 30 minutes at 50° C (125° F). The card-coverglass-plexiglass disc assembly is then placed in a 50° C oven for about 10 hours. The assembly is then removed from the oven and the card separated from the remainder of the unit.

The samples are exposed by grinding off the cover glass on an 850 rpm lap with a slurry of water and #600 aluminum oxide. Being careful to keep the lap damp, grind the disc for 2 to 3 minutes or until the samples are exposed. Also grind the numbered side, being careful not to grind off the numbers. The disc should now be washed thoroughly with soap and water and dried.

The samples are now brought to a rough polish by covering a 600 rpm wheel with a double thickness of brown wrapping paper that has been covered with polishing oil and 3 micron diamond compound. (The diamond compound regularly used is VB–3, produced by the Glennel Corp. of West Chester, Pennsylvania.) The disc should be moved counter to the rotation of the wheel; a lapping time of about 5 minutes is usually required. After washing and drying the polish is examined under a reflected light microscope. If necessary repeat the lapping until the only scratches visible are those made by the 3 micron polishing compound. The numbered side of the disc should also be polished to make the numbers visible.

Next, the disc is lapped on a 150 rpm wheel covered with a polishing cloth. The polishing cloth is covered with water to which 0.05 micron alumina is sparingly added until a damp-dry condition is reached. The disc is moved for 30 turns counter to the rotation of the wheel. The disc, same side down, is rotated 180° and given another 30 turns on the wheel. Once again it is washed and dried.

Finally the disc is lapped on a 50 rpm wheel covered with a clean polishing cloth, giving it only 5 turns with light pressure, counter to the rotation of the wheel. This final polishing is to remove any possible contamination due to smearing.

The disc is now washed and dried and examined under a reflected light microscope at about 80 magnification. The 3 micron scratches should no longer be visible and one should see only highly polished, optically flat grains.

One should exercise care in choosing specimens to be mounted in one disc as some very soft material may smear upon polishing and hence cause contamination of the rest of the specimens. Tests were made here on eight samples of varying hardness (metallic zinc, gold, magnesium, aluminum, silver, platinum. Ni-Fe-Co alloy, and lead sulfide (galena)), and mounted and polished on a single disc. A check was made by electron microprobe to determine any effects of smearing from one sample to another due to the polishing technique. For each sample (sulfur in the case of the galena) the background level above and below the peak was determined. Each sample was then probed for Zn, Au, Mg, Al, Ag, Pt, Fe, Co, Ni, and S. Sulfur was the only element that showed a measurable concentration in some of the other samples on the disc, hence the galena did contaminate the other samples.

Preliminary tests have shown that with judicious choice of samples, microprobe standard discs may be prepared using this technique, thus effecting a considerable saving in time and materials over the one-at-a-time method of polishing microprobe standards.

ACKNOWLEDGMENT.—We wish to thank Charles Obermeyer and William Potts for their assistance in the preparation of this paper.

☆ U.S. GOVERNMENT PRINTING OFFICE: 1975—546–367/32